CHARACTERIZING THE MECHANISM OF DIFFERENTIAL

PHARMACOKINETIC DISPOSITION OF TWO STRUCTURALLY SIMILAR

NUCLEOSIDE REVERSE TRANSCRIPTASE INHIBITORS, ZIDOVUDINE AND

DIDANOSINE

by

SUNG-HACK LEE

A Dissertation submitted to the

Graduate School-New Brunswick

Rutgers, The State University of New Jersey

in partial fulfillment of the requirements

for the degree of

Doctor of Philosophy

Graduate Program in

Pharmaceutical Sciences

written under the direction of

Patrick J. Sinko

and approved by

_____

_____

_____

_____

New Brunswick, New Jersey

[May 2008]

ABSTRACT OF THE DISSERTATION

Characterizing the Mechanism of Differential Pharmacokinetic Disposition of Two

Structurally Similar Nucleoside Reverse Transcriptase Inhibitors, Zidovudine and

Didanosine

By SUNG-HACK LEE

Dissertation Director:
Patrick J. Sinko

The differential contributions of efflux transporters and metabolizing enzymes to the disposition of zidovudine (azidothymidine, AZT) and didanosine (dideoxyinosine, ddI) were investigated using murine and human cells, mouse kidney slices, and mice. Cellular transport, transport in mouse kidney slices, brain uptake, and urinary excretion of AZT and ddI were investigated.

Fumitremorgin C (FTC), a breast cancer resistance protein (BCRP) specific inhibitor), increased AZT accumulation, but had little or no effect on ddI accumulation in either HEK-R482 or in J774. Involvement of BCRP was investigated by comparing results in Mock- and BCRP- transfected cells, and confirmed by repeating the studies after silencing BCRP using siRNA. MK-571, a MRP family inhibitor, blocked the efflux of AZT and ddI in murine and human cells. Silencing MRP3 and MRP4 attenuated the efflux of AZT while silencing MRP1 attenuated ddI efflux. The effect of blocking efflux transporters was found to be minor as compared to inhibition of metabolizing enzymes.

The major form of AZT deposited inside murine cells was AZT-MP, while the major form found inside human cells was AZT-TP. MK-571 abolished the efflux of AZT-MP in both murine and human cells. However, the efflux of AZT, ddI and their metabolites was not affected by FTC. Application of MK-571 also decreased the efflux of GAZT and ddI in kidney slices. The urinary excretion of AZT and ddI with MK-571 in mice was measured. MK-571 did not cause any significant changes in the urinary excretion of AZT, ddI, or their metabolites between the MK-571 untreated and treated groups.

Collectively, the results of these studies indicate that AZT and ddI are substrates of BCRP and MRPs, however since their effects are limited in *in situ* and *in vivo* situation they appear to be relatively minor players in the overall disposition of these drugs.

Dedication

I dedicate this thesis to:

My lovely wife, Ji Young Kim

My precious children, Dong-Jin Lee and Hee-Jin Lee

My mother, Gap-Nam Cho

My late father, Jong-Yeol Lee

My only brother, Jun-Hack Lee

My mother-in-law, Ok-Yeol Ju

My father-in-law, Dae-Sup Kim

My grandmother-in-law, Chin-Sun Kim

My sister-in-law, Ji-Hye Kim

My brother-in-law, Jae Moon Kim

All my friends in Korea and United States

Table of Contents

Lists of tables

List of illustrations

I.   INTRODUCTION

Although zidovudine (AZT) and didanosine (ddI) are the oldest FDA approved drugs for

the treatment of Human Immunodeficiency Virus (HIV) infection, their market is still

among the largest of anti-HIV drugs (~$2 billion in 2004 including combination

formulations, Table 1), and they are clearly prescribed more often than other antiviral

drugs. Since AZT and ddI were launched in 1987 and 1991, respectively, their ADME

properties have been extensively studied. AZT is dominantly metabolized to glucuronides

(Cretton et al., 1990) and ddI is hydrolyzed to hypoxanthine (Stoeckler et al., 1980). But,

there are many other metabolizing enzymes such as phosphorylating kinases or

5-nucleotidase and transporters such as ATP-binding cassette (ABC) transporters and

organic anion transporters (OATs) that are involved with the disposition of AZT and ddI.

Furthermore, the reported mechanisms of metabolism and/or efflux are not sufficiently

understood and cannot explain their pharmacokinetic properties. The major factors

affecting the pharmacokinetic behavior of AZT and ddI are described in the following

sections and this information will be used to develop effective dosing regimens.

Table 1. List of currently available anti-HIV drugs in US (Total 20 drugs including prodrug)

Brand Name	Generic Name	Abbreviation	Experimental Code	Sales (2004)	Change (vs. 03)	Launch	Pharmaceutical Company
Nucleoside/Nucleotide Reverse Transcriptase Inhibitors (NRTIs)							
Videx®	Didanosine: buffered	ddl	BMY-40900	↓	↓	1991	Bristol-Myers Squibb
Videx® EC	Didanosine: delayed-release	ddl		$274M	3%	2000	Bristol-Myers Squibb
Zerit®	Stavudine	d4T	BMY-27857	$272M	-23%	1994	Bristol-Myers Squibb
Emtriva™	Emtricitabine*	FTC		$58M	---	2003	Gilead
Retrovir®	Zidovudine	AZT or ZDV		$80M	4%	1987	GlaxoSmithKline
Epivir®	Lamivudine	3TC		$549M	4%	1995	GlaxoSmithKline
Combivir®	Zidovudine + Lamivudine	AZT + 3TC		$1067M	4%	1997	GlaxoSmithKline
Ziagen®	Abacavir	ABC	1592U89	$290M	0%	1998	GlaxoSmithKline
Trizivir®	Abacavir + Zidovudine + Lamivudine	ABC + AZT + 3TC		$602M	-8%	2000	GlaxoSmithKline
Hivid®	Zalcitabine	ddC		---	---	1992	Roche
Nucleotide Reverse Transcriptase Inhibitors (NtRTI)							
Viread®	Tenofovir DF	TDF or Bis(POC) PMPA		$783M	---	2003	Gilead
Non-Nucleoside Reverse Transcriptase Inhibitors (NNRTIs)							
Viramune®	Nevirapine	NVP	BI-RG-587	$409M	-8%	1996	Boehringer Ingelheim
Sustiva®	Efavirenz	EFV	DMP-266	$621M	14%	1998	Bristol-Myers Squibb
Rescriptor®	Delavirdine	DLV	U-90152S/T	---	---	1997	Pfizer (Agouron)
Protease Inhibitors (PIs)							
Norvir®	Ritonavir	RTV	ABT-538	---	---	1996	Abbott
Kaletra®	Lopinavir + Ritonavir	LPV	ABT-378/r	$896M	19%	2000	Abbott
Reyataz™	Atazanavir*	ATZ	BMS-232632	$414M	---	2003	Bristol-Myers Squibb
Agenerase®	Amprenavir	APV	141W94 or VX-478	↓	↓	1999	GlaxoSmithKline
Lexiva®	Fosamprenavir*	FPV	GW-433908 or VX-175	$121M	80%	2003	GlaxoSmithKline
Crixivan®	Indinavir	IDV	MK-639	$255M	-10%	1996	Merck
Viracept®	Nelfinavir	NFV	AG-1343	~ $200M	-23%	1997	Pfizer (Agouron)
Invirase®	Saquinavir (Hard Gel Cap)	SQV (HGC)	Ro-31-8959	↓	↓	1995	Roche
Fortovase®	Saquinavir (Soft Gel Cap)	SQV (SGC)		~ $110M	14%	1997	Roche
Entry Inhibitors (including Fusion Inhibitors)							
Fuzeon®	Enfuvirtide*	ENF	T-20	$135M	27%	2003	Roche

*Fosamprenavir (2003): prodrug of Amprenavir (Agenerase)
*Atazanavir (2003): 7th FDA-approved HIV protease inhibitor
*Emtricitabine (2003): 7th FDA-approved nucleoside reverse transcriptase inhibitor (NRTI)
*Enfuviritide (2003): new class of fusion inhibitors (SC injection)

II.   BACKGROUND

A.   *Nucleoside Reverse Transcriptase Inhibitors as a treatment of HIV infection*

The HIV is a retrovirus that causes a slow and progressive weakening of the immune system, which results in acquired immunodeficiency syndrome (AIDS)((Figure 1)).
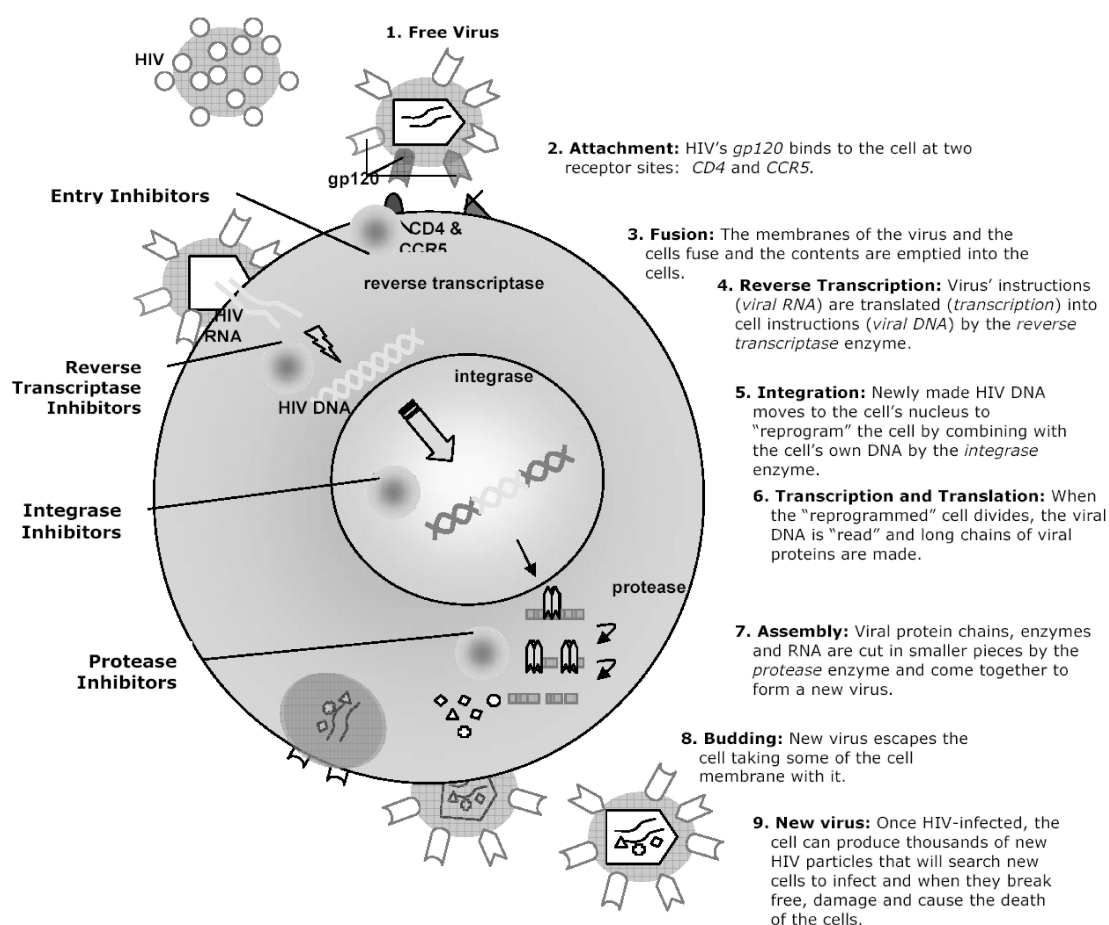
Figure 1. The HIV life cycle. Source from Bedrij et al, HIV/AIDS Industry Report (2005)

The virus inserts its own RNA into host cell DNA, preventing natural cell processes and commencing production of HIV in the host organism. Viral RNA is converted to viral DNA by reverse transcriptase and this DNA is then inserted into the host organism's genome. From one patient infected with HIV, over 10 billion copies of the virus are produced everyday making it easy for HIV to spread quickly through the body. Although HIV infects various types of cells, major target of HIV is T4-lymphocytes (also known as "T-helper" cells). The T4-cell has multiple CD4 receptors, or proteins, and co-receptors such as CCR5 and CXCR-4 on its surface. HIV selectively destroys CD4 expressing cells and, when the number of CD4 cells drops to around 200 cells/μL of blood because of HIV infection, the body's immune system deteriorates (Eyster et al., 1989). When the number of CD4 cells drops below 200 cells/μL of blood, a person with HIV infection is officially said to have AIDS. Reverse Transcriptase Inhibitors block proliferation of HIV by inhibiting reverse transcriptase and the conversion of HIV RNA into viral DNA. Two types of reverse transcriptase inhibitors are introduced for HIV treatment: the "nucleoside" analogue reverse transcriptase inhibitors (NRTIs) and the "non-nucleoside" reverse transcriptase inhibitors (NNRTIs). NRTIs mimic the building blocks used by reverse transcriptase to replicate the HIV genetic material thus disrupting the reverse transcription process. NNRTIs bind directly to reverse transcriptase, and physically prevent the reverse transcriptase from adding new nucleotides to the viral DNA chains.

NRTIs, the main class of reverse transcriptase inhibitors, are converted into their active triphosphate form within cells by phosphorylation. They then resemble natural nucleosides found in human cells and they are able to disrupt the construction of proviral DNA during reverse transcription. In other words, instead of taking up a nucleoside from

the deposited supply in the cell, reverse transcriptase uses a faulty building block (i.e., the nucleoside analogue drug) instead. These "faulty" building blocks do not form the necessary chemical bonds with natural nucleosides and the DNA chain is unable to remain intact. The incomplete chain is unable to correct itself and the process of viral replication is thereby interrupted. The major problem of these drugs is that they may be utilized by healthy reproducing cells thus preventing regular production of healthy new cells as well. The likelihood of nucleoside analogues halting reproduction of healthy cells is not very good, since reverse transcriptase has a much higher affinity for nucleoside analogs rather than DNA polymerase (Zakharova et al., 1995). Also, human cells are able to fix problems with their DNA production process during cell reproduction phase. NRTIs are mainly used in combination therapies also known as "cocktails". When two NRTIs are used with another anti-HIV drug (usually an NNRTI or a protease inhibitor) for a total of 3 drugs, the combination has been found to block HIV replication quite well. Seven NRTIs are currently available: abacavir, didanosine, emtricitabine, lamivudine, stavudine, zalcitabine, and zidovudine. Several drugs in the NRTI class are also currently used as a component of antiretroviral combination therapy. NRTIs are expected to remain as the most robust class of HIV drugs in terms of overall sales (Chrystyna Bedrij, 2005).

B.   *Clinical pharmacokinetic properties of Zidovudine and Didanosine*

Zidovudine Pharmacokinetic parameters of AZT and ddI are listed in Table 2. Oral absorption of AZT is good with a reported bioavailability of between 60% and 70% (Beach, 1998). AZT is subject to hepatic first-pass metabolism (Yarchoan et al., 1986; Blum et al., 1988; Morse et al., 1993). Oral absorption is affected by food consumption, in

particular high-fat meals, resulting in delayed absorption (Unadkat et al., 1990). AZT

achieves cerebrospinal fluid (CSF) levels that are approximately 75% of plasma

concentration by AUC (Rolinski et al., 1997). Thirty-five percent of AZT is protein bound

(Collins and Unadkat, 1989). AZT undergoes metabolism to its glucuronide, the major

plasma and urinary metabolism (Singlas et al., 1989). The major organs in AZT

glucuronidation are the liver, possibly the kidney and the intestinal mucosa. AZT plasma

levels are increased by coadministration of other drugs that are substrates and/or inhibitors

of glucuronidation (Sim et al., 1991). Fourteen percent of parent AZT and 74% of the

glucuronide of the oral dose have been recovered from the urine in healthy volunteers.

Table 2. Pharmacokinetic parameters of AZT and ddI in mouse, rat, and human

	AZT	ddI
Mouse		
$t_{1/2}$ (min)	66	16
CL (ml/min/kg)	23	39
CLr (ml/min/kg)	16	---
Bioavailability (%)	82~92	15
Urine recovery (IV total, %)	86 (87% parent)	---
Kidney T/P ratio (Total)	0.7~53 (inc.)	---
Kidney T/P ratio (unch)	1.97~2.74 (flat)	---
Rat		
$CL_{int,in\ vitro}$	14.3	---
$CL_{int,in\ vivo}$	18.4	---
$t_{1/2}$ (min)	21~26	29~33
CL (ml/min/kg)	28	66
CLr (ml/min/kg)	14~16	14~19
Urine recovery (IV unch, %)	50~57	21~28
Urine recovery (IV total, %)	---	51 (95% parent)
Urine recovery (PO total, %)	78	12
Kidney T/P ratio (Total)	8	2.3
Bioavailability (%)	---	8~11
Human		
$CL_{int,in\ vitro}$	9.87	---
$CL_{int,in\ vivo}$	28.4	---
$t_{1/2}$ (min)	66	84
CL (ml/min/kg)	19	11
CLr (ml/min/kg)	6	6
Plasma protein binding (%)	35	< 5
Bioavailability (%)	60~70	25~43
Urine recovery (IV unch, %)	---	55
Urine recovery (PO unch, %)	14	18
Urine recovery (PO total, %)	90	---

The renal excretion of the drug is mediated by both glomerular filtration and active tubular

secretion (Klecker et al., 1987; Blum et al., 1988). AZT is converted intracellularly to the

triphosphate form like other nucleoside analogues (Figure 2). This conversion is

accomplished via cellular thymidine kinase (Furman et al., 1986). The triphosphate of

AZT (AZT-TP) acts as an inhibitor of HIV RT and as a chain terminator. In the

phosphorylation of AZT, the rate-limiting step is the conversion of the parent drug to its

monophosphate form (Ho and Hitchcock, 1989). This conversion causes the

monophosphate and the diphosphate to accumulate within the cell.
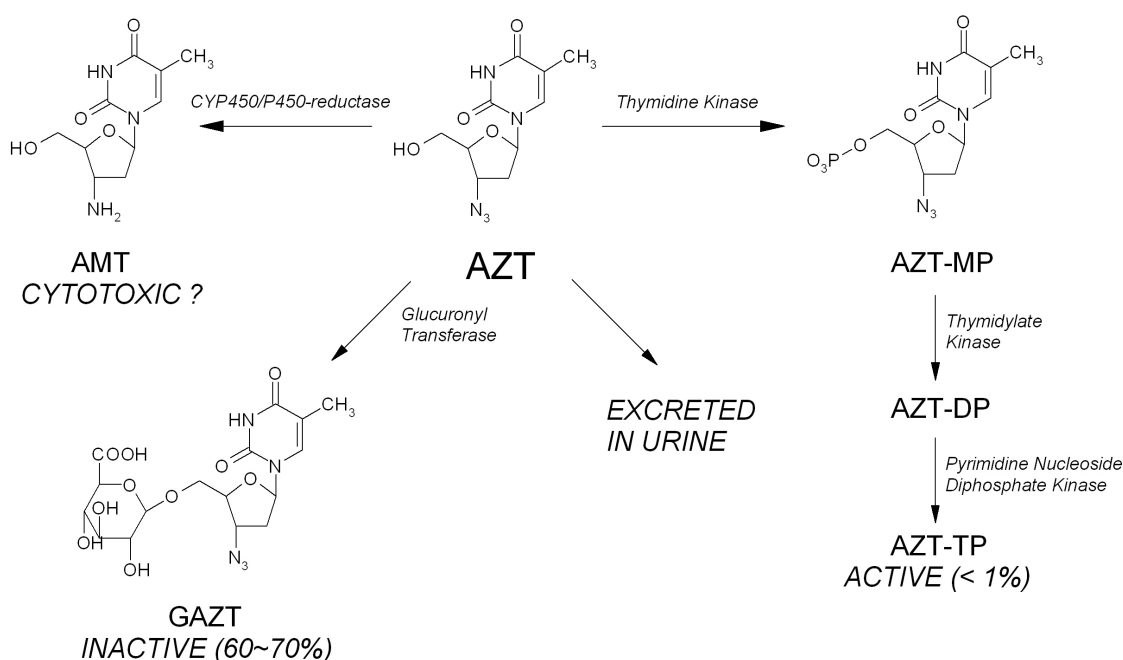
Figure 2. Diagram of metabolism of Zidovudine (AZT) including a sequential enzymatic phosphorylation steps required for activating AZT to the triphosphate moiety. Source from Veal et al., Gen. Pharmac. (1995)

Didanosine Oral bioavailability of ddI ranges from 43% to 25%, depending on whether an antacid or buffer tablet is used (Beach, 1998). Didanosine is very unstable in the stomach because of its' acidic condition. Commercially available formulations of ddI include a buffer solution and tablet. ddI is also given with an antacid. The latter seems to achieve the best bioavailability (Hartman et al., 1991). In addition, it is recommended that ddI be taken in the fasting state because of the high acid condition associated with eating (Hartman et al., 1990; Knupp et al., 1991). Penetration of ddI into the CSF is low, showing a CSF-to-plasma ratio of 0.21 in adults after 60 min infusion (Hartman et al., 1990). Protein binding of ddI is less than 5% (Perry and Balfour, 1996). Renal excretion is the major elimination route for ddI (Beach, 1998). It has been shown to undergo both glomerular filtration and active tubular secretion. Urinary recovery was 55% after single intravenous dose and 20% after single oral dose. Intracellularly, ddI is converted to its monophosphate (ddI-MP) via the cytosolic 5'-nucleotidase, which uses inosine monophosphate as the phosphate donor (Johnson and Fridland, 1989). Monophosphate of ddI is then converted to dideoxy adenosine monophosphate (ddA-MP) by the actions of adenylosuccinate synthetase and adenylosuccinate lyase. The ddA-MP is further phosphorylated to the level of triphosphate, which is an inhibitor of HIV RT and acts as a terminator of the viral DNA chain (Ahluwalia et al., 1987; Johnson et al., 1988).

C.   *Drug metabolism of Zidovudine and Didanosine*

Glucuronidation of AZT   AZT undergoes significant hepatic metabolism via glucuronidation. The metabolite profiles of AZT in rat and human indicated that two metabolites are identified as 5'-O-glucuronide of AZT (GAZT) and

3'-amino-3'-deoxythymidine (AMT), and GAZT is the major metabolite observed in

extracellular as well as in intracellular medium in cultured hepatocytes (Cretton et al.,

1990). However, marked quantitative differences are observed between rats and humans.

24 hr after incubation of AZT, the majority of radioactivity was recovered as unchanged

drug in rat (86% of total extracellular radioactivity). In contrast, higher proportions of

metabolites (~70% of the total extracellular radioactivity) were recovered in culture media

of human hepatocytes (Figure 3).
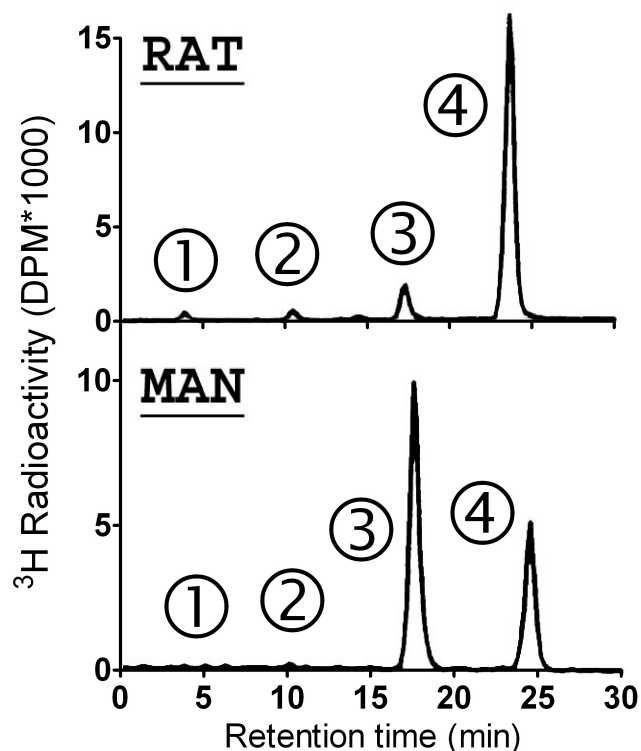
Figure 3. Reverse-phase HPLC profiles of 3H-AZT and its metabolites. Extracellular medium of cultured hepatocytes from rats and humans was analyzed after a 24-hr incubation period with 10 uM AZT. Peaks 1, 2, 3, and 4 represent, respectively, tritiated water (THO), 3'-amino-3'-deoxythymidine (AMT), 5-O-glucuronide of AZT (GAZT), and AZT (total counts applied to column ranged from 57,000 to 62,000 dpm; scale increment: 5,000 dpm). Source from Nicolas et al., Drug Metab. Dispos. (1995)

Unchanged drug represented 88% of the radioactivity excreted in urine after ^{3}H-AZT administration in rats, whereas GAZT represented 52% in human urine samples. This glucuronide was the main metabolite of AZT in both rats and humans. However, some differences are apparent between *in vivo* and *in vitro* metabolic profiles. Besides the formation of GAZT, two other metabolites were formed in humans *in vivo* (Stagg et al.,

1992), and in rat hepatocyte suspensions (Cretton and Sommadossi, 1991; Cretton et al., 1991). They were identified as 3'-amino-3'-deoxythymidine (AMT) and its glucuronide derivative (GAMT).

Phosphorolysis of ddI   Purine nucleoside phosphorylase (PNP) is suspected to be the mechanism of ddI clearance. It is reported that ddI is a good substrate for PNP in enzymatic assays (Stoeckler et al., 1980) and is rapidly degraded in cultured cells, producing hypoxanthine and phosphorylated sugar moiety (Ahluwalia et al., 1987; Weibel et al., 1994). Radiolabeled hypoxanthine appears in dog studies after treatment with 14C-labeled ddI (Kaul et al., 1993) and ddI has a short half-life of 38 min in clinical studies (Hartman et al., 1990). PNP is an omnipresent enzyme, which functions in the purine nucleoside rescue pathway. In physiological situation, the function of PNP is the phosphorolysis of inosine and guanosine nucleosides. Abbreviated models for the activation of ddI to the active antiviral and the metabolism of ddI are proposed (Ray et al., 2004)(Figure 4).
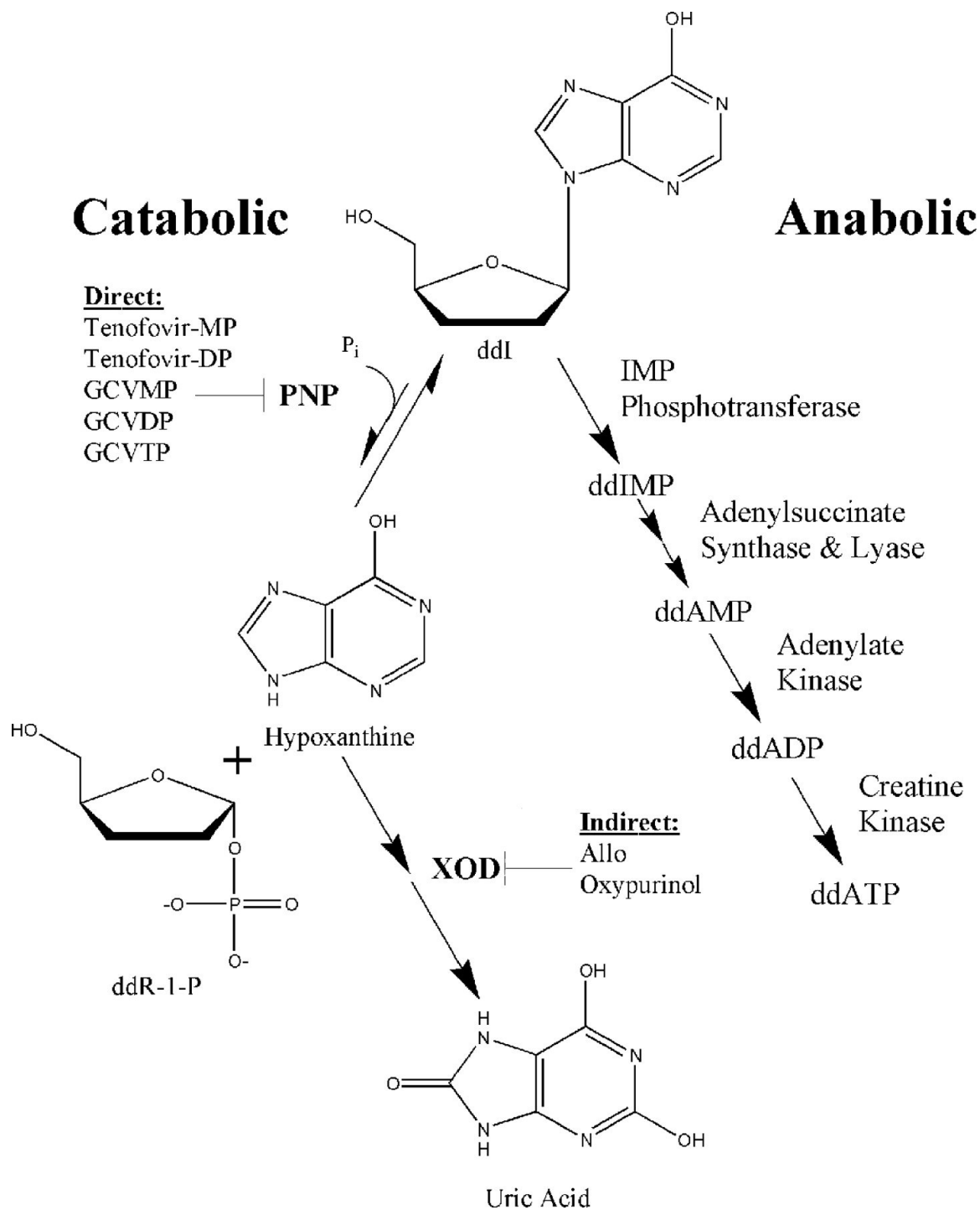
Figure 4. Abbreviated model for ddI metabolism showing both its breakdown and its activation to the active antiviral agent ddATP. The presence of products of PNP may be inhibitory because of the unfavorable equilibrium of PNP. Source from Ray et al., Antimicrob. Agents Chemother. (2004)

The highest levels of PNP activity are found in erythrocytes, granulocytes, peripheral blood lymphocytes, and kidney cells. The large proportion of blood volume occupied by erythrocytes and high PNP levels in erythrocytes make the erythrocyte a likely disposition site of ddI.

Phosphorylation of AZT and ddI   As described in previous section, the nucleoside analogues are taken up by target cells, phosphorylated to the 5'-triphosphate by cellular enzymes and incorporated into target DNA. Drug effect is determined not only by dose and the rate of elimination, but by the rate and extent of intracellular phosphorylation. This explains, in part, why plasma concentrations of nucleoside analogues have proved disappointing in predicting efficacy or toxicity. In the case of AZT phosphorylation, the process appears to be saturable and therefore increases in plasma concentration do not cause proportional increases in total phosphate concentrations. The main intracellular phosphorylated metabolite is AZT monophosphate (AZT-MP) which is explained by the fact that conversion of AZT-MP to AZT diphosphate (AZT-DP) by the enzyme thymidylate kinase is the rate determining step for the AZT intracellular pathway. AZT shares the same intracellular phosphorylating enzymes with stavudine and lamivudine. Therefore, coadministration of these drugs could result in an interaction at the phosphorylation level. Conversely, didanosine is activated by a unique pathway converting it to dideoxyadenosine triphosphate (ddA-TP) instead of dideoxyadenosine triphosphate (ddI-TP).

D.   *Influx and efflux transporters of Zidovudine and Didanosine*

Organic Anion Transporters   Influx of AZT and ddI is facilitated by numerous

transporters. The uptake of AZT and ddI is mediated by the sodium-dependent organic

anion transporter (OAT) system, which includes sodium-ketoglutarate cotransport via the

Na^+/dicarboxylate cotransporter and α-ketoglutarate/organic anion exchange via the

OAT1 (Takeda et al., 2002). During the past decade, several OATs have been cloned from

various tissues and species. OAT1 plays a primary role in the tubular active secretion of

endogenous and xenobiotic organic anions. Uptake by OAT1 is a tertiary active process,

dependent on a dicarboxylate-gradient established by co-transport of Na^+ and

dicarboxylate, a secondary active process, which is, in turn, dependent upon the

Na^+-gradient established by the primary active Na^+/K^+ ATPase (Figure 5).
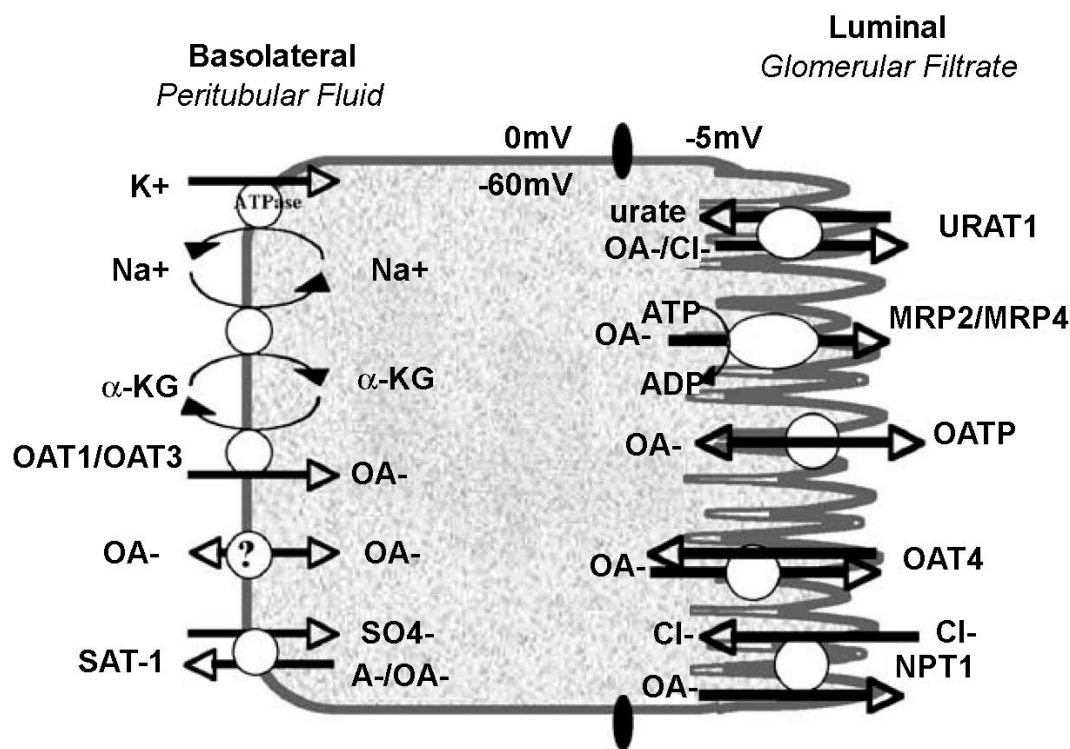
Figure 5. Basolateral and apical organic anion transporters (OATs) of the human proximal tubule. Source from Robertson et al., Pharmacol. Ther. (2006)

Nucleoside transporters Nucleoside transporters (SLC28, SLC29) can also transport NRTIs including AZT and ddI (Anderson et al., 1999; Jennings et al., 2001; Baldwin et al., 2004). There are two families of nucleoside transporters, equilibrative (ENTs, SLC29) and concentrative (CNTs, SLC28). Most cells have low-affinity ENT systems. The human SLC29 family contains four hENTs. The ENT1 and ENT2 systems are driven by the concentration gradient of nucleosides, and can mediate bi-directional nucleoside flux. A study has indicated that ddI, but not AZT, crosses the guinea-pig blood brain barrier by means of the nucleoside transporter (Gibbs et al., 2003). hENT2 transports both ddI and AZT whereas hENT1 only transports ddI (Yao et al., 2001). High affinity CNTs mediate

the flux of nucleosides coupled to the movement of sodium down its electrochemical gradient. Three have been molecularly identified (CNT1~3) and are expressed by the liver, intestine, kidney, and choroids plexus (Gray et al., 2004). CNT1 is implicated in the renal handling and intestinal absorption of AZT. CNT2 is expressed at the blood-brain barrier (BBB) and can transport ddI. hCNT3 transports both AZT and ddI. Considerable species differences exist in the tissue distribution of CNT3 in humans, mice and rats. In epithelia, CNTs are located in the apical membrane, whilst ENTs are detected in the basolateral membrane, suggesting a coordinating role of CNTs and ENTs in transepithelial nucleosides and NRTIs (Gray et al., 2004). The direction of these transporters is absorptive and the function of these transporters is not covered in the current experimental design.

Breast Cancer Resistance Protein   BCRP, a recently discovered transporter, is reported to be a transporter of AZT and ddI (Wang et al., 2004). BCRP belongs to the subfamily G of the large ABC transporter superfamily. BCRP is designated as ABCG2, the second member of subfamily G. At present, 4 members in the subfamily G such as ABCG1, ABCG2, ABCG5, and ABCG8 have been identified in human. Unlike P-gp and MRP1, which are composed of 2 repeated halves, ABCG transporters are half transporters that has a single nucleotide binding domain (NBD) and a single membrane-spanning domain (MSD) (Ross, 2000)(Figure 6).
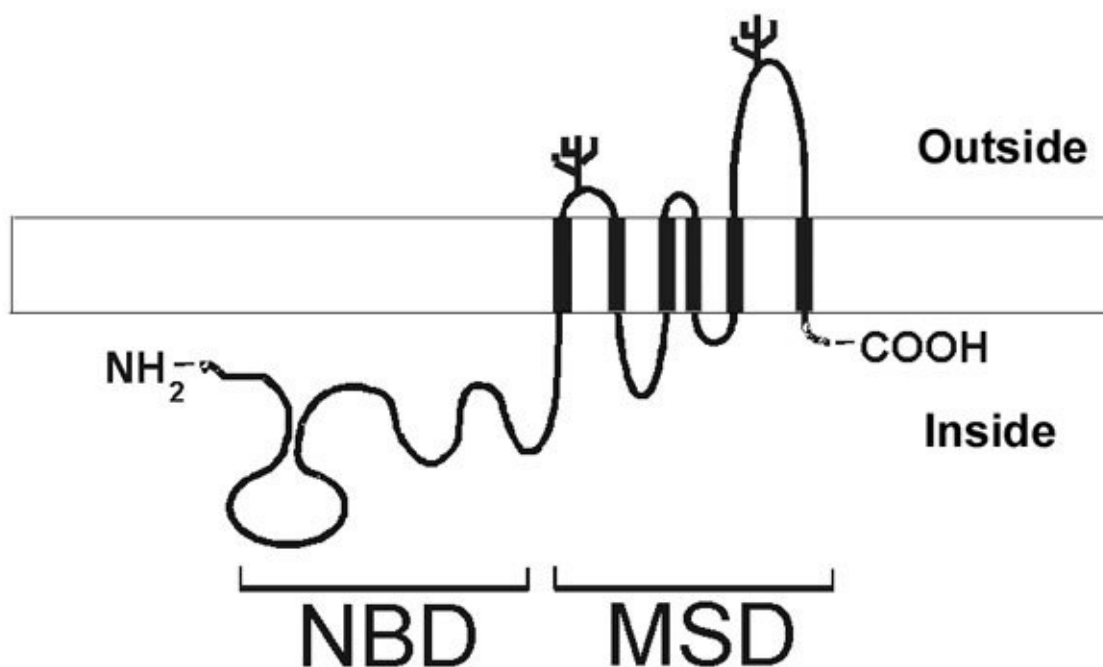
Figure 6. A membrane topology model of BCRP. BCRP contains one nucleotide binding domain (NBD) followed by one membrane-spanning domain (MSD) with 6 predicted transmembrane a-helices. Two or 3 putative N-glycosylation sites (N418, N557, or N596) are predicted to be in the extracellular loops as indicated. Source from Mao et al., AAPS J (2005)

Increasing evidence suggests that ABCG proteins may function as either homodimers or heterodimers (Graf et al., 2003; Xu et al., 2004). Another unique feature of ABCG transporters is the domain arrangement in which the NBD is followed by the MSD, whereas P-gp or MRP1 has an opposite configuration, that is, the MSD precedes the NBD. Such a unique domain configuration is not observed in other human ABC transporters than subfamily G and implies that the transport mechanisms of ABCG transporters may be different from those of other ABC proteins. It has been reported that BCRP transports several NRTIs such as AZT and ddI, but is not an efficient transporter of protease inhibitors (Allen and Schinkel, 2002; Huisman et al., 2002; Wang et al., 2004). Like P-gp,

BCRP is expressed on the apical side of polarized epithelium such as that in the gut, liver, and kidney (Schinkel and Jonker, 2003; Borst et al., 2004), and on the luminal side of the brain capillary endothelium (Maliepaard et al., 2001). This allows removal of AZT and ddI from the body by transporting them into urine, bile, or the intestine.

Multidrug resistance protein 4 Mrp4 expression is highest in the kidney in mice (Maher et al., 2005) and rats (Chen and Klaassen, 2004), and is localized to the apical membrane of proximal tubules in human kidney (van Aubel et al., 2002). Veal et al. reported that AZT-MP was secreted from many different cell types, although the efficiency of secretion varied among cells (Frick et al., 1988; Veal and Back, 1995). Secretion of AZT-MP is not due to leakage or cytotoxicity and is specific for AZT-MP, as AZT diphosphate or AZT triphosphate was not found in the extracellular medium (Frick et al., 1988). Subsequent studies by Fridland et al. confirmed that AZT-MP was effluxed (Fridland et al., 1990). It is notable that AZT-MP efflux appeared inducible as long term incubations with AZT caused an increased rate of AZT-MP efflux. Because AZT cytotoxicity is related to the uptake of AZT-MP, one could speculate that this active transport from cells is a cytoprotective mechanism (Hall et al., 1994; Tornevik et al., 1995). The ability of MRP4 to transport AZT-MP and the localization of MRP4 in kidney suggest that it may play an important role in renal clearance of AZT.

E. *RNA interference of drug transporters*

The successful launch of siRNA as a laboratory tool and therapeutic agent has been cited in more than 1000 publications to date and has led to an application to drug transporters. ATP-binding cassette (ABC) transporters were one of the earlier target candidates of

siRNA since they play a major role in cancer multidrug resistance. Here, we introduce the

in vitro and *in vivo* application of siRNA silencing of drug transporters (Table 3).

Table 3. In vitro and in vivo examples of delivery of transporter siRNA in mammals

Target	Type of siRNA	Delivery of siRNA	Selected Reference
In vitro			
P-gp	Naked siRNA	Lipid based reagent	(Wu et al., 2003)
	Vector shRNA	Stable expression	(Xu et al., 2004)
	Vector siRNA	Lipid based reagent	(Zhang et al., 2005)
	Vector shRNA	Recombinant adeno-associated virus	(Xu et al., 2005)
Mrp1	Naked siRNA	Lipid based reagent	(Lee et al., 2004)
Mrp2,3	Naked siRNA	Lipid based reagent	(Tian et al., 2004)
Bcrp	siRNA + T7 promoter	Lipid based reagent	(Ee et al., 2004)
	Vector siRNA	Adenovirus	(Li et al., 2005b)
	Naked siRNA	Lipid based reagent	(Hori et al., 2005)
In vivo			
P-gp	Modified siRNA	Simple IV injection	(Su et al., 2005)
	Vector shRNA	Hydrodynamic IV injection	(Pichler et al., 2005)
	Naked siRNA	Hydrodynamic IV injection	(Matsui et al., 2005)

In vitro applications

The rate limiting step in siRNA-mediated silencing is the delivery of these small molecules

into the desired cells. Even though siRNA is gene specific, targeted delivery to cells of

interest is important since many transporters are expressed in numerous cell types. This is

not a major concern in the *in vitro* setting because cells are studied in isolation. However,

in vivo use of siRNA becomes a "drug" delivery problem that is quite daunting and similar

in scope to gene and antisense oligonucleotide delivery. The delivery of transporter-

targeted siRNAs is achieved by electroporation or transfection of naked siRNA or by gene

transfer using a vector. Among the 70 articles published to date that relate to siRNA and

transporters, most of them have targeted P-gp as it relates to drug disposition or cancer

chemoresistance. For functional transport analysis, a P-gp knock-down Caco-2 cell line

has been developed (Watanabe et al., 2005). All five MDR1 siRNAs (A1 ~ B2) based on

the guideline for designing effective sequence specifically ablated the MDR1 mRNA and

the uptake of digoxin, p-gp substrate was significantly increased in the siRNA-transfected

cells (Figure 7).

The transcellular transport of typical p-gp substrates was evaluated using two hairpin

siRNAs expressing A2 and B2 sequences (A2-2 and B2-2)(Figure 8). Two MDR1 hairpin

siRNAs lowered the basal-to-apical directional flux of the substrates from 2 ~ 6 times

higher levels to the equivalent levels to the opposite directional fluxes .
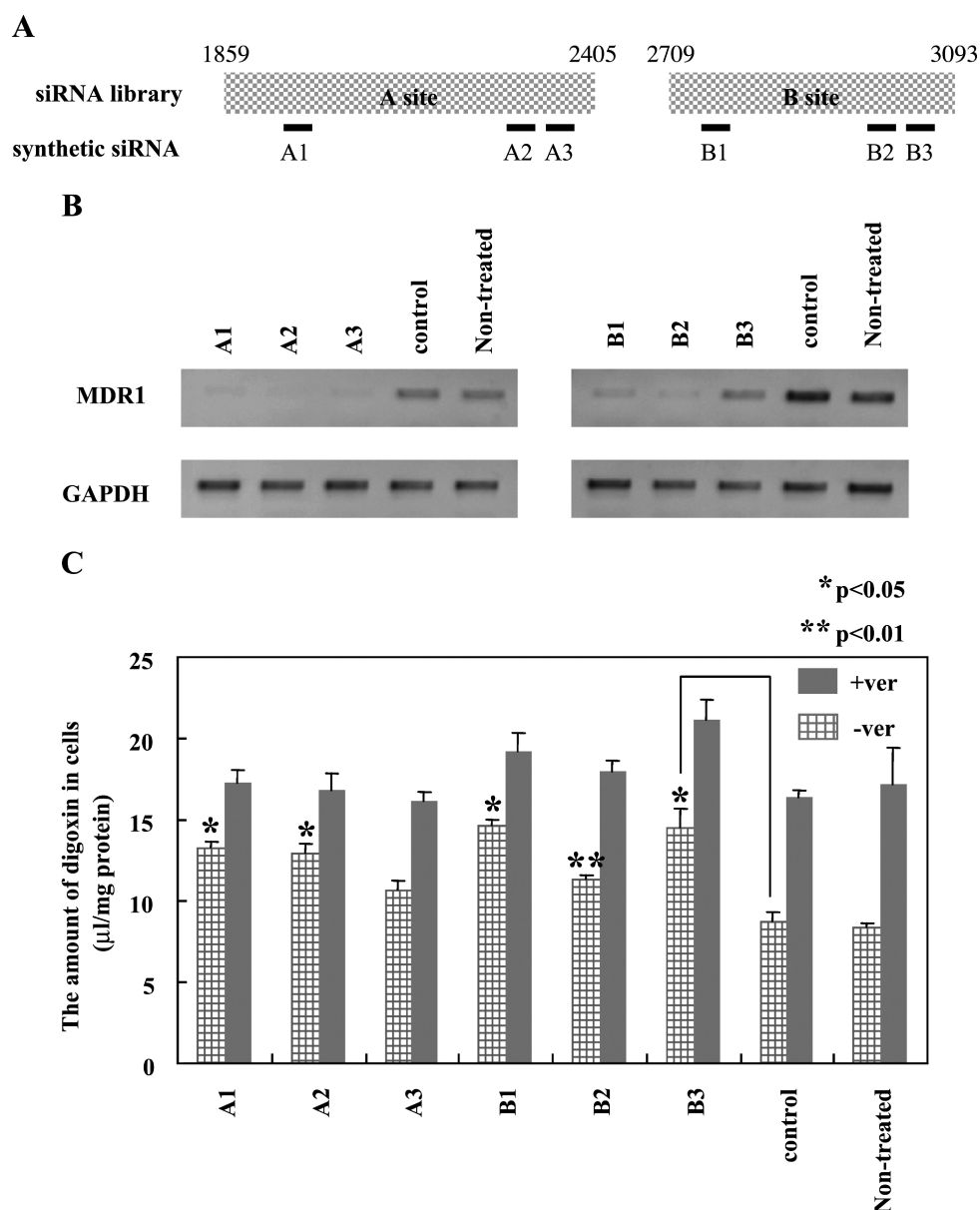
Figure 7. Effects of MDR1 siRNAs in Caco-2 cells. (A) The sequences of the synthetic siRNAs within the sites of siRNA libraries. (B) The level of MDR1 mRNA in the siRNA transfected Caco-2 cells. After transfection for 48 h, GAPDH mRNA (internal control) and MDR1 mRNA were measured by RT-PCR. (C) Accumulation study of the siRNA transfected Caco-2 cells. After transfection for 4 days, the intracellular amount of [3H]digoxin (4 nM), with or without verapamil (100 uM), was examined. Control, control siRNA; non-treated, medium only. Adapted from Pharm Res (2005) by Watanabe et al.
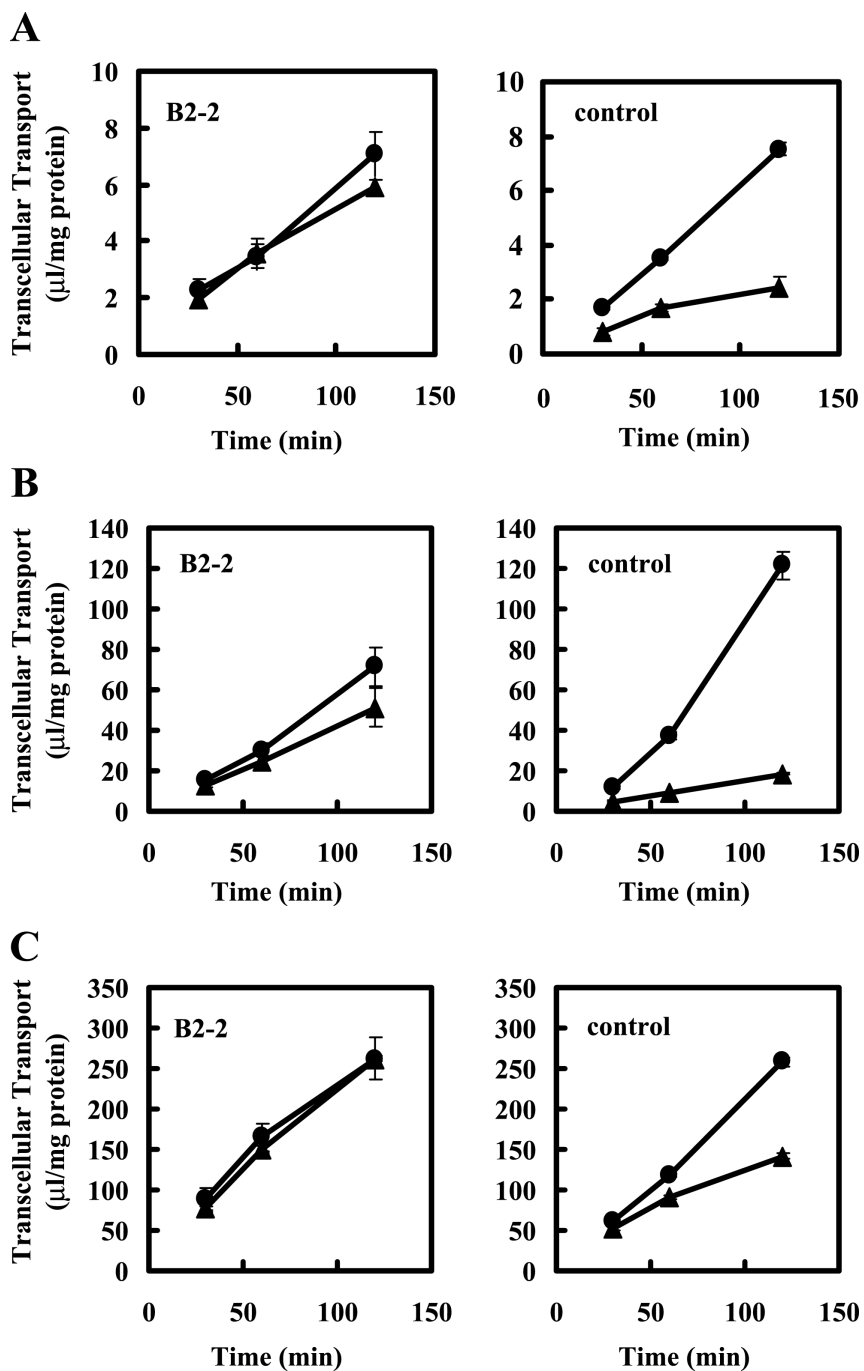
Figure 8. Transcellular transport study of MDR1 substrates. Time profiles for the transcellular transport across the B2-2 clone and the control cells. (A) Vincristine (435 nM). (B) Rhodamine 123 (10 uM). (C) Daunomycin (62.5 nM). The circles and the triangle represent the transcellular transport in the apical-to-basal and the basal-to-apical directions, respectively. Adapted from Pharm Res (2005) by Watanabe et al.

In general, preparing a stable transfectant is a time consuming process, making transient

transfection of naked siRNA and siRNA-plasmid a more favorable option. More recently,

BCRP has become a new target for researchers performing transient transfection with

siRNA (Hori et al., 2005; Li et al., 2005) due to its importance in brain uptake, oral

absorption, and multidrug resistance.

In vivo applications

In contrast to the great interest and progress of *in vitro* siRNA transfection, there are few

reports of *in vivo* use of siRNA. This, of course, is related to the central issue of siRNA

delivery. There are two key siRNA properties that make its *in vivo* delivery difficult. First,

siRNA is rapidly degraded by both extracellular and intracellular nucleases. Chemical

modification increases its stability, also potentially increasing the overall cellular uptake of

siRNA as well. A proprietary stabilized MDR1 siRNA (siSTABLE, Dharmacon) was

recently shown to ablate the expression of P-gp in MCF-7 cancers inoculated into SCID

mice (Su et al., 2005). The second factor that challenges the *in vivo* delivery of siRNA is

poor intrinsic membrane permeability. This is attributed to physicochemical properties

such as the large polar surface area and molecular size of siRNA molecules. A method that

has been used in the preclinical setting with some success involves the hydrodynamic

intravenous injection of naked siRNA or hairpin siRNA. This method has enhanced

siRNA delivery (Lewis et al., 2002; McCaffrey et al., 2002). The technique of

hydrodynamic injection involves injecting a large volume (> 2 ml / mouse) of siRNA

solution over short period of time (< 10 sec). Mouse mdr1a/1b and human MDR1 gene has

been successfully knocked down by using the hydrodynamic injection of the

corresponding siRNA and/or hairpin siRNA (Matsui et al., 2005; Pichler et al., 2005).

Selection of a target gene specific siRNA is critical for proper *in vivo* transfection.

Delivery is still a problem especially in clinical applications since current delivery methods

such as hydrodynamic iv infusion and electroporation can not be safely applied to human

subjects.

III. THE CONTRIBUTION OF EFFLUX TRANSPORTERS SUCH AS BCRP AND MRPS ON CELLULAL EFFLUX PROFILE OF AZT AND DDI

A. *Introduction*

In most cases drug-resistant HIV strains resulting from genetic mutations discovered in

patients treated with antiviral therapy (Berger et al., 1998) explain the mechanisms of drug

resistance. However, some patients show signs of drug resistance even in the absence of

drug-resistant viral strains (Plotkin et al., 1985; Groschel et al., 1997) suggesting

alternative mechanisms of resistance. The alteration of the systemic disposition of

antiviral drugs and the presence of pharmacokinetic sanctuary sites limiting the

accessibility to antiviral agents have been considered as alternative or additional

mechanisms of resistance. Urinary excretion is one of the major dispositional pathways for

AZT and ddI and more than two thirds of AZT total clearance is explained by renal

clearance in mice (Doshi et al., 1989). In the clinical application of AZT, 14% and 76% of

an oral dose is recovered through urinary excretion as parent and its' metabolites,

respectively. Urinary recoveries of unchanged ddI after intravenous and oral

administration are 55% and 18%, respectively. The renal clearances of these drugs are 2 ~

3 times higher than the glomerular filtration rate (GFR) suggesting active tubular secretion

of both drugs. Generally, influx of anionic drugs into kidney tubular cells is predominantly

mediated by OAT transporters (Enomoto et al., 2002). This is consistent with the

observations that an organic anion reduces the renal clearance of AZT *in vivo* (Takeda et

al., 2002). However, the plasma to tissue ratio in the kidney is around two fold, supporting

the existence of efflux transporters in the brush border membrane. Renal ABC transporters

play an important role as drug and metabolite efflux transporters. For all NRTIs including

AZT and ddI, it is important to consider intracellular drug exposures as NRTI triphosphate

concentrations because these are the moieties responsible for antiviral activity and toxicity

(Anderson et al., 2004).

Clinical pharmacokinetic drug-drug interactions give an indirect indication of the

metabolism or efflux of drugs. One example is the interaction of AZT with probenecid.

Coadministration of probenecid increased plasma half-life and maximum plasma

concentration of AZT significantly, and it also doubled the AUC of AZT (de Miranda et

al., 1989; Kornhauser et al., 1989). Probenecid is known to inhibit both AZT metabolism

and the renal elimination of GAZT (Hedaya et al., 1990).

While P-glycoprotein (p-gp) has been proposed as a major efflux transporter for AZT and

ddI, there is evidence that AZT and ddI are not p-gp substrates (Leung and Bendayan,

1999). Wang et al. found that the cytotoxicity of AZT and ddI was reduced in

drug-resistant MT-4/DOX500 (BCRP-overexpressing cells) compared to the parental

MT-4 cells, suggesting that AZT and ddI are BCRP substrates (Wang et al., 2004).   Gene

and protein expression levels of BCRP are measured in our cellular and animal system

using RT-PCR and Western blot. The efflux function of BCRP was investigated using

cellular uptake and efflux studies. Induction of BCRP is regulated by aryl hydrocarbon

receptor (AhR, (Ebert et al., 2005)) and pregnane X receptor (PXR, (Anapolsky et al., 2006)). The cellular model of bcrp1-induction was developed to magnify the role of bcrp1 in the efflux of AZT and ddI. Members of the MRP family are also interesting ABC transporters in the study of AZT and ddI. Two members of the family, MRP4 and MRP5, appear to transport AZT (Schuetz et al., 1999; Wijnholds et al., 2000), while BCRP is responsible for the efflux of both AZT and ddI. The role of MRP4 in NRTI drug resistance was discovered when CEM cells exposed to AZT developed a drug resistance in absence of drug resistant virus (Schuetz et al., 1999). They found that AZT-MP was pumped out of cells in an energy (ATP) dependent manner caused by increased expression of MRP4. Our current work suggested that ddI or its metabolite might also be a substrate of the MRP family. Wijnholds et al. has shown that MRP5 also appears to be an NRTI pump (Wijnholds et al., 2000). Wang et al. found that the cytotoxicity of AZT and ddI was reduced in drug-resistant MT-4/DOX500 (BCRP-overexpressing cells) compared to the parental MT-4 cells, suggesting that AZT and ddI are BCRP substrates (Wang et al., 2003). The objective of this investigation is to identify the role of each efflux transporter on the cellular efflux profile of AZT and ddI. To elucidate the role of each transporter on the cellular efflux of AZT and ddI in mice, intracellular and extracellular concentrations of AZT and ddI were monitored in mouse macrophage 774.1 cells and human embryonic kidney HEK-R482 cells.

B. *Materials and Methods*

1. Materials

AZT and ddI were generously supplied by GlaxoSmithKline (London, UK) and

Bristol-Myers Squibb (New York, NY), respectively. SuperScript First-Strand Synthesis

System for RT-PCR, Platinum® Taq DNA Polymerase, Trizol, Benchmark Protein

Ladder, Opti-MEM I Reduced Serum Medium, and DMEM were purchased from

Invitrogen (Carlsbad, CA). Ready Gel Precast Gels and Laemmli sample buffer were

obtained from Bio-Rad (Hercules, CA). T-PER, BCA protein assay kit, SuperSignal West

Femto Maximum Sensitivity Substrate, and Restore Western Blot Stripping Buffer were

obtained from Pierce (Rockford, IL). All other chemicals were purchased from Sigma

Chemical Co. (St. Louis, MO) or Fisher Scientific (Fair Lawn, NJ) and used as received.

Primary and secondary antibodies were obtained from Kamiya Biomedical (Seattle, WA)

or Santa Cruz Biotechnology (Santa Cruz, CA).

2.   Measurement of genetic and protein expression level

RT-PCR   Total RNA was extracted from cells and animal tissues using TRIZOL reagent

(Invitrogen). Total amount of RNA was calculated by measuring the OD260 of 100x

diluted RNA solution. First-strand reaction and PCR amplification were performed

according to the manufacturer's protocol with modification. The solution containing RNA

sample (1 ~ 2 µg), random hexamers (50 ng/µl), and dNTP mixture (10 mM) was

incubated at 65°C for 5 min, and was mixed into a reaction tube containing 10x RT buffer,

$MgCl_2$ (25 mM), DTT (0.1 M), and RNaseOUT. Fifty units of SuperScript II RT

(Invitrogen) were added per 19 µl, and the first-strand mixture was incubated at 25°C for

10 min, 42°C for 50 min, 70°C for 15 min. To amplify a specific gene from the sample,

oligonucleotide primers were designed using PrimerQuest (Integrated DNA technologies,

Coralville, IA). Amplification reactions of first strand DNA were performed with 10x

PCR buffer, MgCl$_2$ (50 mM), Taq DNA polymerase, dNTP mixture (10 mM), and primers

mixture with the following temperature protocol: 94°C for 3 min to stabilize the sample,

30 cycles (94°C for 30 sec, 60°C for 30 sec, 72°C for 1 min), 72°C for 10 min.

Electrophoresis was performed by the procedure of Meyers et al. (Meyers et al., 1976) on

agarose gels (1%). DNA migrates toward the anode in TAE buffer at 100 V for 1 hr. After

electrophoresis, DNA bands were detected by UV light. Sizes of PCR products were

determined by comparing the migration of the sample in gels to that of a standard DNA

ladder (Invitrogen).

WESTERN BLOTTING   Cells and tissues were lysed using cell lysis buffer (0.1 M

Tris-HCl, 5% Triton X-100, 1.5 M NaCl, 10% SDS, and 0.1 M EDTA) with protease

inhibitors (Sigma). Lysates of cells and tissues were centrifuged for 15 min at 14,000 g at

4°C. The supernatants were transferred to a fresh tube and diluted with sample buffer (x2

volume) containing 5% mercaptoethanol. Samples (50 µg of protein) were separated

under denaturing conditions on a Ready Gel (10% Tris-HCl) precast gel cassette

(Biorad), using TG running buffers supplemented with 0.1% sodium dodecyl sulfate (1 hr

at 4°C at 150 V). Separated proteins were transferred on a PVDF membrane (Novel) for 30

min at 100 V, in a TG transfer buffer with 20% methanol. The membranes were blocked in

5% nonfat milk-0.1% Tween 20 for at least 1 hr and then incubated for at least 2 hr with

gentle shaking and at room temperature with Anti-BCRP primary antibody (Kamiya) after

x5,000 dilution in the blocking buffer. The membranes were then exposed to the

secondary antibody (anti-rat HRP-conjugated IgG, Santa Cruz). Reactive bands were

detected by chemiluminescence using a SuperSignal kit (Pierce). Molecular weights were estimated by comigration with a Benchmark protein ladder (Invitrogen). Positive identification of the BCRP band was made by analyzing in parallel lysates from HEK-R482 cells, BCRP-overexpressing cell.

3.   Electroporation-silencing of specific gene expression

Predesigned siRNAs (siBCRP and siMRP1~4) were purchased from Dharmacon (Lafayette, CO). For cell types proving to be recalcitrant to lipofection-based protocols, electroporation can be a valuable alternative. Electroporation involved applying an electric field pulse to induce the formation of micro-sized pores in the cell's plasma membrane, which then allow the siRNA to cross the membrane. Under specific pulse conditions, the pores resealed quickly and the electroporated cells recovered and resumed growth. A significant advantage of electroporation is that this method is not dependent on cell division, and RNAi-induced mRNA reduction can be detected just a few hours after delivery.

While most of electroporation protocols were developed for delivering plasmid DNA to cell nuclei, siRNAs need to be delivered only into the cytoplasm. Therefore, milder electroporation conditions can be used to minimize cell mortality while ensuring high efficiency of siRNA delivery. Human embryonic kidney HEK-R482 cells and murine macrophage J774.2 cell lines were used. For induction of bcrp1, J774.2 cells were treated with oltipraz and 2-acetylaminofluorene for 2~5 days in 6-well plate. The specific protocol for siBCRP transfection was optimized and is detailed below:

The cells were washed with 10 ml PBS (Phosphate Buffer Saline, pH 7.4) and harvested with a scraper in 10 ml DMEM. The cells were transferred to a centrifuge tube and spun at 1,200 rpm for 2.5 min to pellet the cell. The cells were resuspended in Opti-MEM I (Invitrogen) at a density of 2×10^6 cells/ml. In an electroporation cuvette (4 mm gap), 0.5 ml of the cell suspension was combined with 5 μl of siRNA (final concentration = 200 nM, amount = 1.2 μg), and then the cells were electroporated with ECM830 Electroporator using four 1 ms pulses with a pulse interval of 400 ms.

Electroporation Settings	
Voltage: 500 V (LV mode)	Interval: 400 ms
P. Length: 1 ms	Cuvette gap: 4 mm
# Pulses: 4	Field strength: 1.25 kV/cm

After electroporation, the cells were allowed to recover at 37°C for 10 min and then they were suspended in 2 ml of pre-warmed growth media. The cells were then plated in 6-well plates and incubated in MEM or DMEM supplemented with 10% fetal bovine serum in 5% CO_2 for 24 ~ 72 hr to activate the RNAi pathway.

4.   Cellular uptake and efflux

All experiments were performed with HEK-R482, bcrp-transfected human embryonic kidney cells and J774.1 and J774.2, mouse macrophage cells, grown as monolayers in MEM or DMEM supplemented with 10% fetal bovine serum in 5% CO_2. Cultures were initiated at a density of ca. 5×10^4 cells per cm^2 and used after 2 ~ 3 days of culture upon reaching confluence. For critical determinations, the amount of protein was assessed at the

end of the experiments by measuring absorbance at 570 nm with a BCA protein assay kit (Pierce).

Uptake and efflux assays. After 20 min preincubation with HBSS buffer, cells were treated with 3H-AZT or 3H-ddI with/without transporter inhibitors in 0.5 ml HBSS. At 30 ~ 120 min after incubation, cell monolayers were washed three times with ice-cold phosphate buffer and lysed overnight with 200 µl of 1 N NaOH. The amount of cell-associated AZT or ddI was either analyzed by β-scintillation counting or High Performance Liquid Chromatography (HPLC) analysis as described in the next section. For the efflux study, cells were incubated for 60 ~ 120 min with inhibitors and washed three times with ice-cold PBS. Drug-free media with/without inhibitors were added to each well, and extracellular drug concentrations were measured at 3, 10, 30, and 60 min. Intracellular uptake in efflux study was calculated by summing up the amounts at each time point and the remaining amount in the cell at the end of the experiments. Intracellular uptake in uptake study was calculated by measuring the amount in the cell at specified time point. The cell content of AZT was then expressed by either reference to the total cell protein content or an absolute amount (pmol) per cellular volume. All assays were performed with 24 well plates in triplicates.

Statistical analyses and curve fittings. All the statistical analyses and curve fittings were performed using Graph Pad Prism software (Graph Pad software, San Diego, CA). Data is presented as mean ± SD. Dunnett's multiple comparison test after ANOVA was used to compare the statistical significance of differences between experimental groups and statistical significance was determined at the level of $P=0.05$.

C.   Results

1.   Expression and silencing of BCRP in human and murine cell lines

hBCRP-transfected human embryonic kidney cells (HEK-R482) were used as an *in vitro* model human cell system. We have also used naturally bcrp-expressing mouse macrophage cells (J774) as a model *in vitro* murine cell system. The gene expression level of bcrp and mrps was measured by RT-PCR and protein level of bcrp was determined using Western blot analysis (Figure 9). RNA interference (RNAi) is a sequence-specific gene silencing method using small interfering RNA (siRNA). In our *in vitro* cellular system, RNAi allows us to evaluate the role of specific transporters in the influx and efflux of AZT and ddI. The silencing of BCRP was accomplished by transfecting synthetic siRNA (21 base pairs) using an electroporation method. Three different siRNA duplexes were synthesized by Ambion, Dharmacon (mixture of four different sequences), and Qiagen and the silencing potency of each siRNA was compared in J774 cells (Figure 10). The time dependency of the reduction in expression level of bcrp in J774.1 and J774.2 cells was monitored at day 1 and day 2 after siBCRP transfection. J774 cells were electroporated with 100 pmol of abcg2 siRNAs. Total protein was extracted from the cells and Western blot analysis was performed. The untreated and electroporated treated groups without siRNA were used as controls (Figure 11). Function of the expressed bcrp was verified by monitoring the relative intracellular uptake of topotecan, a known bcrp substrate, in J774.1 cells. J774.1 cells were electroporated with 100 pmol of abcg2 siRNAs. One day later, relative uptake of topotecan was measured 20 min after incubation of J774.1 and J774.2 cells with 10 µM topotecan alone or with topotecan plus 100 µM novobiocin (NOV) or 1 µM GF120918 (GG918)(Figure 12).
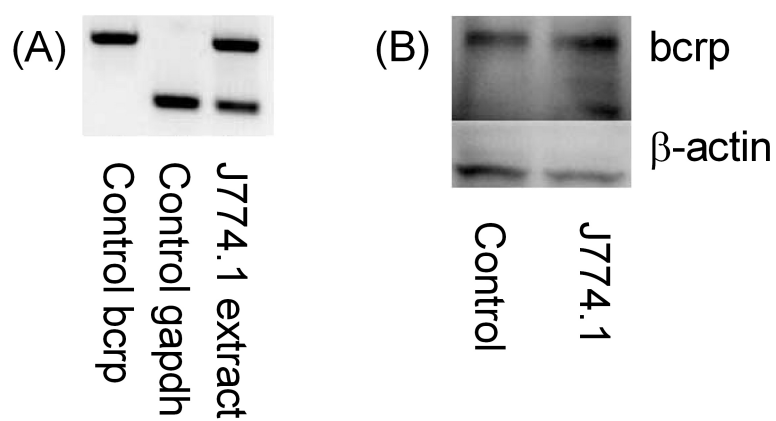
Figure 9. Representative (A) agarose gel from RT-PCR and (B) Western blot of bcrp level in J774.1 cell extracts
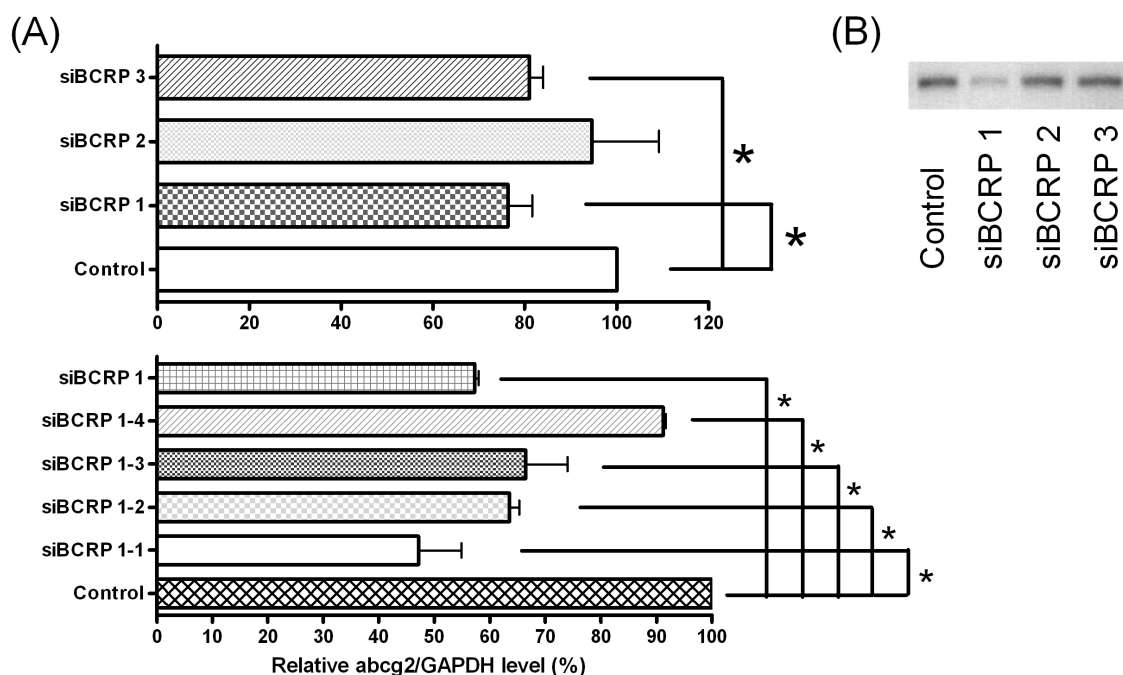
Figure 10. Effect of siRNA on abcg2 mRNA expression in murine macrophage cells. J774.1 and J774.2 cells were electroporated with 100 pmol of abcg2 siRNAs targeting various regions of the abcg2 gene. Electroporation without siRNA was used as control. Twenty-four hours later, total RNA was extracted from the cells and semi-quantitative RT-PCR was performed. (A) Relative bcrp/gapdh level (%) and (B) Representative agarose gel (*: p < 0.05, n = 2)
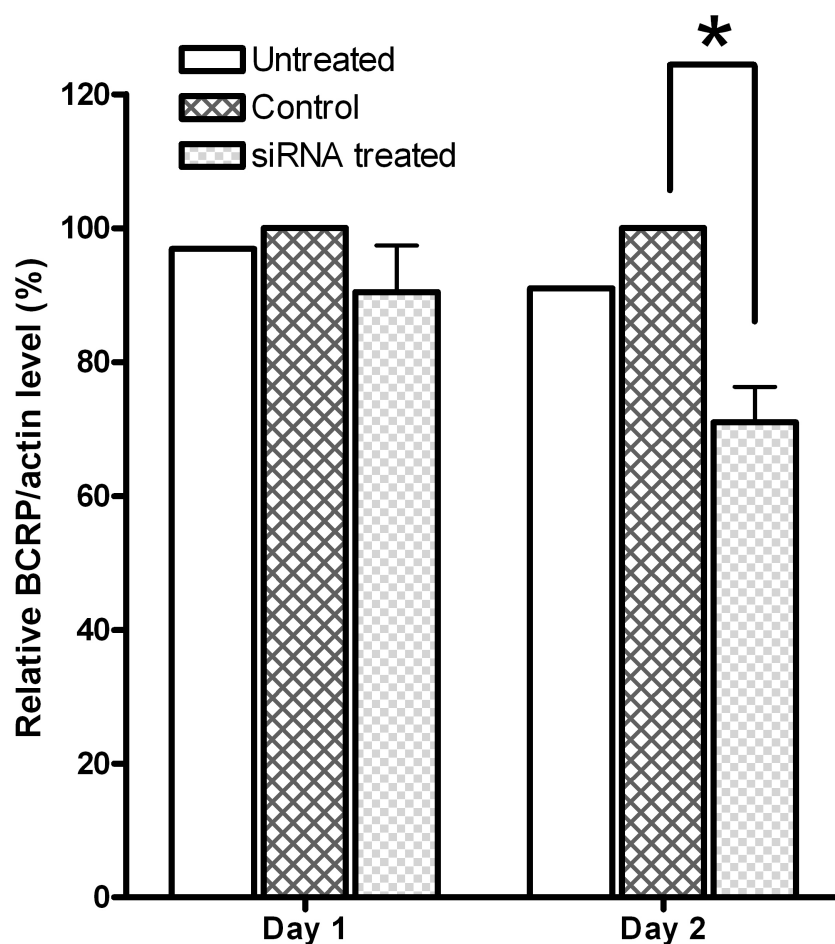
Figure 11. Time dependency of siRNA on abcg2 mRNA expression in murine macrophage cells. J774.1 and J774.2 cells were electroporated with 100 pmol of abcg2 siRNAs targeting various regions of the abcg2 gene. Electroporation without siRNA was used as control. One or two days later, protein was extracted from the cells and Western blot was performed (*: p < 0.05, n = 2)
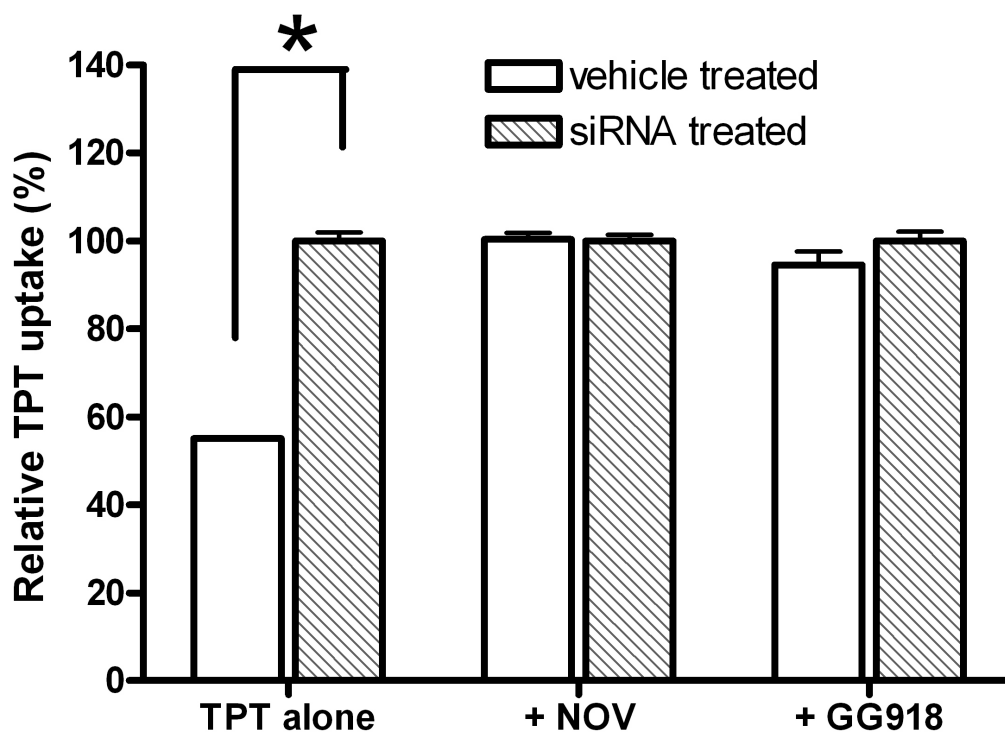
Figure 12. Effect of siBCRP on TPT uptake. Cellular uptake of TPT (10 uM) into J774.1 cells after 20 min incubation with/without GG918 (1 uM), or NOV (100 uM). J774.1 cells were electroporated one day before the uptake study with 100 pmol of bcrp1 siRNAs (*: p < 0.05, n = 3)

2.   Uptake and efflux of AZT and ddI in human and murine cell lines

AZT and ddI were reported to be BCRP substrates (Wang et al., 2004). We verified and investigated the involvement of BCRP in the efflux of AZT and ddI using an established *in vitro* cell model. Chemical inhibitors and siRNA silencing of BCRP were used to suppress BCRP activity.

Effect of BCRP inhibitors in HEK-R482 and J774.2 cells.

The influence of known BCRP inhibitors such as fumitremorgin C (FTC), GF-120918 (GG918), and novobiocin (NOV) on the cellular uptake of AZT and ddI in HEK-R482 and

J774.2 cells were compared in Figure 13. The results demonstrate a significant increase in

AZT uptake due to FTC coincubation (from 13.5 ± 0.8 to 24.5 ± 1.8 pmol/ mg protein in

HEK-R482 and from 1.66 ± 0.25 to 2.91 ± 0.56 pmol/ mg protein in J774.2). Uptake of ddI

increased by the addition of FTC (from 0.99 ± 0.05 to 1.45 ± 0.03 pmol/ mg protein) and, to

a lesser extent, by GG918 (1.31 ± 0.07 pmol/ mg protein) in HEK-R482, whereas J774.2

cells were insensitive to all of the applied BCRP inhibitors including FTC. Currently there

is not sufficient evidence to suggest why ddI uptake is not enhanced in J774.2 cells in the

presence of BCRP inhibitors. We only suspect that there is a species difference in substrate

specificity between human and murine BCRP. This phenomenon is very similar to our

previous experience with two anticancer agents, topotecan (TPT) and SN-38. Even though

both TPT and SN-38 were well known human BCRP substrates, only TPT uptake was

sensitive to GG918 (1 µM) and NOV (100 µM) in our experiments (data not shown). This

suggests that ddI is a BCRP substrate only in humans.
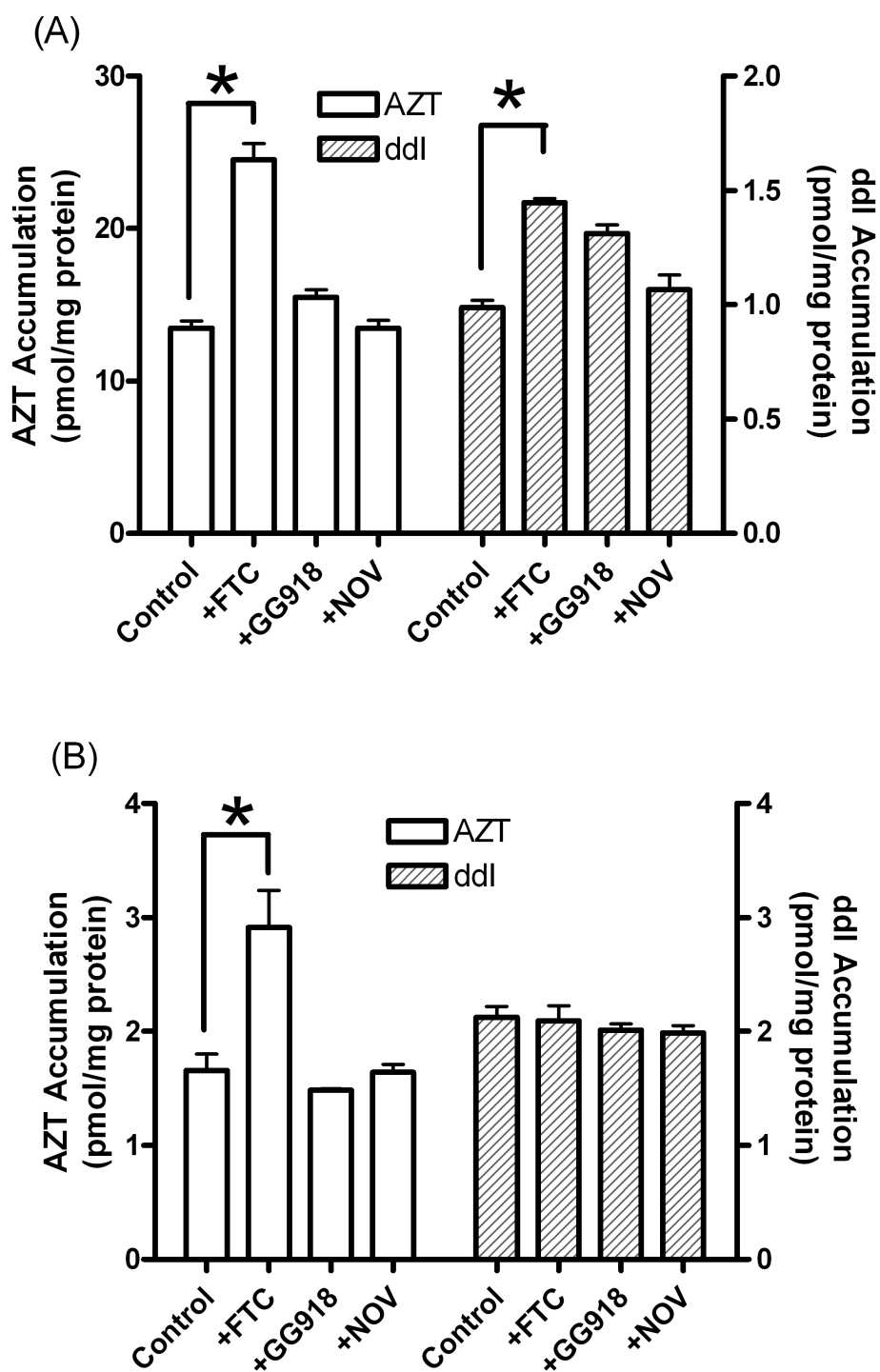
Figure 13. Effect of FTC, GG918, and NOV on 3H-AZT and 3H-ddI uptake. Cellular uptake of 3H-AZT and 3H-ddI (1 uM) into (A) HEK-R482 cells and (B) J774.2 cells after 30 min incubation with/without 10 uM FTC, 1 uM GG918, or 10 uM NOV (*: p < 0.05, n = 3)

Effect of FTC in hBCRP over-expressed cells

The effect of FTC on the uptake of AZT and ddI could be attributed to several mechanisms. For example, FTC might alter the activities of other ABC transporters, or phase I, phase II, or phosphorylating enzymes. HEK-R482 cells are stably transfected human embryonic kidney cells (HEK-293) using PC DNA 3.1 vector (Invitrogen) containing full-length wild-type BCRP whereas HEK-Mock cell is transfected with the control PC DNA 3.1 vector (Morisaki et al., 2005). The comparison between HEK-Mock and HEK-R482 should confirm the role of BCRP in the transport of the two NRTIs (Figure 14). AZT efflux in HEK-Mock was not affected by the addition of FTC, but the efflux rate of AZT in HEK-R482 was faster than in HEK-Mock (k = 0.016 ± 0.001 vs. 0.007 ± 0.001 min^{-1}, $r^2 \geq$ 0.999) and the addition of FTC eliminates the difference, making the efflux profile in HEK-R482 close to the profile in HEK-Mock (k = 0.011 ± 0.001 vs. 0.007 ± 0.001 min^{-1}, $r^2 \geq 0.999$). This trend became more clear for ddI efflux in HEK cells (k = 0.012 ± 0.003 min^{-1} for Mock control, 0.010 ± 0.003 min^{-1} for Mock w/ FTC, 0.036 ± 0.003 min^{-1} for R482 control, and 0.012 ± 0.002 min^{-1}, for R482 w/ FTC, $r^2 \geq 0.99$).
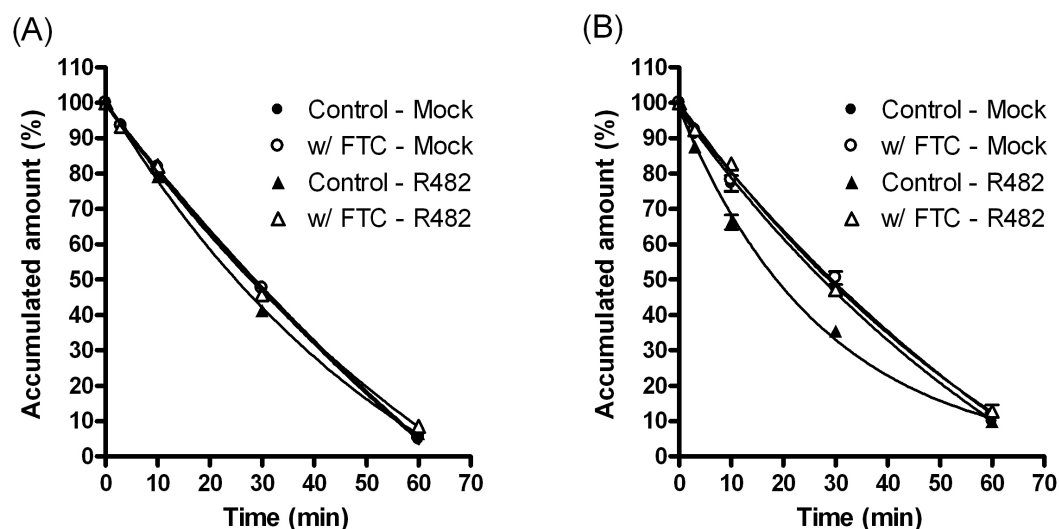
Figure 14. Effect of FTC on the efflux kinetics of (A) 3H-AZT and (B) 3H-ddI in HEK-Mock and HEK-R482 cells. HEK-Mock and HEK-R482 were incubated in a drug-free medium with/without FTC (5 uM) for 60 min after 90 min coincubation of 3H-AZT and 3H-ddI (1 uM) with/without FTC (n = 3)

Effect of siBCRP and siMRPs

The effect of BCRP silencing siRNA was tested in human HEK-R482 cells (Figure 15) and in murine J774.2 cells (Figure 16). The results demonstrated an increase in AZT and ddI uptake in HEK-R482 by silencing BCRP (from 2.06 ± 0.32 to 5.21 ± 0.48 pmol AZT/ well and from 0.15 ± 0.05 to 0.22 ± 0.02 pmol ddI/ well). J774.2 cells were insensitive to bcrp1 silencing attempts in both uptake and efflux of AZT and ddI. ddI results were consistent with our previous results of bcrp1 inhibition by FTC, GG918, and NOV, while AZT results were somewhat unexpected because previous results showed that AZT accumulation increased in the presence of FTC. Considering high specificity of siBCRP mediated silencing, increased uptake of AZT by FTC coincubation observed in Figure 14 might be caused by off-target inhibition of FTC.   In HEK-R482, the efflux rate of AZT was reduced

by applying BCRP silencing as compared to the control group (k = 0.099 ± 0.005 vs. 0.075 ± 0.008 min^{-1}, r^2 ≥ 0.99). Similar results were observed with ddI in HEK-R482. Further experiments are needed to resolve this substrate specificity issue. Based on the results presented in the previous section, Bcrp-mediated efflux alone is not sufficient to explain the differences between the intracellular uptake and efflux of AZT and ddI. We used a series of conditions to demonstrate the role of metabolism and transporters other than bcrp in human and murine cells; depletion of ATP, coincubation with thymidine kinase inhibitors, and coincubation with MK-571, an MRP inhibitor. The effect of siRNAs silencing MRP1~4 were tested in human HEK-R482 cells (Figure 17, Figure 18). The data demonstrated an increase in AZT uptake by silencing MRP3 and MRP4 (from 0.22 ± 0.01 to 0.65 ± 0.02 and 0.47 ± 0.04 pmol AZT/ well, respectively) and an increase in ddI uptake by silencing MRP1 (from 0.031 ± 0.002 to 0.038 ± 0.004 pmol ddI/ well).
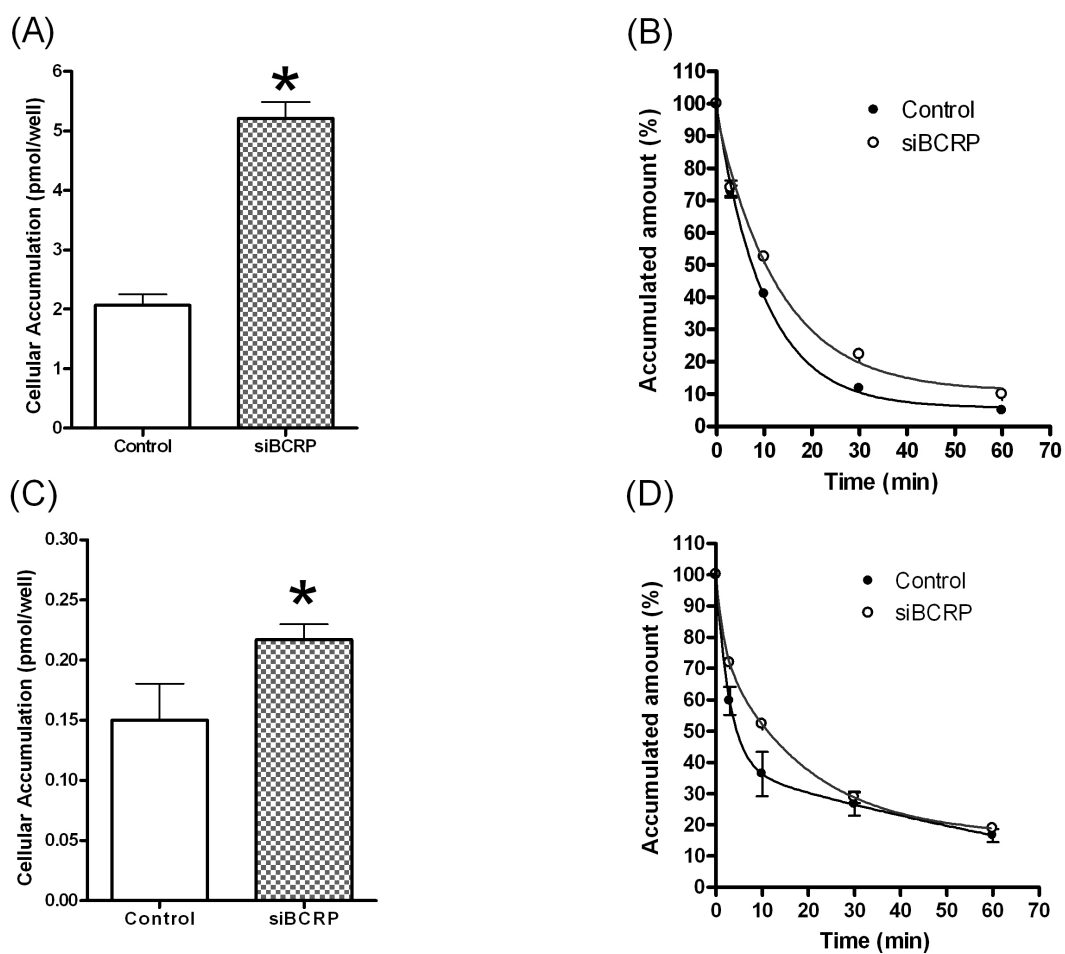
Figure 15. Effect of siBCRP on the uptake and efflux of AZT and ddI. Cellular uptake of (A) 3H-AZT and (C) 3H-ddI after 90 min incubation and efflux kinetics of (B) 3H-AZT and (D) 3H-ddI in a drug-free medium for 60 min. HEK-R482 cells were electroporated one day before the uptake study with 100 pmol of siBCRP (*:p < 0.05, n = 3)
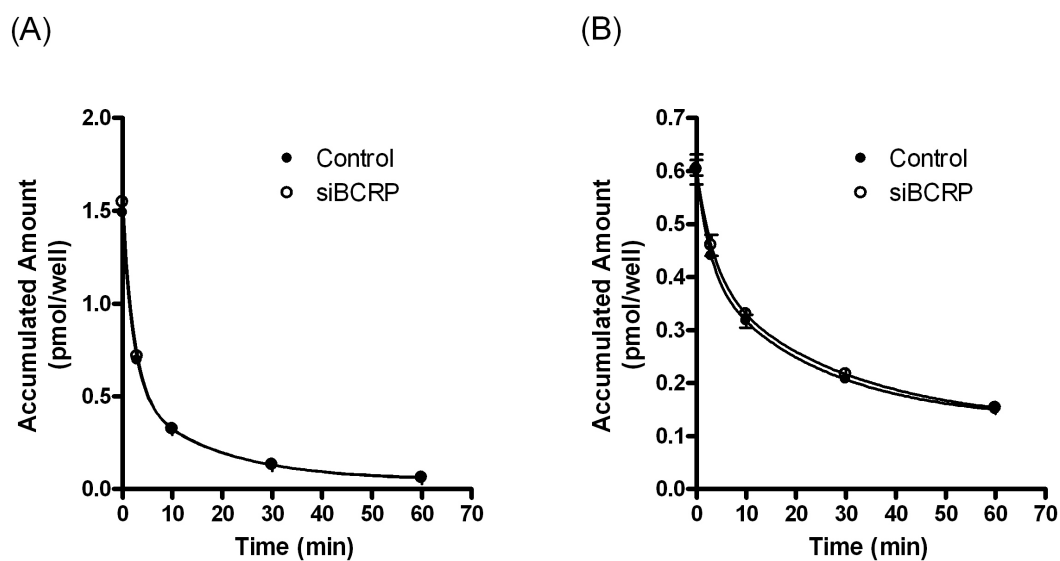
Figure 16. Effect of bcrp1 siRNA on the efflux kinetics of AZT and ddl. Efflux kinetics of (A) 3H-AZT and (B) 3H-ddl in a drug-free medium for 60 min after 90 min incubation of drug. J774.2 cells were electroporated one day before the uptake study with 100 pmol of bcrp1 siRNA (n = 3)
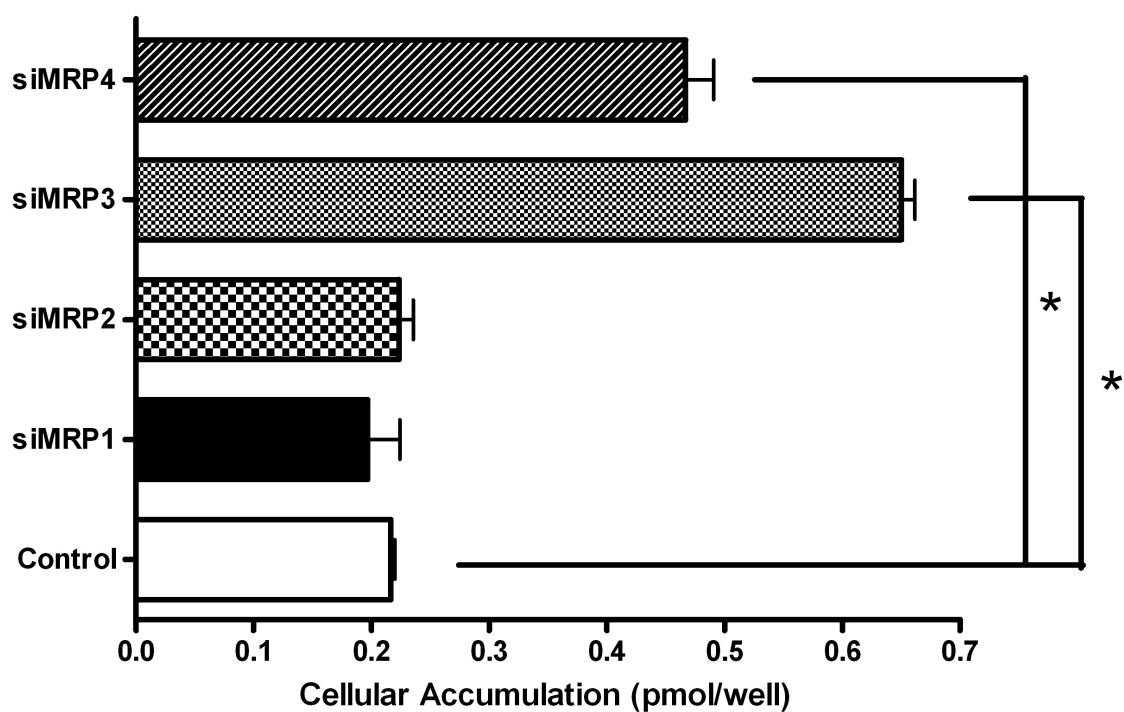
Figure 17. Effect of siMRP1 ~ 4 on the uptake of AZT. Cellular uptake of 3H-AZT after 90 min incubation. HEK-R482 cells were electroporated one day before the uptake study with 100 pmol of siMRP1 ~ 4 (*: p < 0.05, n = 3)
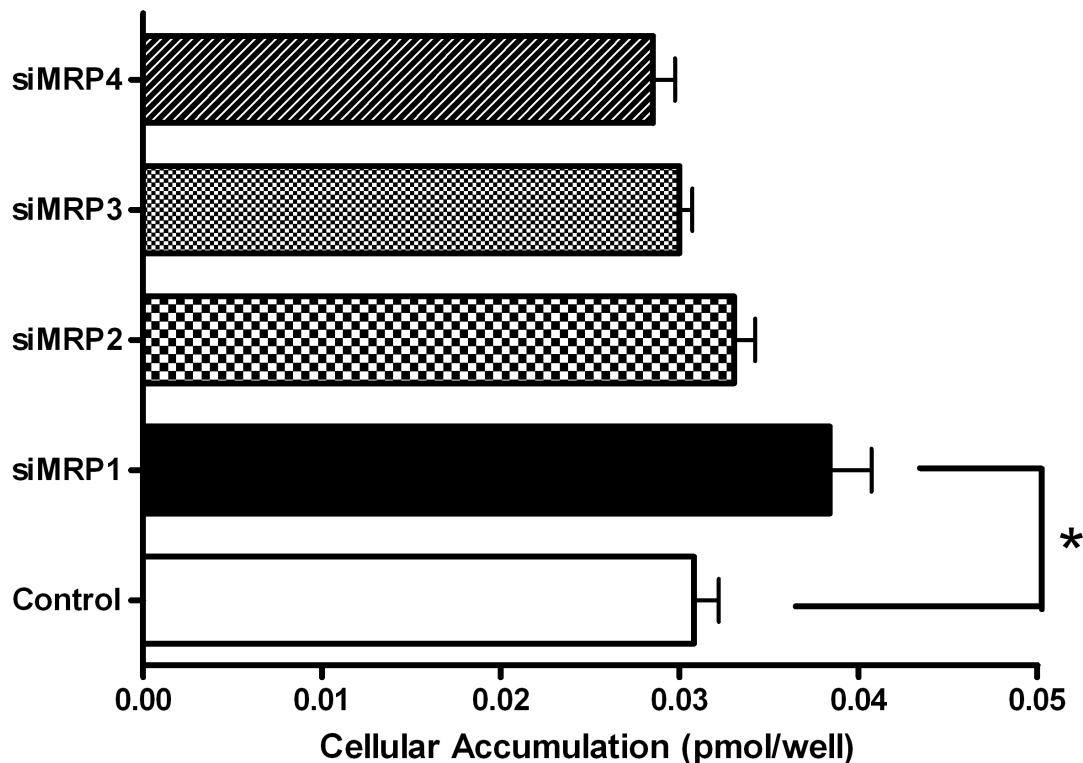
Figure 18. Effect of siMRP1 ~ 4 on the uptake of ddI. Cellular uptake of 3H-ddI after 90 min incubation. HEK-R482 cells were electroporated one day before the uptake study with 100 pmol of siMRP1 ~ 4 (*: p < 0.05, n = 3)

Concentration dependency in efflux of AZT and ddI

The concentration dependence of ddI efflux in HEK-R482 cells was evaluated over the range of 1 ~ 400 μM intracellular concentrations of ddI (Figure 19). The initial efflux rate of the ddI from HEK-R482 cells was calculated from the efflux at 30 sec, which was derived from the linear portion of the efflux – time plot (data not shown). The initial rate of efflux was then plotted against the concentration of the substrate in the cell. The substrate concentration - efflux rate profile was fit to a linear model instead of the nonlinear Michaelis-Menten model since transporter-mediated portion of ddI efflux is negligible. At

the highest concentration of ddI, the velocity of the efflux was proportional to the

intracellular concentration of ddI without any saturation. The concentration dependency of

AZT efflux in HEK-R482 cells was also evaluated over the intracellular concentration

range of 10 ~ 4,000 μM (Figure 20). The efflux rate per unit AZT concentration increases,

which is caused by the saturation of the intracellular concentration of AZT as shown in

Figure 20B. This phenomenon strongly suggests two possibilities: that either an uptake

transporter or metabolizing enzyme became saturated.
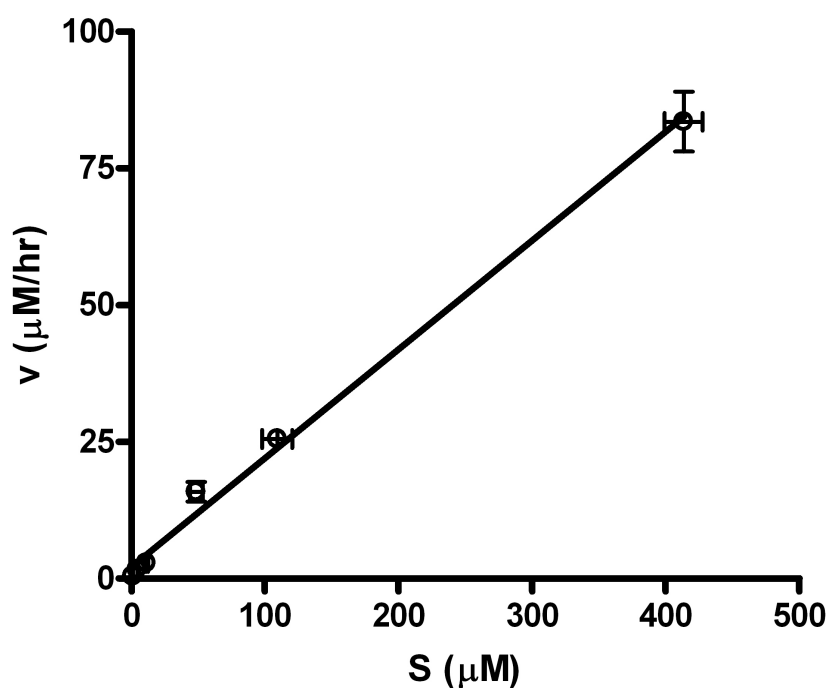
Figure 19. Release of ddI from HEK-R482. Plot of efflux rate at 30 sec from HEK-R482 cell versus estimated intracellular concentration of ddI over the range of 1 ~ 400 uM (n = 3)
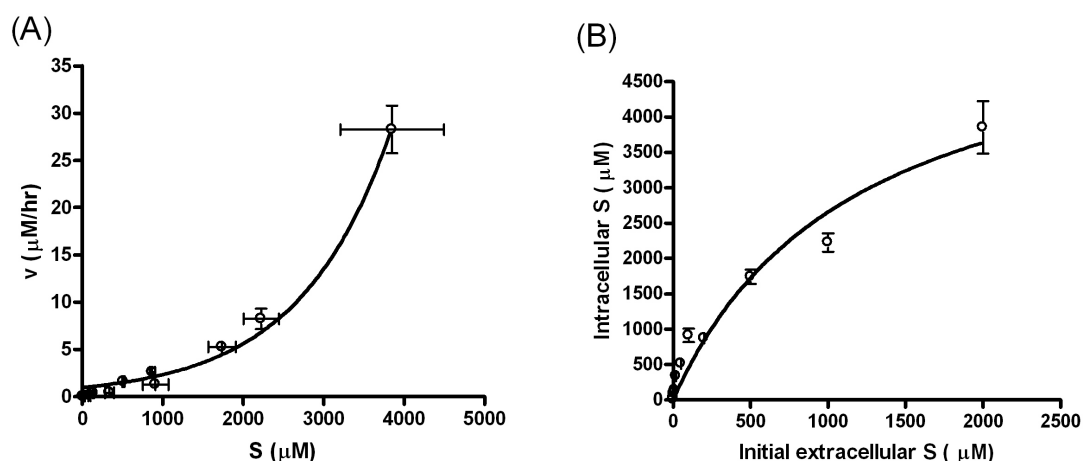
Figure 20. Release of AZT from HEK-R482. (A) Plot of efflux rate at 30 sec from HEK-R482 cells versus estimated intracellular concentration of AZT over the range of 10 ~ 4000 uM. (B) Relationship of the intracellular and the initial extracellular concentration of AZT (n = 3)

Effect of MK-571 in HEK-R482 and J774.2 cells

Since the transporters involved with AZT, ddI, and their metabolites are quite diverse, the delineation of each factor is also quite challenging. MRP4 is reported to be an efflux transporter of AZT-MP (Sampath et al., 2002). The efflux of AZT from HEK-R482 and J774.2 cells was examined (Figure 21). The accumulation of AZT after 90 min uptake in HEK-R482 was 27.2 vs. 30.9 pmol/ well in the control group and in the MK-571-added group. The relative efflux of AZT was delayed in HEK-R482 cells incubated with MK-571 during AZT uptake and efflux (Figure 21A), while the relative efflux of AZT with MK-571 was the same as the control in J774.2 cells (Figure 21B). The accumulation of AZT after 90 min uptake in J774.2 was 3.0 vs. 6.0 pmole in control and MK-571-added group. The efflux processes of ddI in HEK-R482 and J774.2 macrophages were also examined (Figure 22). MK-571 doubled the 90 min uptake of ddI in HEK-R482 (control vs. MK-571 treated; 0.60 vs. 1.11 pmol/well) whereas no effect was observed in a 90 min uptake study of ddI

with MK-571 in J774.2 (control vs. MK-571 treated; 1.13 vs. 0.86 pmol/well). The

relative efflux of ddI with MK-571 in HEK-R482 and J774.2 were slower than in the

control group (Figure 22).
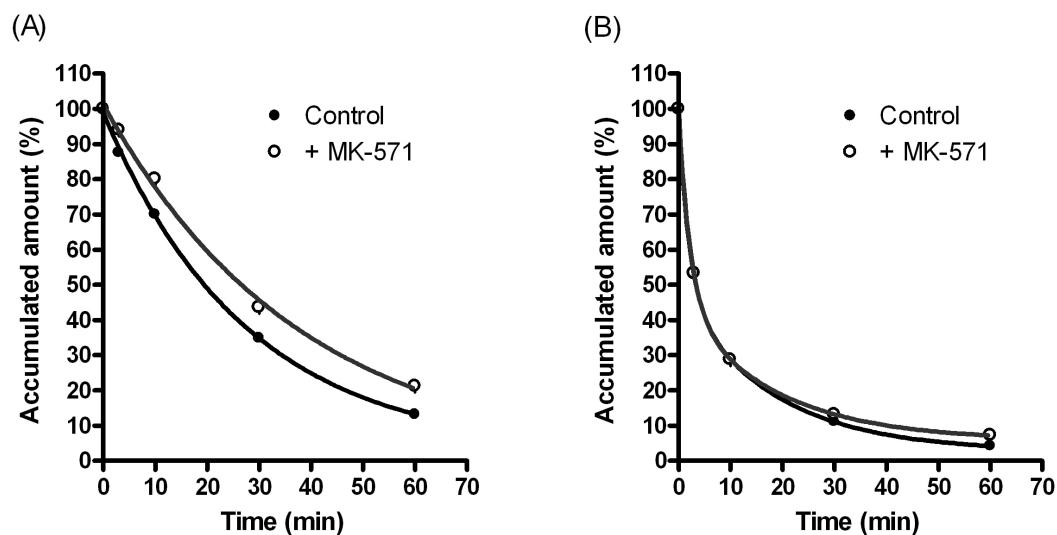
Figure 21. Effect of MK-571 on the efflux kinetics of 3H-AZT in (A) HEK-R482 and (B) J774.2

cells. HEK-R482 and J774.2 cells were incubated in a drug-free medium with/without

MK-571 (100 uM) for 60 min after 90 min coincubation of 3H-AZT (1 uM) with/without MK-571

(n = 3)

(A)

(B)
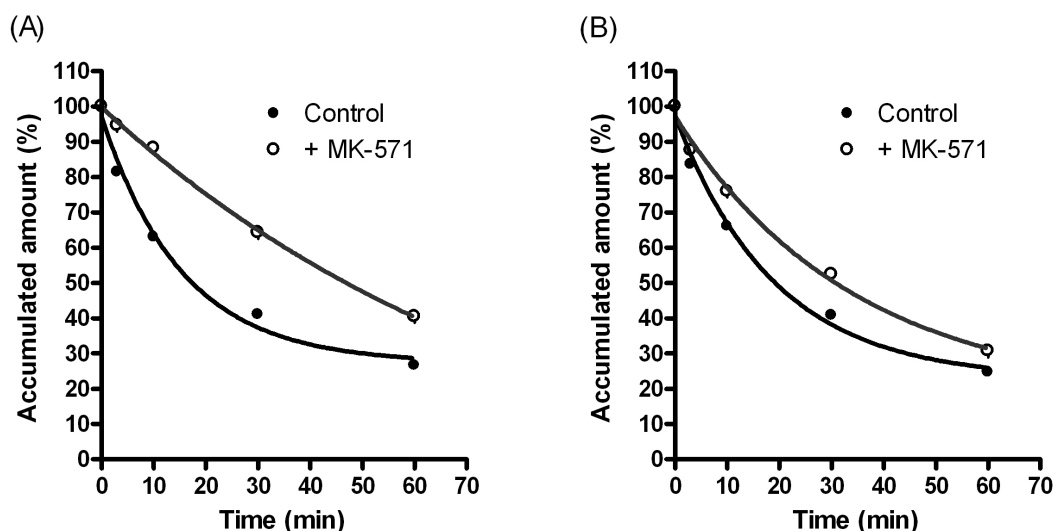
Figure 22. Effect of MK-571 on the efflux kinetics of 3H-ddI in (A) HEK-R482 and (B) J774.2 cells. HEK-R482 and J774.2 cells were incubated in a drug-free medium with/without MK-571 (100 uM) for 60 min after 90 min coincubation of 3H-ddI (1 uM) with/without MK-571 (n = 3)

D.   *Discussion.*

It is essential to dose NRTIs correctly in order to avoid low drug concentrations in target tissues and the subsequent development of resistance, including cross-resistance to other drugs in the class. There are significant differences among the NRTIs with respect to dispositional properties. One of the factors determining the excretion rate of each NRTI is that many NRTIs are substrates for ATP-dependent efflux transporters. Efflux transporters alter the systemic disposition of NRTIs and limit the accessibility of these antiviral agents to pharmacokinetic sanctuary sites. The current experiments address two issues: 1) the study of BCRP and MRPs expression and silencing and 2) the study of uptake and efflux of AZT and ddI in human and murine cell lines. The expression of BCRP has been demonstrated at both the mRNA and protein levels. The expression of bcrp mRNA in J774

cells was confirmed by semi-quantitative RT-PCR. This finding was extended to the protein level. The signal generated with bcrp antibody on Western blots roughly correlates to mRNA level. We established the transfection method of naked siRNA using an electroporation method in this study. The selectivity was checked by measuring the expression level of unrelated GAPDH mRNA. The functional decrease of BCRP was also confirmed in this study.

We demonstrated that AZT uptake into HEK-R482 and J774.2 cells was sensitive to FTC but not to other BCRP inhibitors such as GG918 and NOV (Figure 13). An increase in inhibitor concentration had no effect on AZT uptake (data not shown). The efflux of AZT decreased significantly in the presence of FTC, but the relative difference of efflux rate constant between the control and the FTC-added group was less than 50% (k = 0.016 ± 0.001 vs. 0.011 ± 0.001 min^{-1}, r^2 ≥ 0.999)(Figure 14). Further investigation of the behavior of AZT and each metabolite using radio-HPLC is discussed in the next chapter. These two inhibitors showed clear inhibition of TPT, another well known BCRP substrate. The reason for this phenomenon is not clear, and there are two possibilities: 1) increased uptake of AZT was not mediated by blocking BCRP and 2) the mechanism of BCRP inhibition by these inhibitors did not affect the transport of AZT. The first possibility can be applied to the results in murine J774.2 cells, even though nonspecific inhibition of other efflux transporters by FTC has not been reported to date. siRNA silencing of murine bcrp1 did not decrease efflux of AZT and ddI in murine J774.2 cells (Figure 16), while siRNA silencing of human BCRP significantly increased uptake of AZT and ddI and decreased efflux of both drugs (Figure 15). Neither bcrp1 nor mrps play a significant role in efflux of AZT in the mouse. Contrary to the murine results, both BCRP and MRPs alter the uptake

and efflux profile of AZT significantly in human cells. This species difference in substrate specificity of efflux transporter is a rare and interesting discovery. The effect of bcrp1 or BCRP on the efflux of ddI is minimal. Another interesting finding is that the different MRP subfamily is responsible for the efflux of AZT and ddI. Unlike AZT, whose efflux was delayed by siMRP3 and siMRP4, the efflux of ddI was delayed only by siMRP1 (Figure 18). But, the extent of MRP1 inhibition does not explain the difference in the efflux profile by MK-571. The major inhibition effect of MK-571 treatment in Figure 18 might be caused by inhibition of transporters other than MRP1 ~ 4.

IV.   THE METABOLIC PROFILES OF AZT AND DDI IN MOUSE AND HUMAN CELLS

A.   *Introduction*

Understanding the metabolic profile (i.e., such as the rate of metabolism and the molecular structure of produced metabolites) of a drug is critical in determining a safe dosing regimen. Until now, reports on the metabolism of AZT and ddI have only focused on inter-species differences in hepatic metabolism (Cretton et al., 1990; Pan-Zhou et al., 1997; Collins, 2001). Although the majority of AZT and ddI metabolism occurs in the liver in humans, the effect of renal metabolism can not be ignored particularly in the case of drug-drug interactions. Generally speaking, significant inter-species differences in drug metabolism make interpretation of preclinical and non-clinical results and extrapolation from animals to clinical results difficult. Since there is no single model or method that can extrapolate drug metabolism from animals to humans, extensive preclinical and nonclinical pharmacokinetics and drug metabolism studies are required in laboratory animals prior to

clinical studies. AZT is a well known example of profound species differences in hepatic drug metabolism, since it was shown that most of dosed AZT was found to be glucuronidated in clinical pharmacokinetic and drug metabolism studies (Blum et al., 1988) even though *in vivo* animal studies suggested that metabolism of AZT would be minimal (Chow et al., 1997).

The metabolism of AZT and ddI are not only involved with classical phase I and II metabolizing enzymes but also with PNP and phosphorylating enzymes such as thymidine kinase and 5'-nucleotidase (5'-NT). AZT itself is not active, but it needs to be converted to its phosphorylated anabolites intracellularly by a series of intracellular kinases in order to exert cytotoxic or antiviral activities. Involvement of multiple metabolizing pathways is important because one of the clinical limitations of AZT is rapid clearance with a one hour plasma half-life that requiring a frequent dosing schedule. The intracellular metabolism of AZT has been extensively examined in *in vitro* cell lines and in human PBMCs (Furman et al., 1986; Balzarini et al., 1988; Dhawan et al., 1990; Szebeni et al., 1991).

In this section we investigate the role of thymidine kinase in AZT metabolism. We also monitored the metabolic profiles of AZT and ddI in two kinds of cultured cells, to assess the species differences in drug metabolism. This is important since different levels of enzyme activities are observed in different species from different organs and that can cause inconsistent drug distribution in various organs (Matheny et al., 2001; Ding and Kaminsky, 2003). Completely different patterns of intracellular accumulation of AZT and its metabolites were observed in between J774 and HEK-R482 cells, when the efflux profiles of AZT and its metabolites were similar each other. This suggests that AZT-MP is

a major efluxed form of AZT regardless of intracellular metabolic profile in different organ and/or species.

B.   Materials and Methods

1.   Effect of metabolizing enzymes

HEK-R482 and J774.2 cells were routinely maintained in 75-cm^2 flasks containing DMEM and MEM media supplemented with 10% fetal calf serum at 37°C / 5% CO_2. Cells were incubated with ^{3}H-AZT (1 µM) and either probenecid or thymidine (20 µM or 1 mM) for 2 hr at 37°C in triplicate in 24-well plates. Following incubation, cells were washed three times with ice-cold PBS buffer, lysed by 1N NaOH (0.2 ml) and analyzed using β-scintillation counting. Quantitation of AZT and AZT phosphates in specific samples was achieved using HPLC analysis described in the next section. Data is presented as mean ± SD. Dunnett's multiple comparison test after ANOVA is used to compare the statistical differences between groups and statistical significance is determined at the level of $P = 0.05$.

2.   Radio-HPLC analysis of AZT and its metabolites

Sample Preparation. For the analysis of AZT and its metabolites in HEK-R482 and J774.2 cells using HPLC method, the cells were washed three times with ice-cold media and frozen immediately in liquid nitrogen. The thawed cells were extracted with 60% methanol, and the extracts were heated at 95°C for 1.5 min. The extracts were centrifuged for clarification at 12,000g for 6 min.

Chromatography. AZT and its metabolites was chromatographically separated on a reversed-phase C$_{18}$ column (Nova-pak C18, 5 μm, 4.6 mm × 150 mm Waters) with a mobile phase of phosphate buffer (0.2 M) containing tetrabutylammonium hydrogen sulfate (4 mM, pH 7.5) and acetonitrile in the ratio of 97.5:2.5. Flow rate of the mobile phase was 1.5 ml/min with an Agilent 1050 pump. The eluent is monitored for UV absorbance at 270 nm with an Agilent 1050 UV detector and for beta scintillation counting by using the β-RAM detector and the tritium channel. Identification of the radioactive peaks was achieved by comparing retention times and UV chromatograms of metabolites with those of authentic standards. The HPLC conditions described above allowed the separation of AZT from the phosphorylated metabolites and the concomitant determination of the two major hepatic metabolites, AMT and GAZT. On the day of assay, dried tissue extracts were reconstituted with 150-400 μl of water containing cold AZT and AZT-TP. An aliquot was injected onto HPLC system by an Agilent 1050 autosampler. During the process of our analysis, the coefficient of variation of the radioactivity associated with the injected AZT standards was < 7%.

Quantitation. Concentrations of AZT-MP and AZT in samples were determined from the slopes of standard curves of the peak area ratio of compound to internal standard versus standard compound concentration. Standard curve slopes were generated by either non-weighted or weighted (1/Y^2) least-squares regression analysis.

3.   Radio-HPLC analysis of ddI and its metabolites

HPLC analyses were done with a reversed-phase column C$_{18}$ column (Novapak C18, 5um, 4.6 mm × 150 mm Waters) and mobile phase A (4% acetonitrile, 25 mM pH 6.0 phosphate

buffer, 5 mM hexyl triethylamine ion-pairing reagent (Regis Technologies)) and mobile

phase B (60% acetonitrile, 25 mM phosphate [pH 6.0], 2 mM hexyl triethylamine

ion-pairing reagent). The following gradient was used: (1) 5 min of an isocratic flow with

100% mobile phase A at 1.2 ml/min, (2) 35 min of a linear gradient from 0 to 42% mobile

phase B at 1.2 ml/min, (3) column washing for 2 min with 100% mobile phase B at 2

ml/min, and (4) 8 min of reequilibration with 100% mobile phase A at 1.2 ml/min. The

final eluent was monitored for UV absorbance at 270 nm with an Agilent 1050 UV detector

and for beta scintillation counting by the β-RAM detector using the tritium channel. All

other details were identical to that described in Method #2.

C. Results

1. Metabolism limits the uptake of AZT and ddI in human embryonic kidney cells and murine macrophage cells

Influence of ATP depletion

The cellular accumulation of AZT and the time profiles for AZT efflux were shown for

HEK-R482 (Figure 23) and J774.2 (Figure 24) cells. The efflux profiles follow two

elimination phase kinetics in HEK-R482 and J774.2 cells ($k1 = 0.078, 0.092, 0.082$ min^{-1},

$k2 = 0.067, 0.080, 0.070$ min^{-1} for control, ATP regeneration, and ATP depletion in

HEK-R482; $k1 = 0.55, 0.44, 0.46$ min^{-1}, $k2 = 0.044, 0.040, 0.037$ min^{-1} in J774.2 cells)
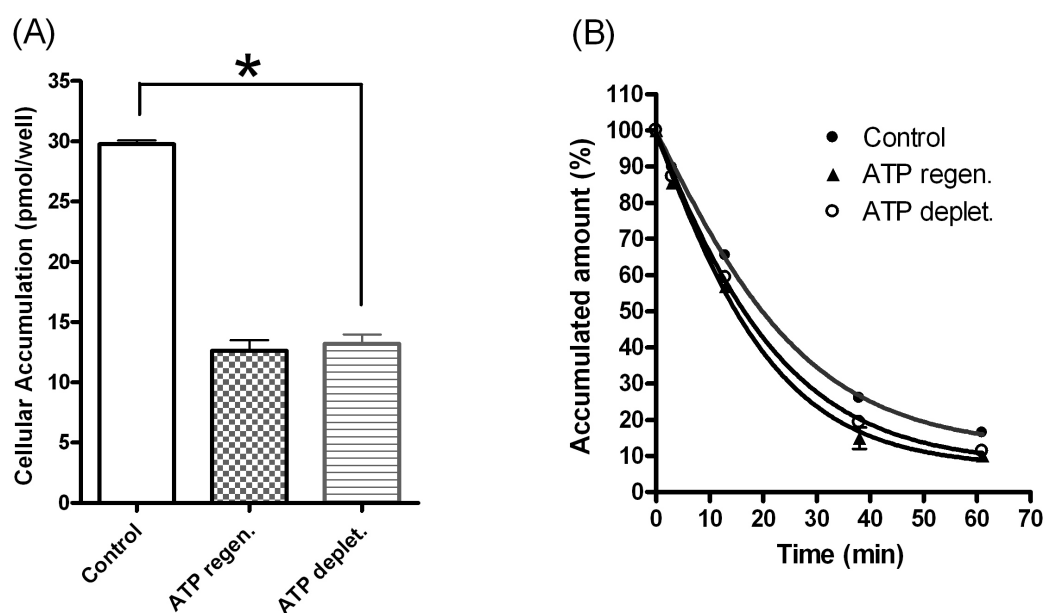
Figure 23. Effect of ATP depletion on (A) cellular uptake and (B) relative efflux of AZT in HEK-R482 cells. ATP depleted cells were maintained in the presence of ATP synthesis inhibitors during the uptake phase. For efflux, cells were either incubated in a substrate-free medium without ATP inhibitors (ATP regen.) or in the continuing presence of the ATP inhibitors (ATP deplet.) (*: p < 0.05, n = 3)
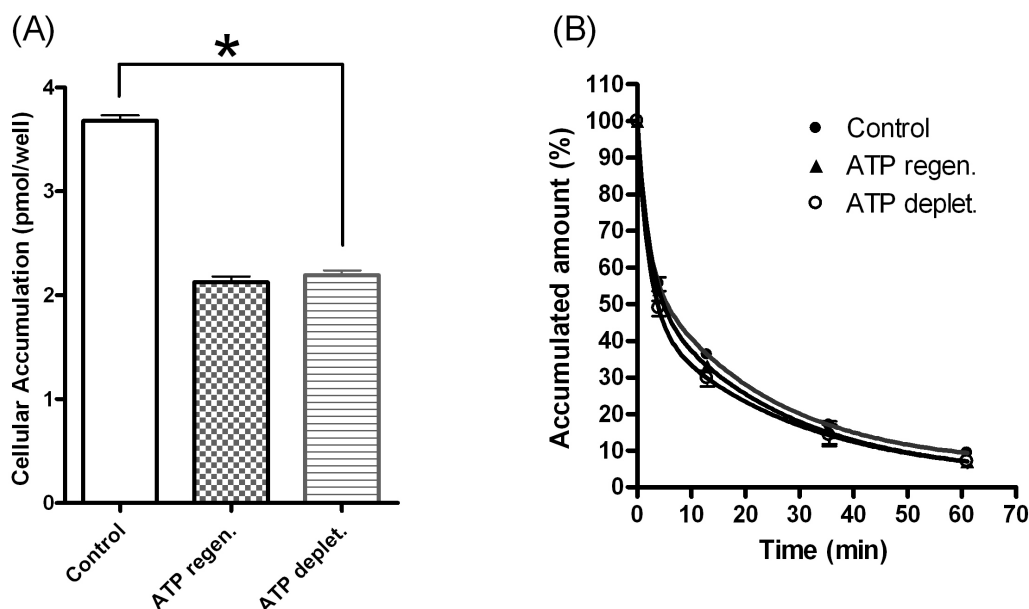
Figure 24. Effect of ATP depletion on (A) cellular uptake and (B) relative efflux of AZT in J774.1 cells. ATP depleted cells were maintained in the presence of ATP synthesis inhibitors during the uptake phase. For efflux, cells were either incubated in a substrate-free medium without ATP inhibitors (ATP regen.) or in the continuing presence of the ATP inhibitors (ATP deplet.) (*: $p < 0.05$, n = 3)

AZT efflux was studied in ATP depleted cells, loaded with AZT in ATP depleting conditions, and transferred to a drug-free medium in ATP depleting conditions. Cells were preincubated for 20 min with NaN_3 and 2-D-deoxyglucose to deplete them of ATP. They were then challenged with 1 µM AZT and ddI for 90 min in ATP depleting condition. ATP depletion was originally designed to ablate the efflux of AZT mediated by ABC transporters such as BCRP, but ATP depletion did not cause an increase but rather a marked decrease of AZT uptake in both HEK-R482 and J774.2 cells (Figure 23, Figure 24). AZT is phosphorylated to the monophosphate (AZT-MP) by thymidine kinase, and further phosphorylated to diphosphate (AZT-DP) and triphosphate (AZT-TP) by

thymidylate kinase and deoxynucleoside diphosphate kinase, respectively. ATP depletion

can block the oxidative phosphorylation of AZT since the source of the phosphate group is

ATP. Inhibition of AZT phosphorylation led to decreased formation of AZT-MP, which is

a substrate of MRP4 (Schuetz et al., 1999). The mixed function of ATP supports the efflux

data in Figure 23B and Figure 24B showing that the relative efflux rate of AZT in ATP

depleting and regenerating conditions was not different compared to the observation in the

control group (no ATP depletion). The effect of ATP depletion on the efflux transporters

can be segregated from the metabolism by separately measuring the parent AZT and

metabolites. Cellular uptake of ddI was also compared among control, ATP regeneration,

and ATP depletion conditions. The effect of ATP depletion was minimal in both

HEK-R482 cells (control vs. ATP regeneration vs. ATP depletion; 1.36 vs. 1.71 vs. 1.60

pmol/ well) and J774.2 cells (control vs. ATP regeneration vs. ATP depletion; 1.17 vs. 0.93

vs. 0.87 pmol/ well).

Role of thymidine kinase in cellular uptake of AZT

The effect of ATP depletion on AZT uptake strongly suggests the involvement of

phosphorylation (Elwell et al., 1987), glucuronidation (Resetar and Spector, 1989), and/or

uptake transporters (Griffiths et al., 1991). Thymidine kinase is the first in line of the

successive phosphorylation of AZT to AZT-TP, and this enzyme is inhibited by an

excessive amount of thymidine (Hoggard et al., 1995). Probenecid is known to be an

inhibitor of both organic anion transporters (Somogyi, 1996) and glucuronidation (Hauser

et al., 1988). The influence of thymidine kinase inhibitors and probenecid on the

intracellular uptake of AZT in HEK-R482 and J774.2 cells is compared (Figure 25). It has

been reported that AZT was metabolized predominantly to AZT-MP (approximately 75%

of total phosphates) with less AZT-DP and AZT-TP formed (Hoggard et al., 1995).
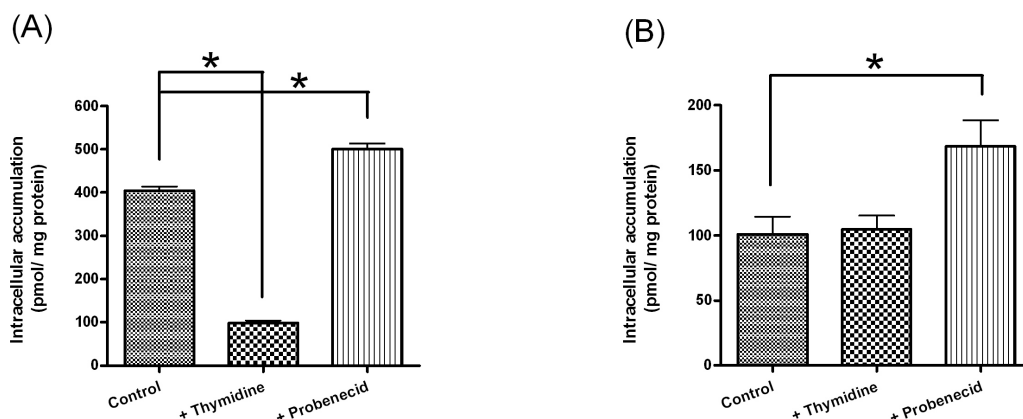
Figure 25. Effect of thymidine and probenecid on 3H-AZT accumulation. Cellular accumulation of 3H-AZT (1 uM) in (A) HEK-R482 cells and (B) J774.2 cells after 90 min incubation with/without 20 uM thymidine or 1 mM probenecid (*: p < 0.05, n = 3)

The addition of thymidine (20 μM) resulted in a marked reduction in AZT accumulation in

HEK-R482 cells compared to controls whereas the addition of probenecid (1 mM)

increased AZT uptake in both HEK-R482 and J774.2 cells. Reduced uptake of AZT by

thymidine suggests that ATP depletion is caused by the inhibition of thymidine kinase.

2.   *Effect of AZT phosphorylation on AZT efflux*

To investigate MRPs' role in the transport of AZT and its metabolites, we examined the

uptake and efflux processes in J774 (Figure 26, Figure 27) and HEK-R482 (Figure 28,

Figure 29) cells. A typical radiochromatogram had two radioactive peaks. Peaks were

characterized by using HPLC cochromatography with authentic cold standards such as

AZT and AZT-MP (Figure 30). MK-571 abolished the efflux of AZT-MP in J774 cells

whereas it had no effect on AZT efflux. A similar pattern was observed in HEK-R482 cells

suggesting that AZT-MP is a substrate of MRPs.
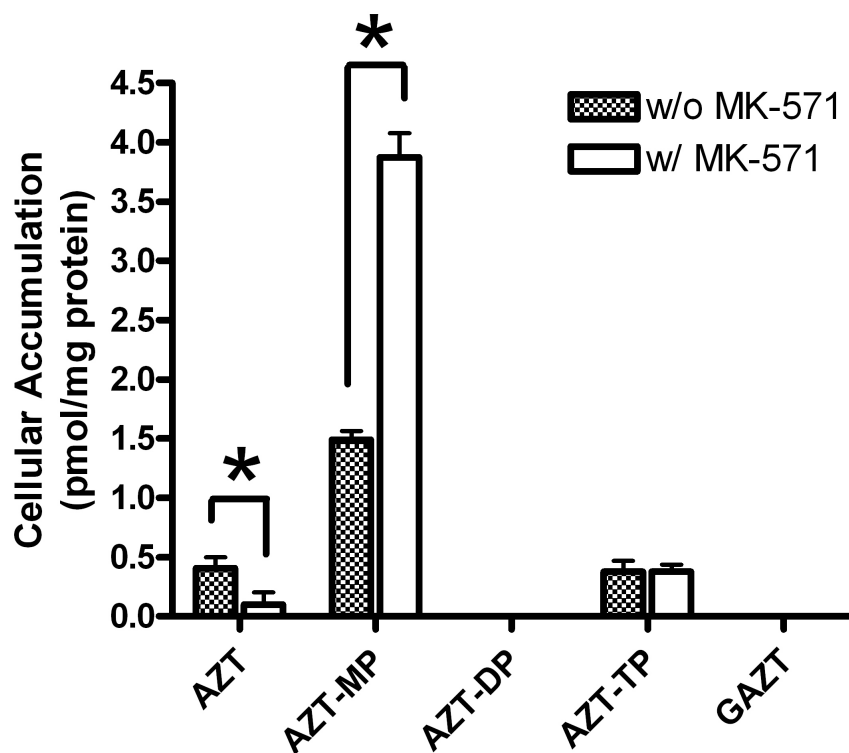
Figure 26. Effect of MK-571 on 3H-AZT and its metabolites uptake. Cellular uptake of

3H-AZT (1 uM) and its metabolites into J774.2 cells after 30 min incubation with/without 100
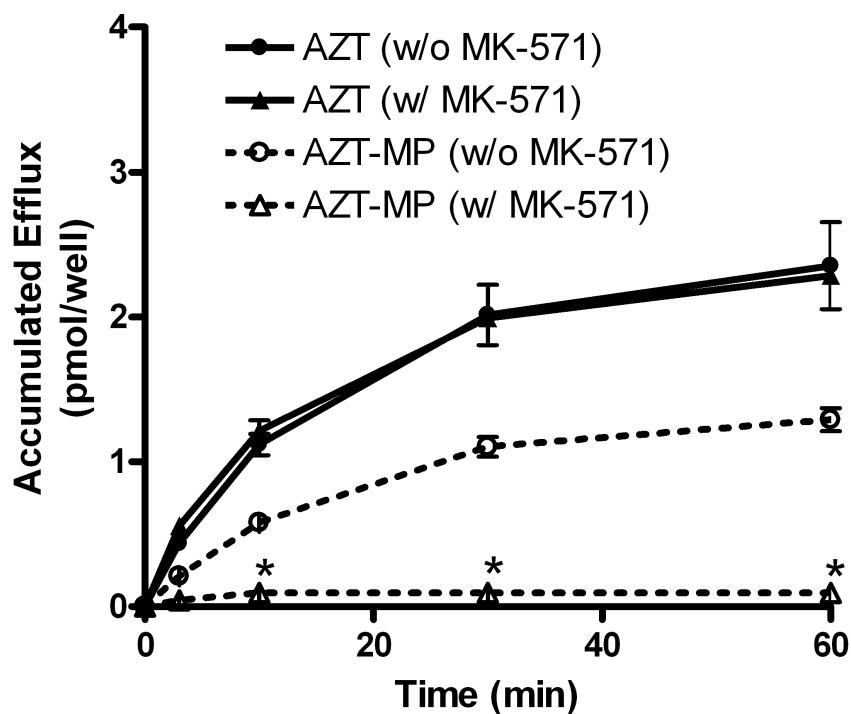
uM MK-571 (*: p < 0.05, n = 3)

Figure 27. Effect of MK-571 on the efflux kinetics of 3H-AZT and AZT-MP in J774.2 cells.

J774.2 cells were incubated in a drug-free medium with/without MK-571 (100 uM) for 60 min

after 90 min coincubation of 3H-AZT (1 uM) with/without MK-571 (*: p < 0.05, n = 3)
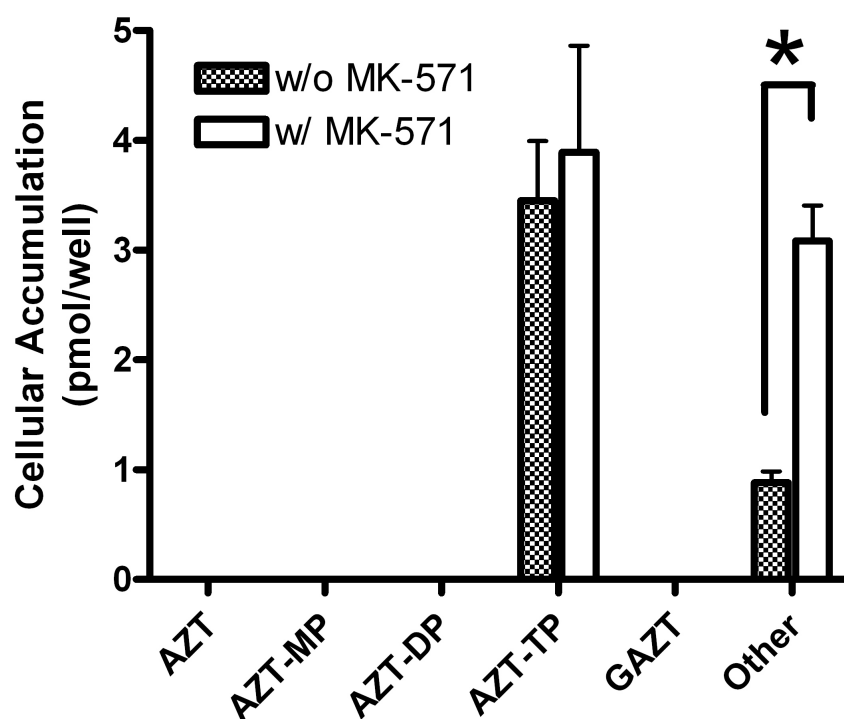
Figure 28. Effect of MK-571 on 3H-AZT and its metabolites uptake. Cellular uptake of 3H-AZT (1 uM) and its metabolites into HEK-R482 cells after 30 min incubation with/without 100 uM MK-571 (*: p < 0.05, n = 3)
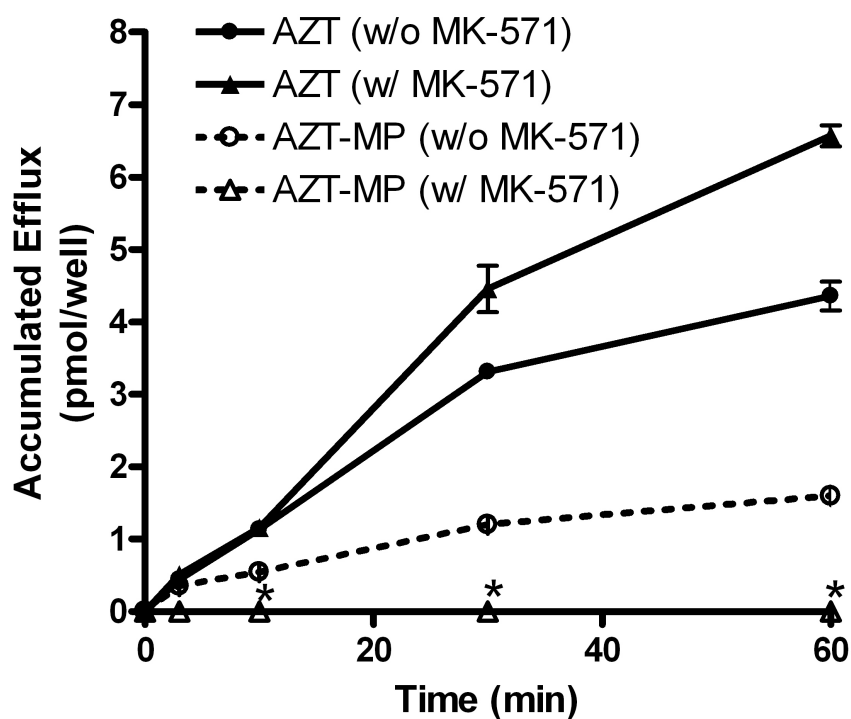
Figure 29. Effect of MK-571 on the efflux kinetics of 3H-AZT and AZT-MP in HEK-R482 cells.

HEK-R482 cells were incubated in a drug-free medium with/without MK-571 (100 uM) for 60

min after 90 min coincubation of 3H-AZT (1 uM) with/without MK-571 (*: $p < 0.05$, n = 3)
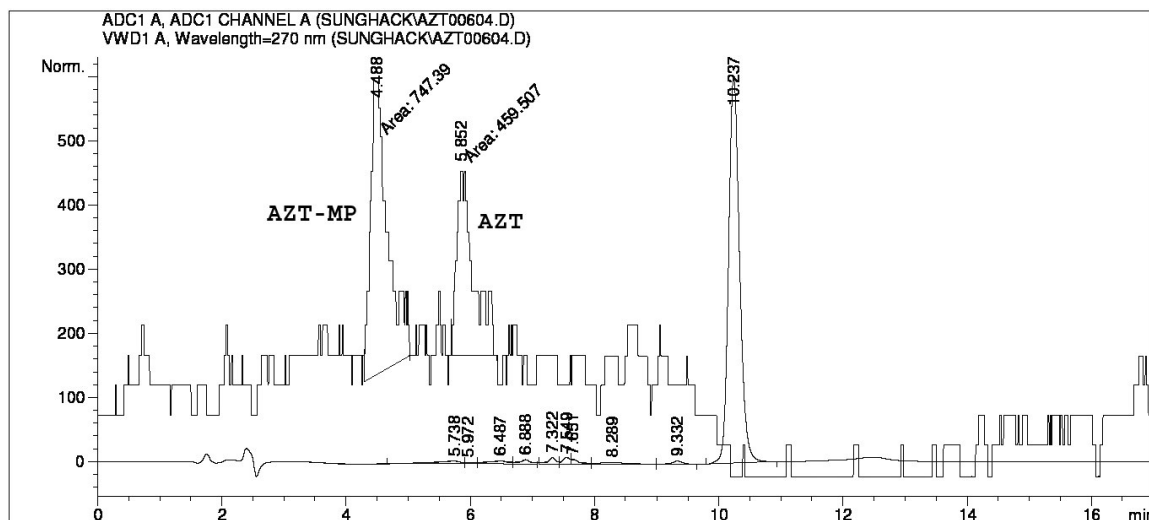
Figure 30. Typical HPLC radiochromatogram of an efflux media sample incubated with

3H-AZT in HEK-R482 cells

3.   Effect of ddI phosphorylation on ddI efflux

The effect of MK-571 on the cellular deposition of ddI-originated molecular species in

HEK-R482 cells was shown in Figure 31. A typical radiochromatogram, presented in

Figure 32 showed only one radioactive peak. The peak was characterized as ddA-TP by

using HPLC cochromatography with an authentic cold standard. The major effluxed form

of ddI was also examined using radio-HPLC, and it was identified as ddI itself (data not

shown). The peak size of ddI was slightly over the detection limit, and it was difficult to

claim that ddI was the only effluxed form found in the media.
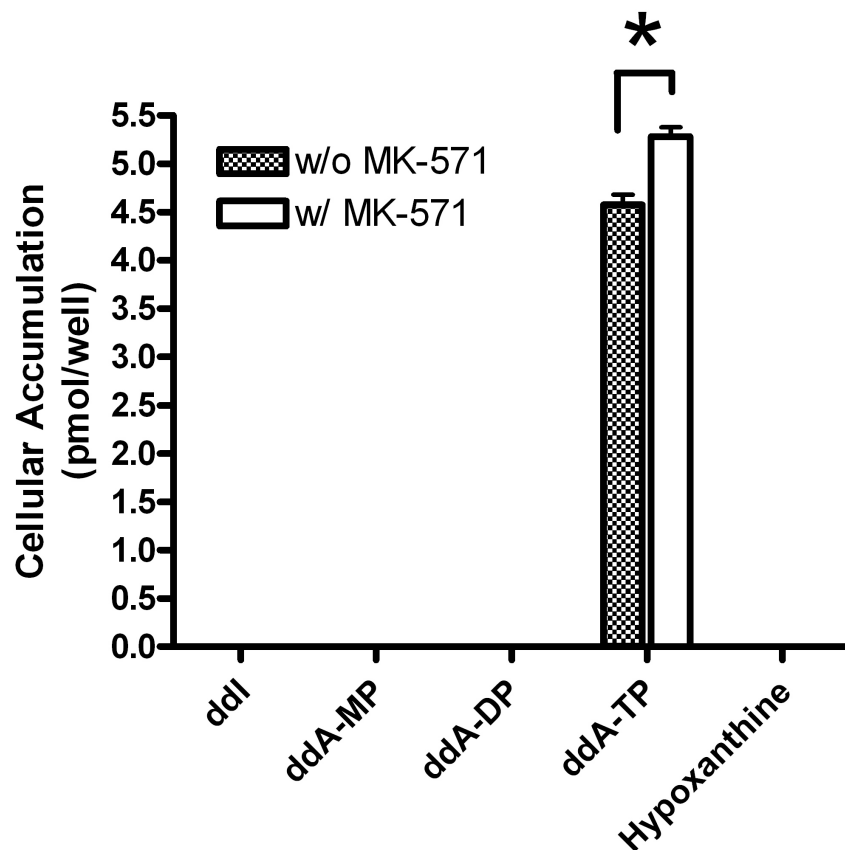
Figure 31. Effect of MK-571 on 3H-ddI and its metabolites uptake. Cellular uptake of 3H-ddI (1 uM) and its metabolites into HEK-R482 cells after 30 min incubation with/without 100 uM MK-571 (*: $p < 0.05$, n = 3)
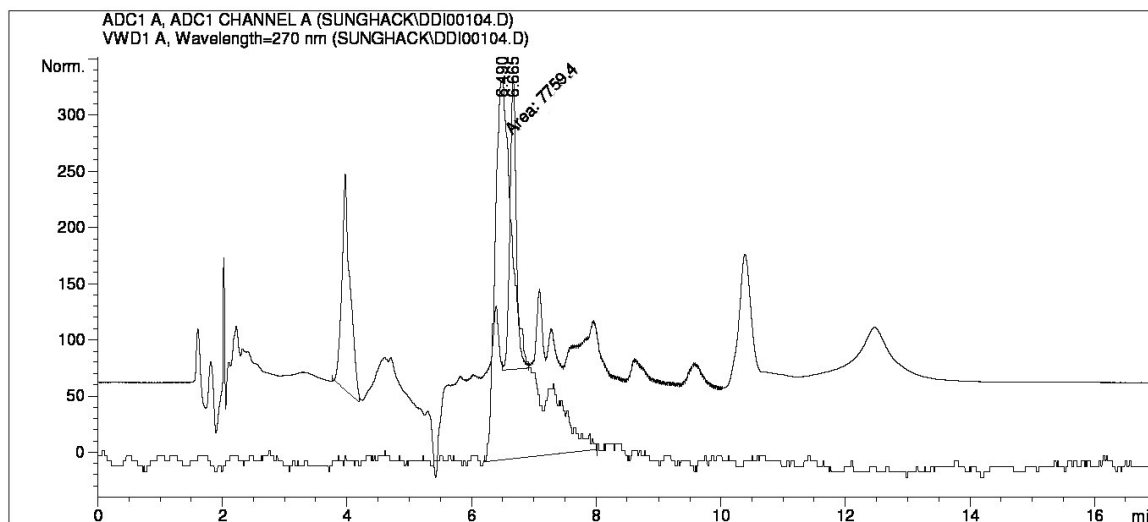
Figure 32. Typical HPLC radiochromatogram of an uptake media sample incubated with

3H-ddI in HEK-R482 cells

D.   *Discussion*

Literature reports have suggested that the tissue-to-plasma ratio (T/P ratio) of AZT was

high in the kidney due to the involvement of uptake transporters. Detection of extracellular

AZT-MP indicated that AZT-MP was transported outward by an efflux transporter.

Sampath et al. reported that AZT-MP is a substrate of MRP4 (Sampath et al., 2002). The

low ratios of AZT-MP to AZT in tissue and of AZT-TP to AZT in the mouse kidney (9.6%

and 0.1%) indicate that the major intracellular AZT form is AZT itself (Chow et al., 1997;

Chow et al., 1998). The current uptake studies of AZT indicated rapid phosphorylation in

cultured cells such as human embryonic kidney (HEK-R482) and mouse macrophage

(J774.2) cells. Incubation of AZT resulted in the formation of AZT-MP in J774.1 and most

of the AZT was effluxed as a parent AZT or AZT-MP. Different patterns of AZT

metabolism were monitored depending on the applied cell systems. In HEK-R482 cells,

AZT-TP was the predominant metabolite instead of AZT-MP indicating more rapid serial

phosphorylation of AZT than in murine J774.1 cells. In the case of ddI, the metabolic

pathway is more complicated than for AZT. ddI-MP was aminated by the adenylsuccinate

synthase and lyase enzymes to ddA-MP, which was phosphorylated to the ddA-DP and

ddA-TP forms. In the cultured cells, ddI showed lower intracellular level than AZT,

probably because ddI has lower permeability to the cell membrane as compared to AZT.

The predominant metabolite found in human HEK-R482 was the triphosphate form of ddA

(ddA-TP) similar to AZT.

ATP depletion was originally designed to ablate the efflux of AZT mediated by ABC

transporters such as BCRP, but ATP depletion did not cause an increase but rather a

marked decrease of AZT uptake in both HEK-R482 and J774.2 cells. AZT is

phosphorylated to the monophosphate (AZT-MP) by thymidine kinase, and further

phosphorylated to diphosphate (AZT-DP) and triphosphate (AZT-TP) by thymidylate

kinase and deoxynucleoside diphosphate kinase, respectively. ATP depletion blocks the

oxidative phosphorylation of AZT since the source of the phosphate group is ATP.

Inhibition of AZT phosphorylation led to decreased formation of AZT-MP, which is a

substrate of MRP4 (Schuetz et al., 1999). The mixed function of ATP supports the efflux

data showing that the relative efflux rate of AZT in ATP depleting and regenerating

conditions was not different compared to the observation in the control group (no ATP

depletion). Cellular uptake of ddI was also compared among control, ATP regeneration,

and ATP depletion conditions. The effect of ATP depletion was minimal in both

HEK-R482 cells and J774.2 cells.

The experiments presented here show that metabolism is closely related to the efflux of

AZT and ddI, and the deposited forms of these drugs are sometimes different compared

with effluxed form.

V. THE ROLE OF DRUG EFFLUX AND METABOLISM ON THE URINARY DISPOSITION OF AZT AND DDI

A. *Introduction*

For most drugs, the major routes of drug disposition are hepatic extraction and renal excretion. While hepatic extraction of drugs is mediated by biotransformation and biliary excretion, renal excretion of drugs encompasses glomerular filtration, tubular secretion, tubular reabsorption, intracellular storage, and metabolism. Although glomerular filtration and tubular reabsorption are responsible for the renal clearance of drugs in a number of cases, other mechanisms, such as tubular secretion, intracellular storage, or metabolism of drugs, may also be involved in the renal clearance of drugs. Since the renal clearance of AZT (7.4 ml/min/kg) and ddI (15.7 ml/min/kg) exceeded the normal glomerular filtration rate of rats (5.2 ml/min/kg) it suggests a significant role of tubular secretion in the elimination of these drugs (Doshi et al., 1989). Unlike glomerular filtration, tubular reabsorption and secretion are saturable processes, as transporters mediate vectorial transepithelial transport of drugs. Besides the well-known ability of absorptive transporters to recycle nutrients back to the body (Le Hir and Dubach, 1985; Franco et al., 1990; Gutierrez and Giacomini, 1993), secretory transporters mediate the export of drugs via the basolateral and apical membrane of renal proximal tubular cells into urine thus playing a critical role in drug elimination.

The identification and characterization of organic ion transporters at the basolateral membranes of the kidney are now better understood (Inui et al., 2000). In addition to these organic ion transporters, the ATP-binding cassette (ABC) transporter family located at the

apical membrane such as P-glycoprotein (P-gp), multidrug resistance-associated proteins (MRPs), and breast cancer resistance protein (BCRP) have been suggested as efflux transporters in the kidney (Siegmund et al., 2002; Dietrich et al., 2003; Ito et al., 2005; Cascorbi, 2006). In previous two chapters, it was shown that MRPs and BCRP are responsible for the efflux of AZT and ddI in species specific way and phosphorylation plays a great role in the metabolism of AZT and ddI. Also, the metabolism and efflux of both drugs appear to be closely related to each other. Phosphorylation and transport work as tandem processes in the disposition of AZT and ddI, which introduces an extra complexity to the interpretation of their efflux kinetics. The excretion of AZT and ddI from systemic blood, through renal tubular epithelial cells, and into urine can be considered a three-step process. The first step involves the filtration of AZT and ddI from blood through glomerulus, a passive filtration process dependent only upon size and charge. The second step is reabsorption into renal tubular epithelial cells. Entry of drugs from urine into tubular cells can be achieved via a variety of apical carrier systems. Alternatively, uptake of drugs from systemic blood into tubular cell is achieved through the basolateral membrane. Once inside the tubular cells, the third step of urinary clearance involves transferring drugs back to the microtubular space through the tubular apical membrane. This step of urinary clearance at the tubular apical membrane involves unchanged drug and/or metabolites. Many transporting proteins have been shown to be present on the tubular apical membrane to mediate this process (Thiebaut et al., 1987; Schaub et al., 1997; Schaub et al., 1999; van Aubel et al., 2002). Renal clearance of AZT and ddI including their metabolites accounts for half of the total clearance in our results with mice and in the literature (Doshi et al., 1989; Ahmed et al., 1991). The main scope of

this investigation is to determine whether MK-571 altered the urinary excretion of AZT, ddI, and their metabolites. To elucidate the effect of MK-571 on urinary excretion of AZT and ddI in mice, we collected urine for up to 24 hrs after intravenous injection of AZT and ddI.

B. Materials and Methods

1. Urinary excretion of AZT and ddI in mice

AZT was mixed with ^{3}H-AZT in water and this aqueous mixture was used as AZT dosing solution in mice studies. Same procedures were applied to ddI dosing solution. AZT and ddI dosing solutions were intravenously administered at a dose of 10 mg/kg into FVB mice through the tail vein, and administered mice were kept in a metabolic cage (Nalgene, Rochester, NY). During the time of 0 ~ 12 hr and 12 ~ 24 hr, urine samples were collected, the metabolic cage was washed with water, and washing solution was also collected. For specific assay of ^{3}H-AZT or ^{3}H-ddI itself and metabolites in urine samples, radio-HPLC analysis was applied. A 10x diluted urine sample was vortex mixed in a 1.5-ml polypropylene tube for approximately 10 sec, centrifuged for 20 min at 15,800 g to achieve a clear supernatant, and 100 μL of the supernatant was injected directly onto a radio-HPLC system. ^{3}H-AZT and ^{3}H-ddI were analyzed using a reverse-phase HPLC on a Nova-Pak C8 column (150×4.6 mm, 5-μm particle size, Waters) fitted with a Nova-Pak C8 Guard-Pak precolumn (Waters). The HPLC system consisted of an Agilent Chemstation control software, Agilent 1050 pumps, Agilent 1050 autoinjector, and IN/US β-RAM radioactivity detector.

2. *Measurement of intrinsic clearance*

FVB mice were euthanized by CO_2 inhalation, and the kidneys were immediately placed into freshly oxygenated ice-cold saline. Tissue slices (≤ 0.5 mm; 5~10 mg wet weight) were cut with a Stadie-Riggs microtome and maintained in ice-cold modified Cross and Taggart saline (in mM: 95 NaCl, 80 mannitol, 5 KCl, 0.74 $CaCl_2$, and 9.5 Na_2PO_4, pH 7.4). Slices were incubated for 1 hr with AZT or ddI with/without inhibitors (10 µM Fumitremorgin C or 50 µM MK-571). After incubation, the slices were removed from the uptake medium, blotted, and weighed. Slices were dissolved in scintillation cocktail and analyzed by liquid scintillation counting method. For radio-HPLC analysis, samples were deproteinized with methanol instead of dissolution with scintillation cocktail. Data were presented as the tissue to medium (T/M) ratios (*i.e.,* dpm/mg tissue divided by dpm/µl medium).

3. *Pharmacokinetic analysis*

The peak plasma concentration (C_{max}) and time to reach a C_{max} (T_{max}) are read directly from the plasma concentration-time data. The V_{max} (the maximum velocity) and K_m (Michaelis-Menten constant; the concentration at which the rate is one-half of V_{max}) for the disappearance of AZT and ddI are determined after incubating the liver and kidney slices and drugs The kinetic constants (K_m and V_{max}) for the disappearance of AZT and ddI are calculated using the Lineweaver-Burk plot with the method of least squares. Data is presented as mean $\pm$ SD. Dunnett's multiple comparison test after ANOVA is used to compare the statistical significance of differences between experimental groups and statistical significance is determined at the level of $P=0.05$.

C.   Results

1.   Effect of novobiocin on oral absorption of ddI in rats

An LC-MS/MS assay for the determination of ddI was developed for use with the heparin anticoagulated rat plasma matrix. Mass spectra for ddI are shown in Figure 33 and two strong molecular ions were observed at m/z 495 and 295. ddI is coupled with sodium atom producing the adducts of [M+Na]$^+$ (m/z 495) and [2M+Na]$^+$ (m/z 259).
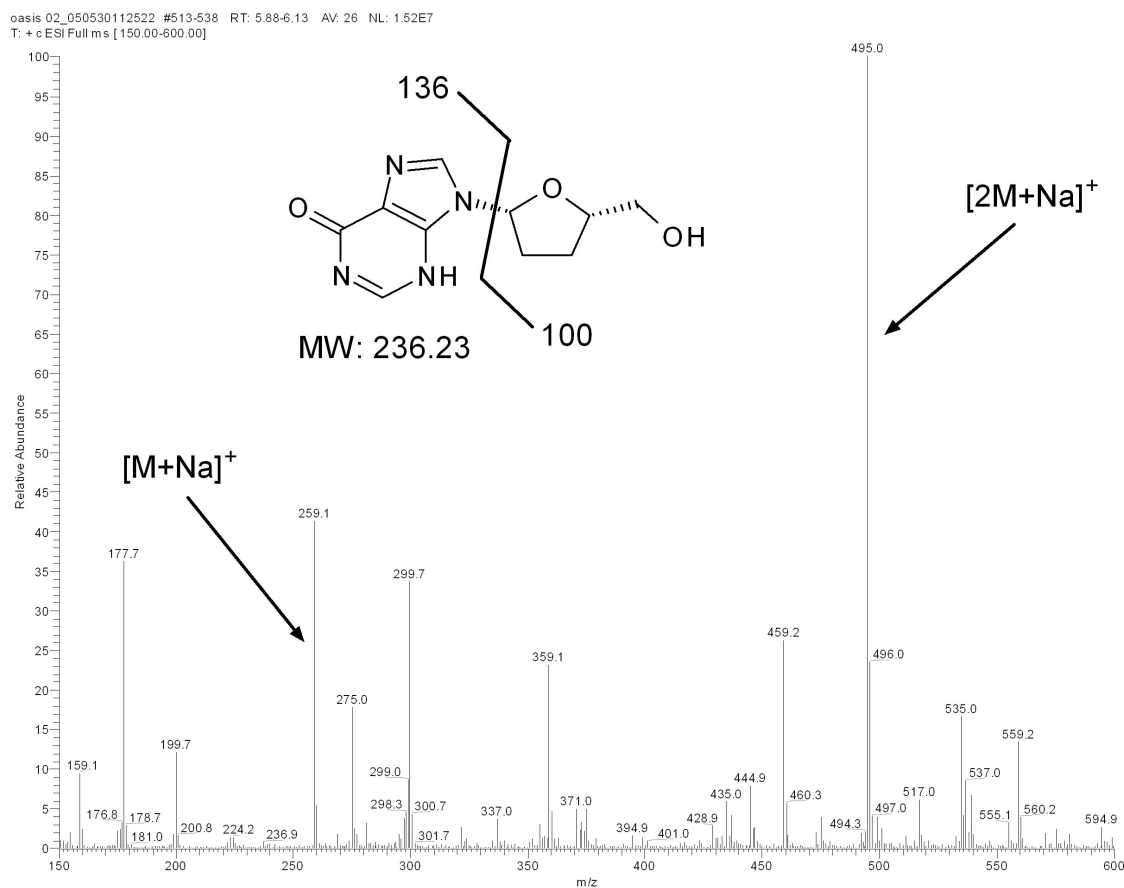
Figure 33. Mass spectra of ddI at the full scan mode (m/z range = 150 ~ 600).

Detection of ddI was achieved by ESI MS/MS in the positive ion mode using two channels:

495/259 and 259/159 for ddI, 445/234 and 423/212 for ddC (Figure 34).
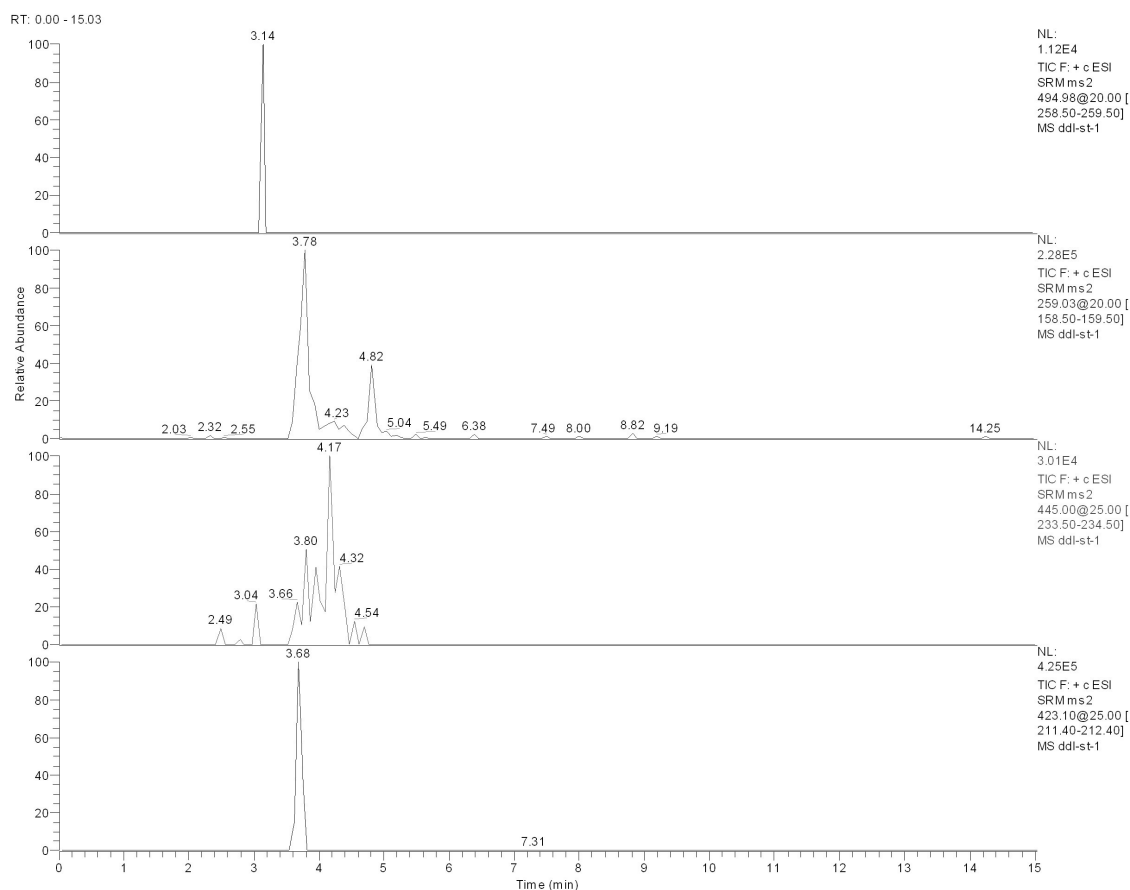
Figure 34. Chromatogram of ddI and internal standard ddC from the standard sample (2 ug/ml). Multiple reaction monitoring (MRM) mode at four channels: m/z of parent /daughter ion = 495/259 and 259/159 for ddI, 445/234 and 423/212 for ddC, in control serum when methanol was used for deproteinization

The calibration curve was linear in two phases of 10 ~ 80 ng/ml and 80 ~ 2,000 ng/ml. The

usefulness of this LC-MS/MS method to monitor plasma concentrations of ddI was

demonstrated in subsequent rat pharmacokinetic results. The plasma concentration–time

profile of ddI is shown in the absence and presence of NOV, a known BCRP inhibitor

(Figure 35). The group with NOV showed higher ddI concentrations than in the control group even though the difference was not statistically significant ($p > 0.05$).
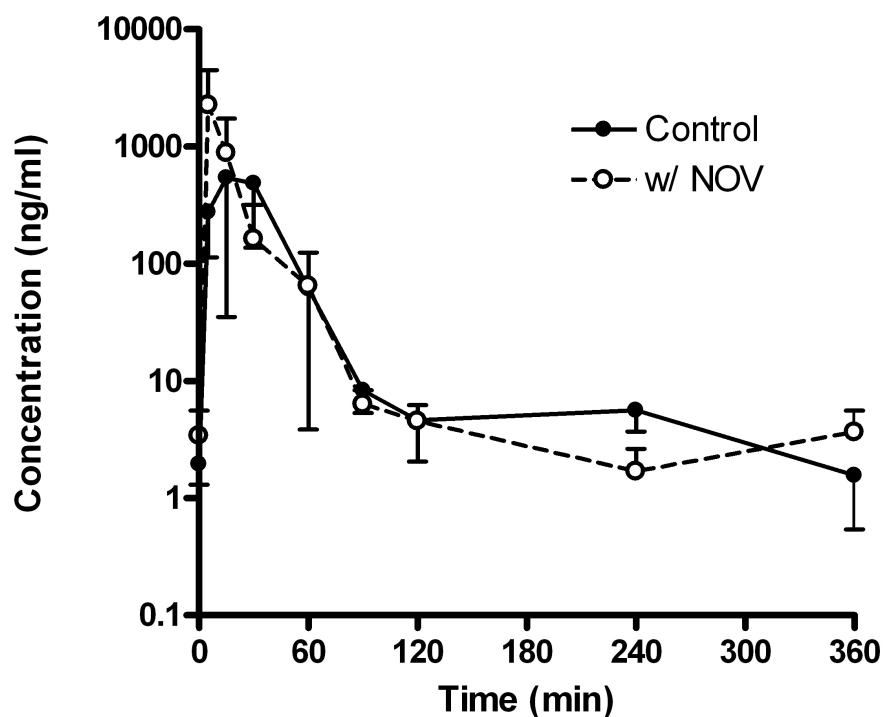
Figure 35. Mean arterial plasma concentration-time profile of didanosine (ddI) after oral administration at a dose of 20 mg/kg in Sprague-Dawley rats. ddI was administered with/without 50 mg/kg novobiocin (NOV). Each points represents means +/- SD (n = 3)

In vitro uptake of ddI suggested that ddI was not a substrate for mouse bcrp1 (Figure 13). It is unclear if the NOV effect is mediated by bcrp1 or by other factors.

2. *Intrinsic clearance from mouse kidney slices*

We have observed the efflux processes of AZT and the effect of FTC and MK-571 in mouse kidney slices have been examined in Figure 36 and Figure 37, respectively. The

efflux of AZT and GAZT during the first 60 min in mouse kidney slices was not changed in

the presence of FTC (Figure 36). The efflux of GAZT was delayed in mouse kidney slices

incubated with MK-571, while the efflux of AZT was same as control (Figure 37). The

relative efflux rates of AZT and GAZT was different: the same efflux rate of AZT and

GAZT regardless of the presence of MK-571.
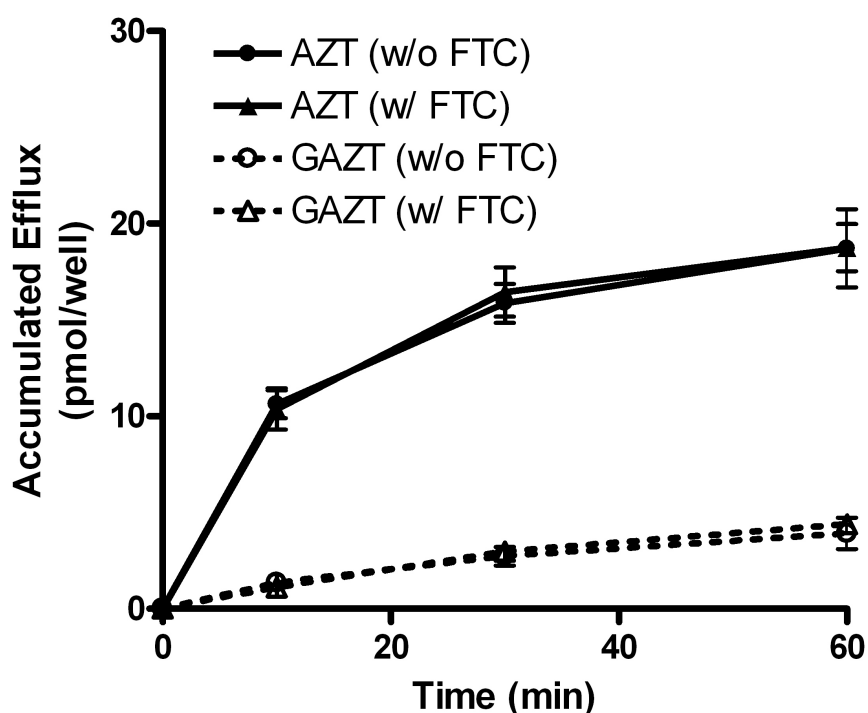
Figure 36. Effect of Fumitremorgin C (FTC) on the efflux kinetics of 3H-AZT and GAZT in mouse kidney slices. Mouse kidney slices were incubated in a drug-free medium with/without FTC (10 uM) for 60 min after 90 min coincubation of 3H-AZT (1 uM) with/without FTC (*: p < 0.05, n = 3)

(A)   (B)
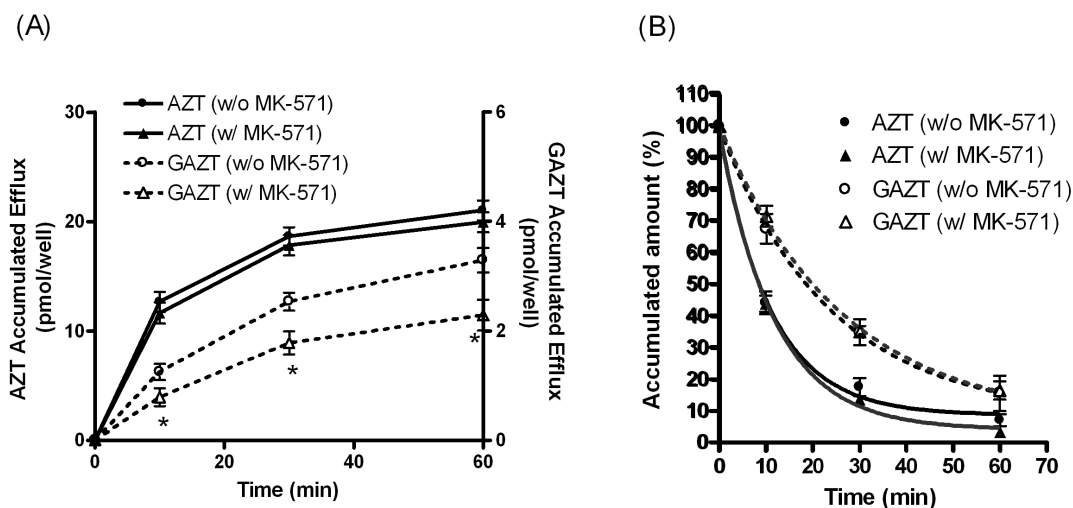
Figure 37. Effect of MK-571 on (A) the efflux profile and (B) the relative efflux profile of 3H-AZT and GAZT in mouse kidney slices. Mouse kidney slices were incubated in a drug-free medium with/without MK-571 (100 uM) for 60 min after 90 min coincubation of 3H-AZT (1 uM) with/without MK-571 (*: $p < 0.05$, n = 3)

We have also observed the efflux of ddI and the effect of FTC and MK-571 in mouse kidney slices have been examined in Figure 38 and Figure 39, respectively. The efflux of ddI and ddA-MP during the first 60 min in mouse kidney slices did not change in the presence of FTC (Figure 38). The efflux of ddA-MP was the same as the control, while the efflux of ddI itself was delayed in mouse kidney slices incubated with MK-571 (Figure 39). The relative efflux rates of ddI and ddA-MP with MK-571 was opposite: the same efflux rate of ddI vs. increased efflux rate of ddA-MP.
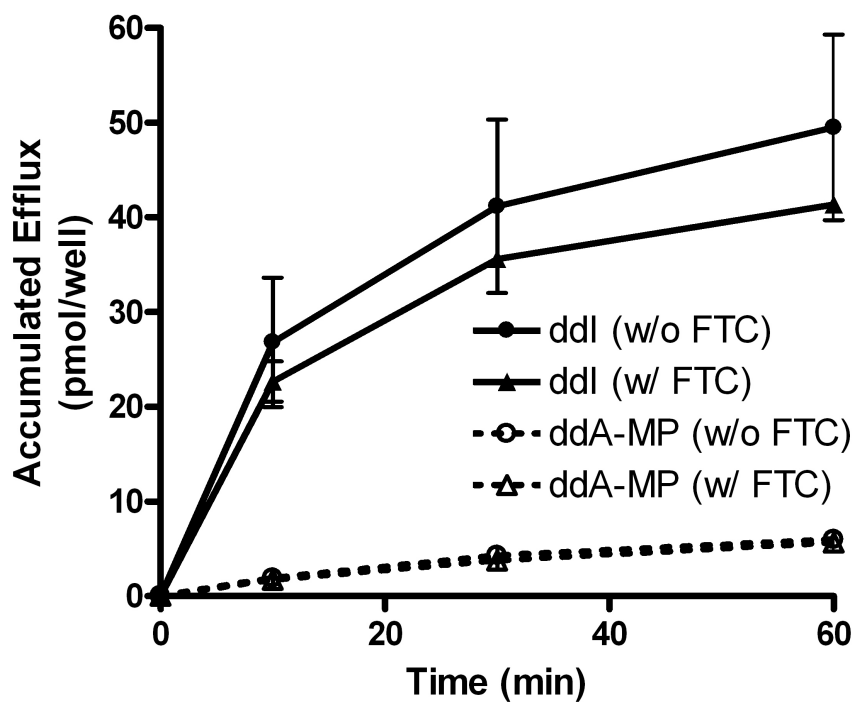
Figure 38. Effect of Fumitremorgin C (FTC) on the efflux kinetics of 3H-ddI and ddA-MP in mouse kidney slices. Mouse kidney slices were incubated in a drug-free medium with/without FTC (10 uM) for 60 min after 90 min coincubation of 3H-ddI (1 uM) with/without FTC (*: p < 0.05, n = 3)
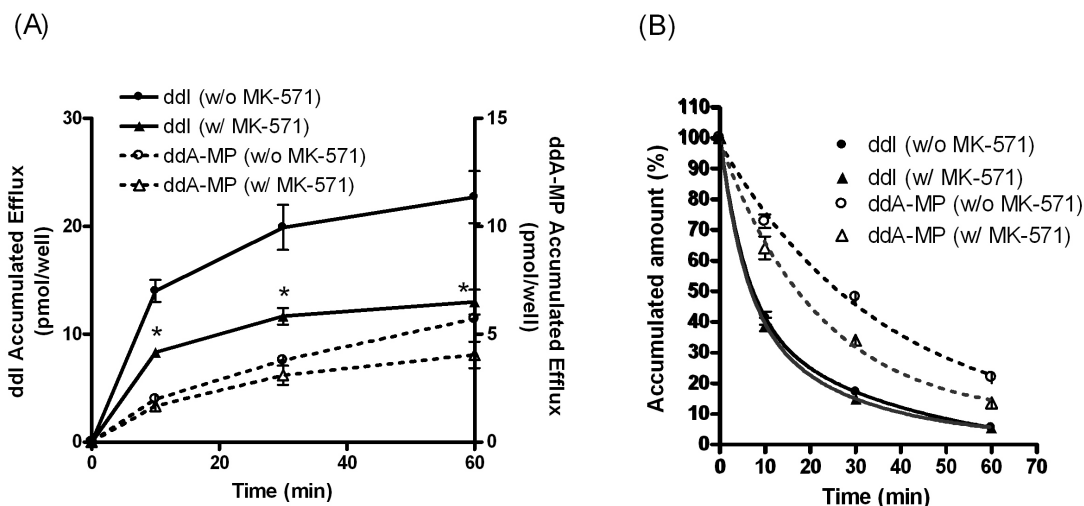
Figure 39. Effect of MK-571 on (A) the efflux profile and (B) the relative efflux profile of 3H-ddI and ddA-MP in mouse kidney slices. Mouse kidney slices were incubated in a drug-free medium with/without MK-571 (100 uM) for 60 min after 90 min coincubation of 3H-ddI (1 uM) with/without MK-571 (*: $p < 0.05$, n = 3)

3.   Urinary excretion of AZT and ddI in mice

AZT appeared in the urine and constituted almost all of urinary excreta for 24 hr after intravenous administration of AZT (Figure 40). 32% and 29% of the AZT dose was delivered into urine as AZT throughout the experiment in the absence/presence of MK-571 administered orally at 30 min prior to AZT dosing (50 mg/kg), respectively. The average excreted amount of GAZT was much lower, as it was found only occasionally in the urine.

Injected ddI was also excreted into the urine and, in fact it was one of the main forms of urinary excreted ddI (Figure 41). ddI that appeared in the urine accounted for 38% of the total excreted ddI, and the remaining was excreted as the ddA monophosphate form (ddA-MP). The existence of ddA-MP was confirmed by comparing the retention time of the metabolite peak in urine sample with that of cold authentic ddA-MP. 21% and 35% of

the ddI dose was delivered into urine as ddI and ddA-MP in the absence of MK-571, while

17% and 28% of the ddI dose was delivered as ddI and ddA-MP in the presence of
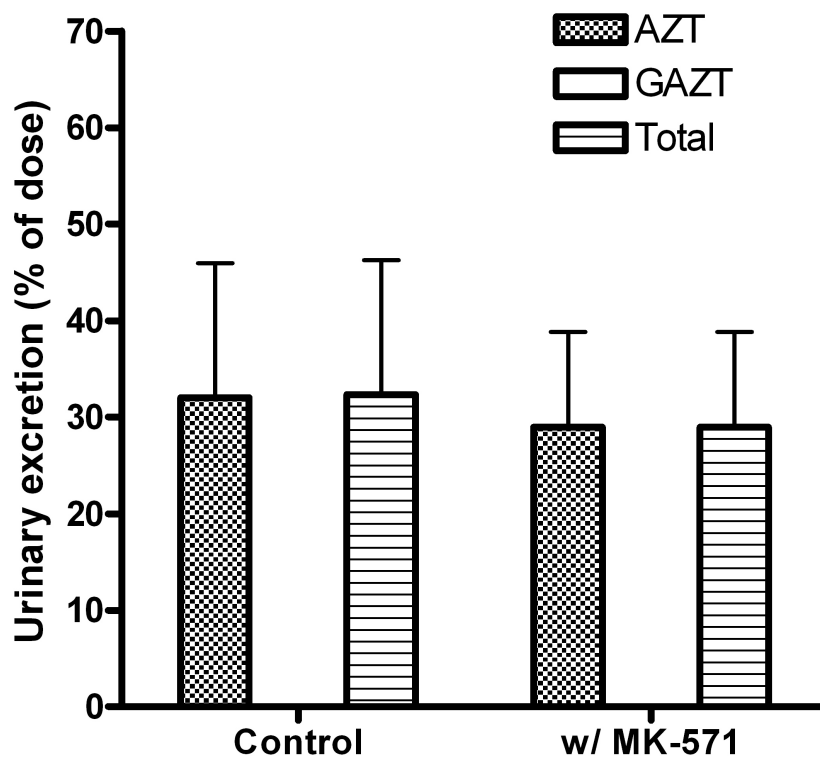
MK-571.

Figure 40. Effects of MK-571 on the urinary excretion of AZT in mice. AZT (10 mg/kg) with trace amount of 3H-AZT was injected through the tail vein with or without MK-571 (50 mg/kg). The excreted amount of AZT and GAZT over a period of 24 hr in a urine sample to the percent of the injected amount were determined (p < 0.05, n = 3)
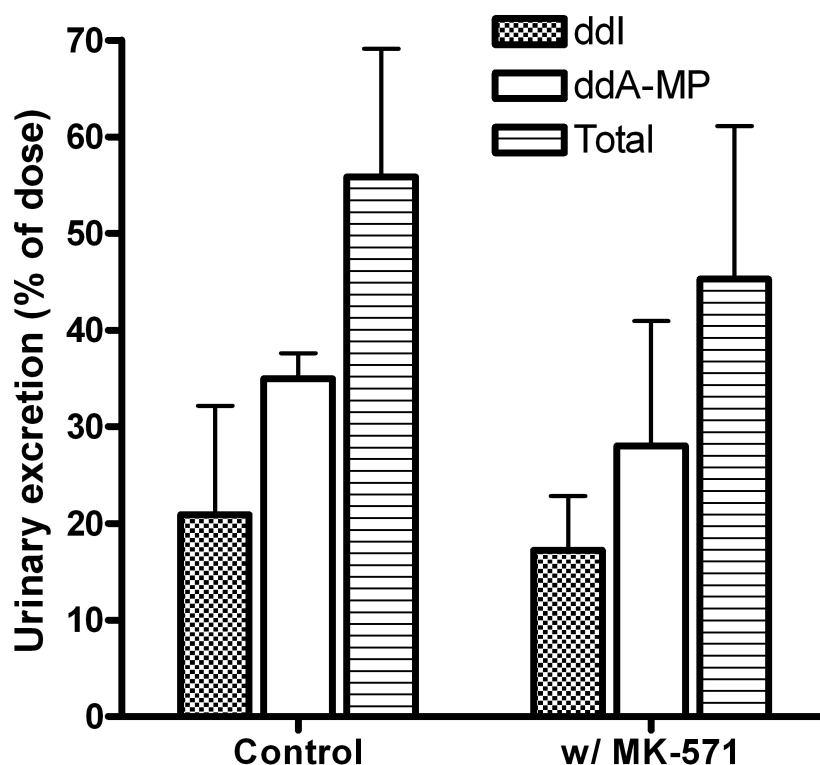
Figure 41. Effects of MK-571 on the urinary excretion of ddI in mice. ddI (10 mg/kg) with trace amount of 3H-ddI was injected through the tail vein with or without MK-571 (50 mg/kg). The excreted amount of ddI and ddAT-MP over a period of 24 hr in a urine sample to the percent of the injected amount were determined (p < 0.05, n = 3)

The inhibitory effect of MK-571 on the urinary excretion of AZT and ddI in mice was examined. The excreted amount of AZT and ddI was not altered by coadministration of MK-571, and thus the urinary clearance values of AZT and ddI in the presence of MK-571 were not affected by MK-571 coadministration.

D.   *Discussion*

In a preliminary study, the systemic exposure of ddI after oral dosing to rats was slightly higher when treated with NOV, a known BCRP inhibitor (Figure 35). However, the *in*

vitro ddI uptake study in cultured cells and kidney slices suggested that ddI was not a substrate of mouse bcrp1 (Figure 13, Figure 38). MK-571 was used in the mouse *in vivo* model as a putative transporter inhibitor to determine if efflux was caused by the MRPs instead of bcrp1. Urinary excretion of AZT and ddI were monitored in mice treated with/without MK-571. As a corresponding *in vitro* model, the metabolism and efflux of AZT and ddI in mouse kidney slices were also investigated. Incubation of AZT in mouse kidney slices resulted in the formation of GAZT with one unknown metabolite in contrast to the results from mouse J774.1. The reason for the unexpected difference of major intracellular metabolites between cultured cells and mouse kidney slices is uncertain. One possible reason for this phenomenon is the variable expression of glucuronidating enzymes, UDP-glucuronosyltransferases. This is supported by the fact that trimethylcyclohexanol was converted to its glucuronide in J774 cells at much slower rate than in rat hepatocytes (White et al., 1990). Contrary to our expectation, no change in AZT or ddI urinary excretion was observed between the MK-571 treated and untreated groups. It is probably because the binding affinity of AZT or ddI to MRPs was not strong enough to show an *in vivo* effect. Generally, significant *in vivo* pharmacokinetic changes by efflux transporters are observed only when *in vitro* inhibition is quite strong. In these experiments, we demonstrate a discrepancy between *in vitro* and *in vivo* inhibition of efflux transporters.

VI.   DEVELOPMENT OF A NOVEL STRATEGY FOR THE PENETRATION OF NRTIS TO HIV RESERVOIR SITES

A.   *Introduction*

Among the available antiviral drugs approved for the treatment of HIV-1 infected patients, AZT and ddI are still among the most effective drugs. AZT is a drug of choice for the prevention and management of AIDS dementia complex (ADC), because it is the best understood and certainly has better CNS penetration than other drugs such as nucleotide analog reverse transcriptase inhibitors and protease inhibitors. Patients receiving AZT show a general improvement in cognitive functions including attention, memory, motor function, and general cognitive ability (Sidtis et al., 1993). The success of AZT treatment has been attributed to its effective penetration into the brain and spinal fluid unlike recently developed nucleotide analogs such as adefovir. The transport of AZT across blood-brain barrier has been estimated from determinations of AZT levels in the brain tissue of mice. Larger doses (1,000 mg compared to the standard 600 mg/day) of AZT appear to be necessary for the treatment of ADC. However, continued use of AZT has been prohibited in a significant portion of patient population, because of dose-related hematologic toxicity. On the contrary, ddI has not been extensively studied for the treatment of cognitive impairment. Several small studies from clinicians suggest that ddI is less effective than AZT for treating AIDS dementia (Yarchoan et al., 1990). It seems that ddI does not cross the blood-brain barrier well as AZT does. It is estimated that only about 20% of ddI crosses the blood-brain barrier. However, ddI should be considered for people who are not be able to tolerate high doses of AZT.

In addition to brain, lymphocytes are also considered important target cells in HIV-1 treatment, since they are closely related to infectivity and propagation of HIV-1 (Gartner et al., 1986; Ho et al., 1986). To function as reverse transcriptase inhibitors, most NRTIs including AZT and ddI must first be phosphorylated to the triphosphate forms by

intracellular kinases. Unfortunately, the activity level of these enzymes depends on the cell activation state and on the cell type. Resting cells usually have low level of the enzymes responsible for the phosphorylation of nucleoside analogue, whereas activation causes increased activity levels (Gao et al., 1993; Gao et al., 1994).

In the brain and lymphocytes it is now understood that efflux transporters, such as P-glycoprotein, play a significant role in the secretory efflux of drugs from these sanctuary sites thereby attenuating the penetration of drug into brain and lymphocytes (Gupta and Gollapudi, 1993; Schinkel, 1999). Efflux transporters are saturable, inducible, inhibitable and display some degree of polymorphism. All of this needs to be considered with respect to variability in drug disposition and response (Liu and Hu, 2000).

Recent studies demonstrated that some of multidrug resistance related proteins (MRPs) are involved in pumping anionic substances out against a concentration gradient (Borst et al., 2000), which can be overcome by MRP inhibitors such as MK-571. MRPs are present in various organs: MRP1 and MRP5 are expressed in kidney, MRP2 and MRP3 are highly expressed in liver, only MRP5 is expressed in brain in substantial amount, and MRP4 is expressed at very low levels in a few tissues (Kool et al., 1997). Experiments performed on the mouse macrophage cells (J774), and human embryonic kidney cells (HEK) in previous chapters suggested that AZT and ddI are substrates of MRPs. Currently, two of the MRP family, MRP4 and MRP5, are known to be capable of transporting NRTIs such as adefovir as well as AZT-MP (Schuetz et al., 1999; Lee et al., 2000; Chen et al., 2001).

For successful therapy of AIDS patients using NRTIs, improvement of pharmacological and pharmacokinetic properties of NRTIs is required. Since intracellular phosphorylation is a key event for the anti-HIV effect of AZT and ddI, it is important to investigate if the

increased intracellular concentration of AZT or ddI generates an increased anti-HIV effect.

Our preliminary results suggest that suppression of drug efflux transporters can increase

the exposure of viral reservoirs to AZT and ddI. If boosting can be applied to the clinical

situation, effective treatment of AIDS, especially AIDS dementia, will be possible.

However, there are few cases of significant *in vivo* inhibition of efflux transporters

suggesting that *in vivo* inhibition may not occur even though transporter inhibition may

occur at the cellular level. Thus, it is important to verify if the *in vitro* inhibition of efflux

transporters leads to pharmacokinetic boosting in an animal model.

B.   *Materials and Methods*

1.   *In vivo silencing of efflux transporters*

Predesigned siRNAs (siBCRP) were purchased from Dharmacon. In mouse studies, male

Balb/c or FVB mice, age 4 ~ 8 weeks, weighing 15 ~ 40 g, were purchased from Taconic

(Hudson, NY). Anesthesia was induced with ketamine/xylazine (80/10 mg/kg, ip

injection). The mice were dosed intravenously via a fast tail vein injection over 7-10

seconds with the siRNA dissolved in Ringers' solution. The total injection volume per

mouse (in ml) was calculated by dividing the weight of the mouse (in g) by 10. In siRNA

distribution studies, mice have free access to food and water. One or more days after

intravenous administration of siRNA, mice were euthanized by CO_2 inhalation. Selected

tissues, such as the liver, intestine, brain, lung, and kidney were collected to measure the

transporter expression in each tissue by Western blot or RT-PCR. Each organ were stored

in 1.5 ml tube and frozen in liquid nitrogen right after taken from the body. They were

stored in a freezer at -80°C until further analysis. Each set were tested in 3 mice to achieve

adequate statistic power.

2.   *In situ brain perfusion*

Male FVB mice (20 ~ 30g, 5 ~ 8 weeks old, Taconic) were used in *in situ* brain perfusion

experiments. Mice were maintained under standard conditions with *ad libitum* access to

food and water. Mice were anesthetized with ketamine/xylazine (140/8 mg/kg, ip

injection). The common carotid artery was exposed and ligated caudally, then the external

carotid artery was ligated at the bifurcation of the common carotid artery with the internal

carotid artery as shown in Figure 42.
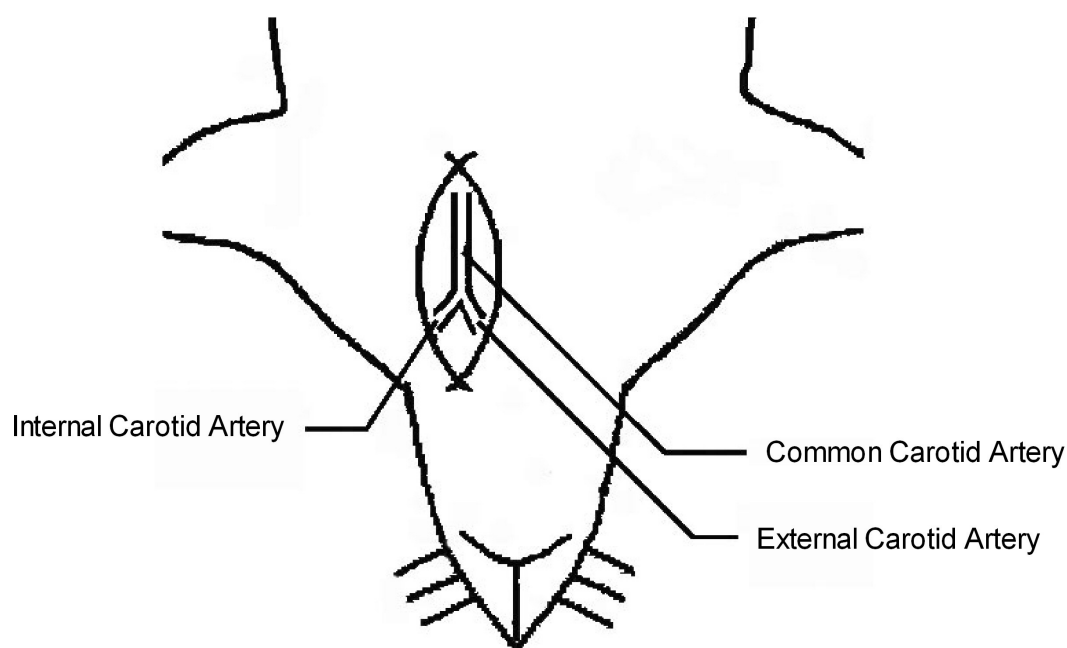
Figure 42. Structure of the carotid arteries around the neck of FVB mouse.

The left common carotid artery was catheterized with the polyethylene tubing (0.28-mm ID X 0.65-mm OD, A-M systems, WA) filled with heparin (25 U/mL). Immediately before perfusion, the heart beat was stopped by cutting the cardiac ventricles. Brains were perfused for various times at 37 °C using an infusion pump (Harvard, MA). The perfusate contains target compound in Krebs/bicarbonate buffer containing D-glucose, gassed with 95% O_2/5% CO_2 for pH control (7.4).

Components	Concentration (mM)
NaCl	128
KCl	4.2
$NaHCO_3$	24
NaH_2PO_4	2.4
$CaCl_2$	1.5
$MgSO_4$	0.9
Distilled water	Remaining

In the case of measuring the brain vascular volume, ^{3}H inulin was used instead of the target compound as a vascular volume marker. The perfusion was terminated by decapitating the mouse. The brain was removed from the skull and cleaned with paper tissue, then stored in -80°C until analysis. Right and left hemispheres must be separated immediately and so does the removal of Cerebellum. All data were reported for the perfused hemisphere. Brain vascular volume (V_{vasc}, ml·100g^{-1}), the ratio of the vascular marker concentration in brain to that in perfusate, was determined using the following equation: $V_{vasc} = X^{*}/C^{*}$, where X^{*} was the amount of radiolabeled inulin in the brain (dpm · 100 g^{-1}) and C^{*} was the perfusate concentration. Initial brain uptake clearances (Cl_{up}, ml · 100 g^{-1} · min^{-1}) was the following relationship: $Cl_{up} = dX_{brain}/dt/C_{pf}$, where X_{brain} was the amount of target compound in the brain corrected for vascular contamination ($X_{total} - V_{vasc} · C_{pf}$) and C_{pf} was the tracer concentration in the perfusate. In single time point experiment, X_{brain}/T replaced dX_{brain}/dt, where T was the perfusion time (min). Apparent brain distributional volumes

(V_{brain}, ml· 100 g^{-1}) were calculated from $V_{brain} = X_{brain}/C_{pf}$. In order to obtain the *PA*

product, the Crone Renkin model of capillary transport was used: *PA* was defined as *F*

ln(1-K_{in}/*F*), where *F* was the regional cerebral perfusion fluid flow, which was determined

using ^{14}C diazepam in separate experiments; K_{in} was the unidirectional transfer coefficient

from blood to brain which can be estimated in the same way of *Cl*$_{up}$; *P* was the apparent

permeability coefficient of the BBB for a test compound; and *A* was the mouse brain

capillary surface area. *P* can be calculated by dividing *PA* by *A*. Data was presented as

mean ± SD. Dunnett's multiple comparison test after ANOVA was used to compare the

statistical significance of differences between experimental groups and statistical

significance was determined at the level of *P*=0.05.

C.   Results

1.   In vivo silencing of efflux transporters

Hydrodynamic injection of siBCRP was developed for the knock-down of mouse bcrp1,

and the expression level of bcrp1 was measured for the control and siBCRP group (Figure

43). Expression of bcrp1 in the liver of the siBCRP treated mouse was significantly lower

than in the control group (*: $p < 0.05$). Expression levels of mouse bcrp1 in the kidney

showed no changes, consistent with published studies (Giladi et al., 2003; Lewis and

Wolff, 2005). This knock-down system can be utilized to monitor the effect of bcrp1 on

disposition, especially hepatic excretion of AZT and ddI.
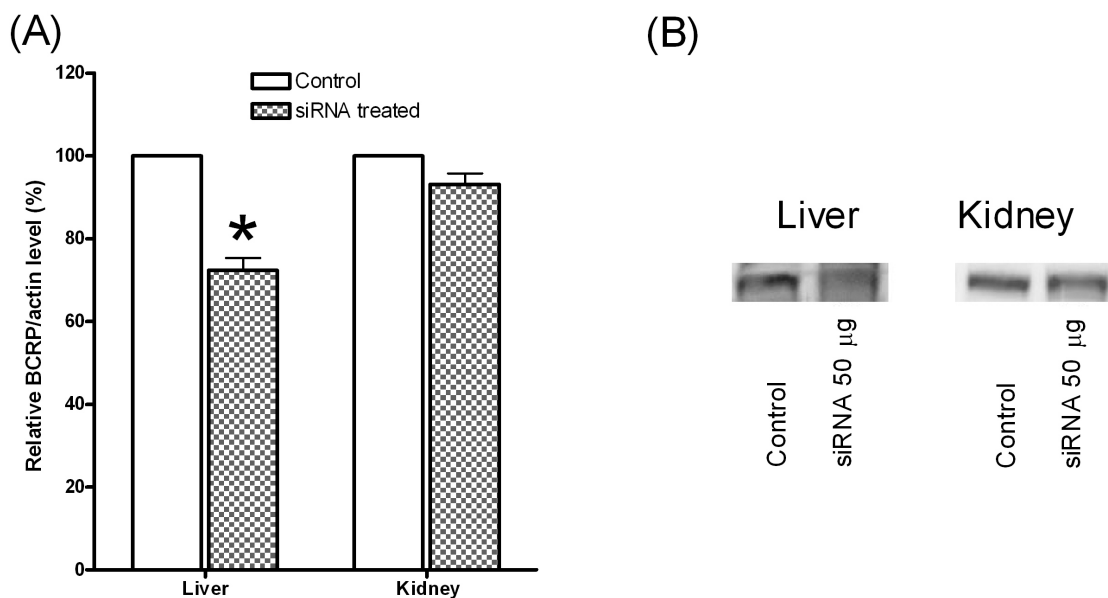
Figure 43. Effect of in vivo injection of naked siRNA of bcrp1. One day after IV injection (50 ug siRNA), protein was extracted respectively from liver and kidney and Western blot were performed. Each points represents means+SD (*: $p < 0.05$, n = 3)

2. *In situ brain perfusion*

The brain uptake properties of ddI in the presence of MK-571, a specific MRPs inhibitor were characterized using the brain perfusion technique to investigate the *in vivo* contribution of MRPs on brain uptake of ddI (Figure 44). The addition of MK-571 (100 μM) in the perfusates did not increased the V_{brain} values of ddI compared with ddI alone. As a positive control for MRPs inhibition by MK-571, inhibition of SQV brain uptake was examined (Figure 45). The V_{brain} values of ddI in the absence of MK-571 were constant over the range of 10 nM to 10 μM (Figure 46). The selected concentration range covered the plasma concentrations of ddI at clinically recommended dose; C_{max} of ddI equals 5.5 ± 2.3 μM at 200 mg b.i.d. dose (Sahai et al., 1995). Concentration independent brain uptake confirmed that no influx or efflux transporters were involved in brain uptake of ddI.
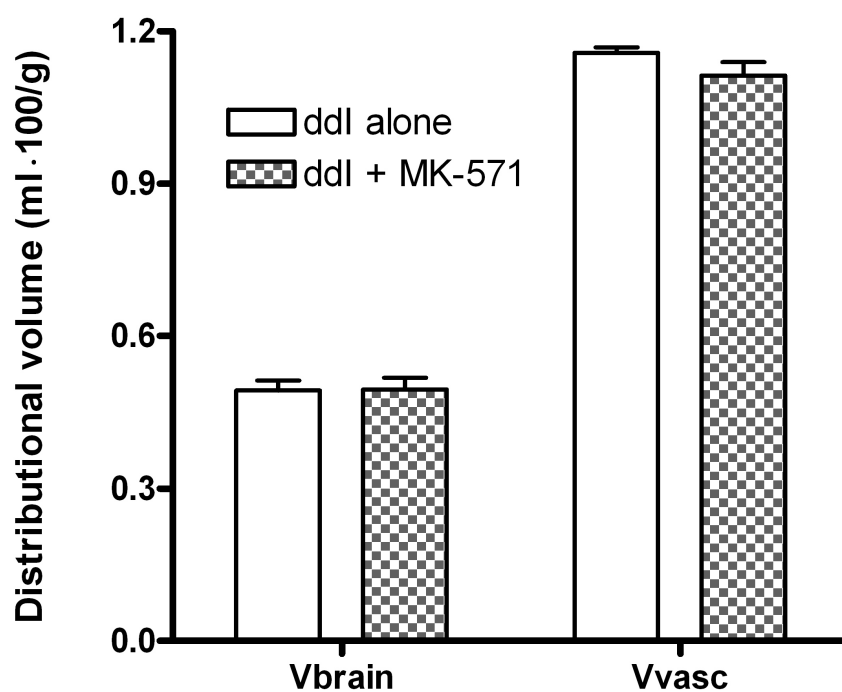
Figure 44. Apparent brain distributional volumes of 3H-ddI (1 uM) in the absence and presence of MK-571 (100 uM), which was included in the perfusates. Brain vascular volume was measured using 14C-sucrose. The mice were perfused for 60 sec and perfusion flow rate was 2.1 ml/min (n = 4)
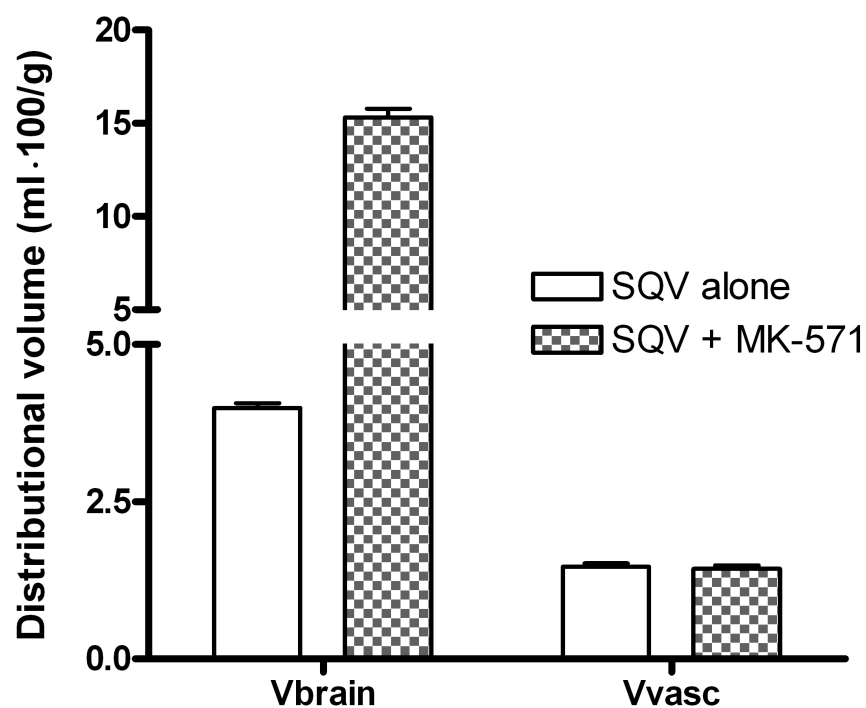
Figure 45. Apparent brain distributional volumes of 14C-SQV (1 uM) in the absence and presence of MK-571 (100 uM), which was included in the perfusates. Brain vascular volume was measured using 3H-mannitol. The mice were perfused for 60 sec and perfusion flow rate was 2.1 ml/min (n = 4)
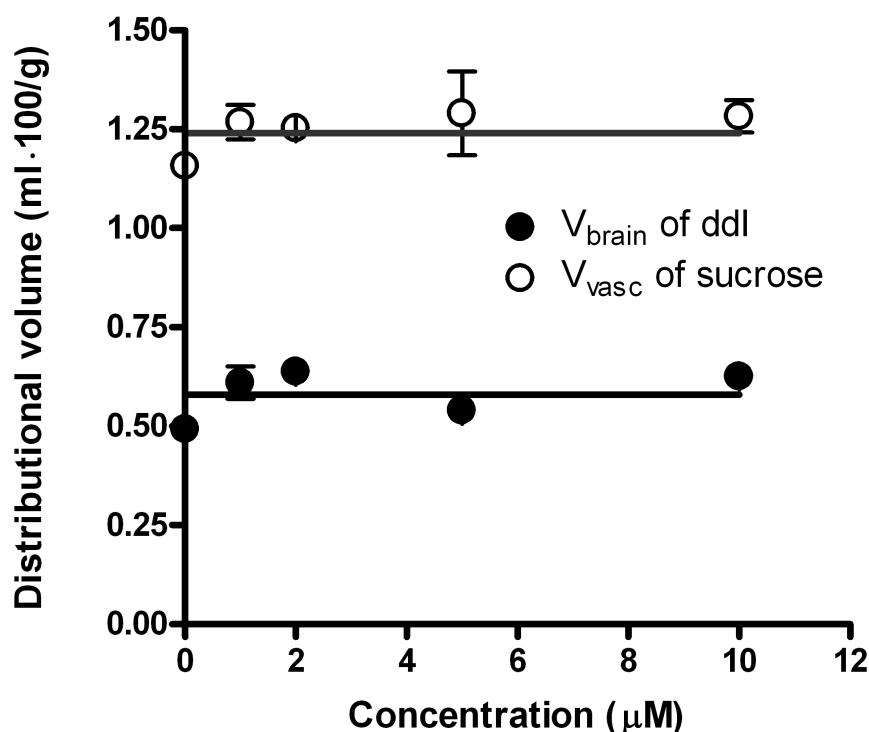
Figure 46. Apparent brain distributional volumes of ddl versus concentration of ddl, which was included in the perfusates. Brain vascular volume was measured using 14C-sucrose. The mice were perfused for 60 s. Perfusion flow rate was 2.1 ml/min (*: p < 0.05, n = 4)

D.   *Discussion*

The aim of this chapter was to develop an effective delivery strategy for NRTIs to HIV reservoir sites such as brain by circumventing the efflux mediated by ABC transporters such as BCRP and MRPs. In preliminary work, *in vivo* hydrodynamic injection of siRNA has been used to silence the mouse bcrp1 gene. This work is critical since high systemic exposure to NRTIs eventually leads to high accumulation of NRTIs in HIV reservoir sites. However, effective knockdown of the mouse bcrp1 gene by siRNA has been achieved only in liver and not in other tissues such as brain and kidney after hydrodynamic injection to mice. Hydrodynamic tail vein injection needs large dosing volumes over a short period.

Although this harsh dosing condition makes it difficult to apply hydrodynamic injection to clinical use, this technique is still promising as an experimental tool to evaluate the *in vivo* role of various uptake and efflux transporters especially in the mouse liver. Unfortunately, literature search suggested that no gene suppression in brain is expected after hydrodynamic injection of siRNA. Thus, effect of efflux transporters in brain uptake of ddI were investigated with chemical inhibitor MK-571 instead of siRNA. Brain uptake expressed as V_{brain} of ddI was not affected by MK-571, while saquinavir as positive control showed significant increase of brain uptake (Figure 44).

VII. OVERALL SUMMARY AND CONCLUSIONS

AZT and ddI are potent NRTIs and the oldest drugs to be approved by FDA for the treatment of HIV infection. These two NRTIs have been prescribed more often than any other antiviral drugs since the FDA approved them. Although AZT and ddI have been studied extensively for more than 20 years, the mechanisms behind their significant differences in absorption and disposition have not been well characterized. The focus of this research was to delineate the contribution of each pharmacokinetic process and metabolizing enzyme or transporters that affect the pharmacokinetics of AZT and ddI, and the specific objectives of this research were to:

1. Identify the contribution of efflux transporters such as BCRP and MRPs on the renal excretion of AZT and ddI.

2. Characterize the diverse metabolic pathways of AZT and ddI in animal and human cells.

3. Evaluate the role of drug efflux and metabolism on the urinary disposition of AZT and ddI.

4. Develop the novel strategy of the penetration of NRTIs to HIV reservoir site.

For the first objective, uptake and efflux studies of 3H-AZT or 3H-ddI with/without transporter inhibitors were performed in human HEK-R482 and mouse J774.1 and J774.2 cells. The renal clearances of two NRTIs are much greater than the Glomerular Filtration Rate (GFR) suggesting active secretion of these two drugs. Although AZT is assimilated into the epithelial kidney cells by organic anion transporters, the tissue distribution of AZT is moderate indicating the presence of AZT efflux transporter. The influx of ddI is also mediated by organic anion transporters, and the distribution in the kidney is only two-fold higher than plasma levels in rats. Interestingly, species differences in substrate specificity to the efflux transporter were observed. Neither bcrp1 nor mrps play a significant role in the efflux of AZT in mice, while both BCRP and MRPs altered the uptake and efflux of AZT significantly in human. The efflux properties of ddI were quite different from those of AZT: the effect of bcrp1 or BCRP on efflux of ddI was minimal; only MRP1 out of the four tested MRP subfamilies (MRP1 ~ 4) was responsible for ddI efflux and only to a marginal extent. Another key finding was that different MRP subfamilies were responsible for efflux of AZT and ddI. The efflux of AZT was greatly modulated by siMRP3 and siMRP4, and efflux of ddI was delayed only by siMRP1 to a moderate degree indicating that the major inhibition effect of MK-571 treatment might be caused by the inhibition of transporters other than MRPs. The identification of the efflux transporters is important for

understanding the elimination profiles of these NRTIs. The information obtained can be used to predict drug-drug interactions between AZT or ddI and other prescribed drugs. Metabolic profiles of 3H-AZT and 3H-ddI were characterized using radio-HPLC. Cellular uptake studies indicated rapid phosphorylation of AZT in HEK-R482 and J774.2 cells. Incubation of AZT resulted in the formation of AZT-MP in J774.1 and most of AZT was effluxed as a form of AZT or AZT-MP. However, AZT-TP was the predominant metabolite indicating faster serial phosphorylation of AZT in HEK-R482 cells than in J774.1 cells. In the case of ddI, the metabolic pathway was more complex than AZT. In cell systems, ddI showed lower intracellular concentrations compared to those of AZT, probably because ddI is less permeable to cell membranes than AZT. The predominant metabolite found in human HEK-R482 was the triphosphate form of ddA (ddA-TP) similar to AZT. ATP depletion and subsequent inhibition of AZT phosphorylation led to decreased formation of AZT-MP, which is a substrate of MRP4. The mixed function of ATP supports the efflux data showing that the relative efflux rate of AZT in ATP depleting and regenerating conditions was not different compared to the observation in the control group (no ATP depletion). Cellular uptake of ddI was also compared among control, ATP regeneration, and ATP depletion conditions. The effect of ATP depletion was minimal in both HEK-R482 cells and J774.2 cells. The experiments presented here show that metabolism is closely related to drug efflux of AZT and ddI, and the deposited forms of these drugs are sometimes different compared to the effluxed form.

Preliminary data indirectly suggested that BCRP was involved in plasma disposition of ddI in rats. But, subsequent *in vitro* studies did not support that BCRP was a substrate of ddI in cultured cells and kidney slices. The effect of MRP on mouse renal excretion of AZT and

ddI was assessed instead of the BCRP effect in mice *in vitro* and *in vivo* models. Outward transport of AZT was not apparently affected by FTC or by MK-571 in mouse kidney slices suggesting no involvement of efflux transporters in outward transport of AZT itself. However, accumulated efflux of GAZT significantly decreased when treated with MK-571. The overall process of AZT disposition involves the intracellular metabolism of AZT to GAZT and the subsequent pumping GAZT out possibly by MRPs in mouse kidney. Renal excretion of AZT was measured in mice when coadministered with MK-571. Far from *in vitro* results, no change of AZT or ddI urinary excretion was observed between MK-571 treated and untreated group. It is probably because the binding affinity of AZT or ddI to MRPs was not strong enough to show significant *in vivo* effect.

In case of ddI, efflux of ddI itself was decreased when treated with MK-571 and ddA-MP was not significantly changed by addition of MK-571. Urinary excretion of ddI or ddA-MP was not changed when coadministered with MK-571 and the possible cause of this phenomenon is same as the case of AZT. The kidney and liver are two of the major organs involved in drug disposition in gerenal. The renal clearance of AZT and ddI accounts for 30 ~ 50% of total body clearance after intravenous dosing while hepatic clearance is expected to cover the major portion of nonrenal clearance. Urinary excretion profile of AZT and ddI can be an indirect marker of these two drug's plasma disposition profile. The different renal disposition profile between AZT and ddI could not be explained by efflux transporters and rather the renal metabolism might be a main governing factor in renal disposition of these drugs.

Last objective is related with our long term goal to <u>develop a more effective dosing regimen for NRTIs in treating HIV/AIDS.</u> As long as an appropriate dosing regimen is established, chemical and biological inhibitors of efflux transporters can circumvent the low assimilation into viral reservoirs thus improving pharmacokinetics. Literatures suggest that drug efflux might hamper NRTI therapy in AIDS patients. Preliminary work was focused on the development of mouse model with specific transporter knock-down. The hydrodynamic injection itself was proven to be an effective tool to ablate the expression of target transporter gene and protein, but influence of efflux transporters on AZT and ddI could not be investigated with this technique, because it did not silence transporter in target organ such as brain and kidney. Chemical inhibition using MK-571 was used in *in situ* brain perfusion study as an alternative inhibition tool. Future study for developing enhanced dosing regimen must be focused more on metabolism than on efflux in these two reservoir sites.

Inhibitors of efflux transporters will be characterized at the cellular level and in animal studies. Effect of these inhibitors on pharmacodynamics of NRTIs using an HIV-infected cell system will be also assessed.

VIII. REFERENCES

Ahluwalia, G., Cooney, D. A., Mitsuya, H., Fridland, A., Flora, K. P., Hao, Z., Dalal, M., Broder, S. and Johns, D. G., 1987. Initial studies on the cellular pharmacology of 2',3'-dideoxyinosine, an inhibitor of HIV infectivity. *Biochem Pharmacol* **36,** 3797-3800.

Ahmed, A. E., Jacob, S., Loh, J. P., Samra, S. K., Nokta, M. and Pollard, R. B., 1991. Comparative disposition and whole-body autoradiographic distribution of [2-14C]azidothymidine and [2-14C]thymidine in mice. *J Pharmacol Exp Ther* **257,** 479-486.

Allen, J. D. and Schinkel, A. H., 2002. Multidrug resistance and pharmacological protection mediated by the breast cancer resistance protein (BCRP/ABCG2). *Mol Cancer Ther* **1,** 427-434.

Anapolsky, A., Teng, S., Dixit, S. and Piquette-Miller, M., 2006. The role of pregnane X receptor in 2-acetylaminofluorene-mediated induction of drug transport and -metabolizing enzymes in mice. *Drug Metab Dispos* **34,** 405-409.

Anderson, C. M., Baldwin, S. A., Young, J. D., Cass, C. E. and Parkinson, F. E., 1999. Distribution of mRNA encoding a nitrobenzylthioinosine-insensitive nucleoside transporter (ENT2) in rat brain. *Brain Res Mol Brain Res* **70,** 293-297.

Anderson, P. L., Kakuda, T. N. and Lichtenstein, K. A., 2004. The cellular pharmacology of nucleoside- and nucleotide-analogue reverse-transcriptase inhibitors and its relationship to clinical toxicities. *Clin Infect Dis* **38,** 743-753.

Baldwin, S. A., Beal, P. R., Yao, S. Y., King, A. E., Cass, C. E. and Young, J. D., 2004. The equilibrative nucleoside transporter family, SLC29. *Pflugers Arch* **447,** 735-743.

Balzarini, J., Pauwels, R., Baba, M., Herdewijn, P., de Clercq, E., Broder, S. and Johns, D. G., 1988. The in vitro and in vivo anti-retrovirus activity, and intracellular metabolism of 3'-azido-2',3'-dideoxythymidine and 2',3'-dideoxycytidine are highly dependent on the cell species. *Biochem Pharmacol* **37,** 897-903.

Beach, J. W., 1998. Chemotherapeutic agents for human immunodeficiency virus infection: mechanism of action, pharmacokinetics, metabolism, and adverse reactions. *Clin Ther* **20,** 2-25; discussion l.

Berger, E. A., Moss, B. and Pastan, I., 1998. Reconsidering targeted toxins to eliminate HIV infection: you gotta have HAART. *Proc Natl Acad Sci U S A* **95,** 11511-11513.

Blum, M. R., Liao, S. H., Good, S. S. and de Miranda, P., 1988. Pharmacokinetics and bioavailability of zidovudine in humans. *Am J Med* **85,** 189-194.

Borst, P., Balzarini, J., Ono, N., Reid, G., de Vries, H., Wielinga, P., Wijnholds, J. and Zelcer, N., 2004. The potential impact of drug transporters on nucleoside-analog-based antiviral chemotherapy. *Antiviral Res* **62,** 1-7.

Borst, P., Evers, R., Kool, M. and Wijnholds, J., 2000. A family of drug transporters: the multidrug resistance-associated proteins. *J Natl Cancer Inst* **92,** 1295-1302.

Cascorbi, I., 2006. Role of pharmacogenetics of ATP-binding cassette transporters in the pharmacokinetics of drugs. *Pharmacol Ther*

Chen, C. and Klaassen, C. D., 2004. Rat multidrug resistance protein 4 (Mrp, Abcc4): molecular cloning, organ distribution, postnatal renal expression, and chemical inducibility. *Biochem Biophys Res Commun* **317,** 46-53.

Chen, Z. S., Lee, K. and Kruh, G. D., 2001. Transport of cyclic nucleotides and estradiol 17-beta-D-glucuronide by multidrug resistance protein 4. Resistance to 6-mercaptopurine and 6-thioguanine. *J Biol Chem* **276,** 33747-33754.

Chow, H. H., Brookshier, G. and Li, P., 1998. Tissue disposition of zidovudine and its phosphorylated metabolites in zidovudine-treated healthy and retrovirus infected mice. *Pharm Res* **15,** 139-144.

Chow, H. H., Li, P., Brookshier, G. and Tang, Y., 1997. In vivo tissue disposition of 3'-azido-3'-deoxythymidine and its anabolites in control and retrovirus-infected mice. *Drug Metab Dispos* **25,** 412-422.

Chrystyna Bedrij, T. F., Scott C. Matchett, CFA, 2005. MAJOR DEVELOPMENTS IN THE TREATMENT OF HIV / AIDS. *HIV/AIDS Industry Report* 12.

Collins, J. M., 2001. Inter-species differences in drug properties. *Chem Biol Interact* **134,** 237-242.

Collins, J. M. and Unadkat, J. D., 1989. Clinical pharmacokinetics of zidovudine. An overview of current data. *Clin Pharmacokinet* **17,** 1-9.

Cretton, E. M. and Sommadossi, J. P., 1991. Modulation of 3'-azido-3'-deoxythymidine catabolism by probenecid and acetaminophen in freshly isolated rat hepatocytes. *Biochem Pharmacol* **42,** 1475-1480.

Cretton, E. M., Waterhous, D. V., Bevan, R. and Sommadossi, J. P., 1990. Glucuronidation of 3'-azido-3'-deoxythymidine by rat and human liver microsomes. *Drug Metab Dispos* **18,** 369-372.

Cretton, E. M., Xie, M. Y., Bevan, R. J., Goudgaon, N. M., Schinazi, R. F. and Sommadossi, J. P., 1991. Catabolism of 3'-azido-3'-deoxythymidine in hepatocytes and liver microsomes, with evidence of formation of 3'-amino-3'-deoxythymidine, a highly toxic catabolite for human bone marrow cells. *Mol Pharmacol* **39,** 258-266.

de Miranda, P., Good, S. S., Yarchoan, R., Thomas, R. V., Blum, M. R., Myers, C. E. and Broder, S., 1989. Alteration of zidovudine pharmacokinetics by probenecid in patients with AIDS or AIDS-related complex. *Clin Pharmacol Ther* **46,** 494-500.

Dhawan, R. K., Kharbanda, S., Nakamura, M., Ohno, T. and Kufe, D., 1990. Effects of granulocyte-macrophage colony-stimulating factor on 3'-azido-3'-deoxythymidine uptake, phosphorylation and nucleotide retention in human U-937 cells. *Biochem Pharmacol* **40,** 2695-2700.

Dietrich, C. G., Geier, A. and Oude Elferink, R. P., 2003. ABC of oral bioavailability: transporters as gatekeepers in the gut. *Gut* **52,** 1788-1795.

Ding, X. and Kaminsky, L. S., 2003. Human extrahepatic cytochromes P450: function in xenobiotic metabolism and tissue-selective chemical toxicity in the respiratory and gastrointestinal tracts. *Annu Rev Pharmacol Toxicol* **43,** 149-173.

Doshi, K. J., Gallo, J. M., Boudinot, F. D., Schinazi, R. F. and Chu, C. K., 1989. Comparative pharmacokinetics of 3'-azido-3'-deoxythymidine (AZT) and 3'-azido-2',3'-dideoxyuridine (AZddU) in mice. *Drug Metab Dispos* **17,** 590-594.

Ebert, B., Seidel, A. and Lampen, A., 2005. Identification of BCRP as transporter of benzo[a]pyrene conjugates metabolically formed in Caco-2 cells and its induction by Ah-receptor agonists. *Carcinogenesis* **26,** 1754-1763.

Elwell, L. P., Ferone, R., Freeman, G. A., Fyfe, J. A., Hill, J. A., Ray, P. H., Richards, C. A., Singer, S. C., Knick, V. B., Rideout, J. L. and et al., 1987. Antibacterial activity and mechanism of action of 3'-azido-3'-deoxythymidine (BW A509U). *Antimicrob Agents Chemother* **31,** 274-280.

Enomoto, A., Takeda, M., Tojo, A., Sekine, T., Cha, S. H., Khamdang, S., Takayama, F., Aoyama, I., Nakamura, S., Endou, H. and Niwa, T., 2002. Role of organic anion transporters in the tubular transport of indoxyl sulfate and the induction of its nephrotoxicity. *J Am Soc Nephrol* **13,** 1711-1720.

Eyster, M. E., Ballard, J. O., Gail, M. H., Drummond, J. E. and Goedert, J. J., 1989. Predictive markers for the acquired immunodeficiency syndrome (AIDS) in

hemophiliacs: persistence of p24 antigen and low T4 cell count. *Ann Intern Med* **110,** 963-969.

Franco, R., Centelles, J. J. and Kinne, R. K., 1990. Further characterization of adenosine transport in renal brush-border membranes. *Biochim Biophys Acta* **1024,** 241-248.

Frick, L. W., Nelson, D. J., St Clair, M. H., Furman, P. A. and Krenitsky, T. A., 1988. Effects of 3'-azido-3'-deoxythymidine on the deoxynucleotide triphosphate pools of cultured human cells. *Biochem Biophys Res Commun* **154,** 124-129.

Fridland, A., Connelly, M. C. and Ashmun, R., 1990. Relationship of deoxynucleotide changes to inhibition of DNA synthesis induced by the antiretroviral agent 3'-azido-3'-deoxythymidine and release of its monophosphate by human lymphoid cells (CCRF-CEM). *Mol Pharmacol* **37,** 665-670.

Furman, P. A., Fyfe, J. A., St Clair, M. H., Weinhold, K., Rideout, J. L., Freeman, G. A., Lehrman, S. N., Bolognesi, D. P., Broder, S., Mitsuya, H. and et al., 1986. Phosphorylation of 3'-azido-3'-deoxythymidine and selective interaction of the 5'-triphosphate with human immunodeficiency virus reverse transcriptase. *Proc Natl Acad Sci U S A* **83,** 8333-8337.

Gao, W. Y., Agbaria, R., Driscoll, J. S. and Mitsuya, H., 1994. Divergent anti-human immunodeficiency virus activity and anabolic phosphorylation of 2',3'-dideoxynucleoside analogs in resting and activated human cells. *J Biol Chem* **269,** 12633-12638.

Gao, W. Y., Cara, A., Gallo, R. C. and Lori, F., 1993. Low levels of deoxynucleotides in peripheral blood lymphocytes: a strategy to inhibit human immunodeficiency virus type 1 replication. *Proc Natl Acad Sci U S A* **90,** 8925-8928.

Gartner, S., Markovits, P., Markovitz, D. M., Kaplan, M. H., Gallo, R. C. and Popovic, M., 1986. The role of mononuclear phagocytes in HTLV-III/LAV infection. *Science* **233,** 215-219.

Gibaldi, M. and Perrier, D. (1982) *Pharmacokinetics*. M. Dekker, New York.

Gibbs, J. E., Jayabalan, P. and Thomas, S. A., 2003. Mechanisms by which 2',3'-dideoxyinosine (ddI) crosses the guinea-pig CNS barriers; relevance to HIV therapy. *J Neurochem* **84,** 725-734.

Giladi, H., Ketzinel-Gilad, M., Rivkin, L., Felig, Y., Nussbaum, O. and Galun, E., 2003. Small interfering RNA inhibits hepatitis B virus replication in mice. *Mol Ther* **8,** 769-776.

Graf, G. A., Yu, L., Li, W. P., Gerard, R., Tuma, P. L., Cohen, J. C. and Hobbs, H. H., 2003. ABCG5 and ABCG8 are obligate heterodimers for protein trafficking and biliary cholesterol excretion. *J Biol Chem* **278,** 48275-48282.

Gray, J. H., Owen, R. P. and Giacomini, K. M., 2004. The concentrative nucleoside transporter family, SLC28. *Pflugers Arch* **447,** 728-734.

Griffiths, D. A., Hall, S. D. and Sokol, P. P., 1991. Interaction of 3'-azido-3'-deoxythymidine with organic ion transport in rat renal basolateral membrane vesicles. *J Pharmacol Exp Ther* **257,** 149-155.

Groschel, B., Cinatl, J. and Cinatl, J., Jr., 1997. Viral and cellular factors for resistance against antiretroviral agents. *Intervirology* **40,** 400-407.

Gupta, S. and Gollapudi, S., 1993. P-glycoprotein (MDR 1 gene product) in cells of the immune system: its possible physiologic role and alteration in aging and human immunodeficiency virus-1 (HIV-1) infection. *J Clin Immunol* **13,** 289-301.

Gutierrez, M. M. and Giacomini, K. M., 1993. Substrate selectivity, potential sensitivity and stoichiometry of Na(+)-nucleoside transport in brush border membrane vesicles from human kidney. *Biochim Biophys Acta* **1149,** 202-208.

Hall, E. T., Yan, J. P., Melancon, P. and Kuchta, R. D., 1994. 3'-Azido-3'-deoxythymidine potently inhibits protein glycosylation. A novel mechanism for AZT cytotoxicity. *J Biol Chem* **269,** 14355-14358.

Hartman, N. R., Yarchoan, R., Pluda, J. M., Thomas, R. V., Marczyk, K. S., Broder, S. and Johns, D. G., 1990. Pharmacokinetics of 2',3'-dideoxyadenosine and 2',3'-dideoxyinosine in patients with severe human immunodeficiency virus infection. *Clin Pharmacol Ther* **47,** 647-654.

Hartman, N. R., Yarchoan, R., Pluda, J. M., Thomas, R. V., Wyvill, K. M., Flora, K. P., Broder, S. and Johns, D. G., 1991. Pharmacokinetics of 2',3'-dideoxyinosine in patients with severe human immunodeficiency infection. II. The effects of different oral formulations and the presence of other medications. *Clin Pharmacol Ther* **50,** 278-285.

Hauser, S. C., Ziurys, J. C. and Gollan, J. L., 1988. A membrane transporter mediates access of uridine 5'-diphosphoglucuronic acid from the cytosol into the endoplasmic reticulum of rat hepatocytes: implications for glucuronidation reactions. *Biochim Biophys Acta* **967,** 149-157.

Hedaya, M. A., Elmquist, W. F. and Sawchuk, R. J., 1990. Probenecid inhibits the metabolic and renal clearances of zidovudine (AZT) in human volunteers. *Pharm Res* **7,** 411-417.

Ho, D. D., Rota, T. R. and Hirsch, M. S., 1986. Infection of monocyte/macrophages by human T lymphotropic virus type III. *J Clin Invest* **77,** 1712-1715.

Ho, H. T. and Hitchcock, M. J., 1989. Cellular pharmacology of 2',3'-dideoxy-2',3'-didehydrothymidine, a nucleoside analog active against human immunodeficiency virus. *Antimicrob Agents Chemother* **33,** 844-849.

Hoggard, P. G., Veal, G. J., Wild, M. J., Barry, M. G. and Back, D. J., 1995. Drug interactions with zidovudine phosphorylation in vitro. *Antimicrob Agents Chemother* **39,** 1376-1378.

Hori, S., Ohtsuki, S., Ichinowatari, M., Yokota, T., Kanda, T. and Terasaki, T., 2005. Selective gene silencing of rat ATP-binding cassette G2 transporter in an in vitro blood-brain barrier model by short interfering RNA. *J Neurochem* **93,** 63-71.

Huisman, M. T., Smit, J. W., Crommentuyn, K. M., Zelcer, N., Wiltshire, H. R., Beijnen, J. H. and Schinkel, A. H., 2002. Multidrug resistance protein 2 (MRP2) transports HIV protease inhibitors, and transport can be enhanced by other drugs. *Aids* **16,** 2295-2301.

Inui, K. I., Masuda, S. and Saito, H., 2000. Cellular and molecular aspects of drug transport in the kidney. *Kidney Int* **58,** 944-958.

Ito, K., Suzuki, H., Horie, T. and Sugiyama, Y., 2005. Apical/basolateral surface expression of drug transporters and its role in vectorial drug transport. *Pharm Res* **22,** 1559-1577.

Jennings, L. L., Hao, C., Cabrita, M. A., Vickers, M. F., Baldwin, S. A., Young, J. D. and Cass, C. E., 2001. Distinct regional distribution of human equilibrative nucleoside transporter proteins 1 and 2 (hENT1 and hENT2) in the central nervous system. *Neuropharmacology* **40,** 722-731.

Johnson, M. A., Ahluwalia, G., Connelly, M. C., Cooney, D. A., Broder, S., Johns, D. G. and Fridland, A., 1988. Metabolic pathways for the activation of the antiretroviral agent 2',3'-dideoxyadenosine in human lymphoid cells. *J Biol Chem* **263,** 15354-15357.

Johnson, M. A. and Fridland, A., 1989. Phosphorylation of 2',3'-dideoxyinosine by cytosolic 5'-nucleotidase of human lymphoid cells. *Mol Pharmacol* **36,** 291-295.

Kaul, S., Shyu, W. C., Shukla, U. A., Dandekar, K. A. and Barbhaiya, R. H., 1993. Absorption, disposition, and metabolism of [14C]didanosine in the beagle dog. *Drug Metab Dispos* **21,** 447-453.

Klecker, R. W., Jr., Collins, J. M., Yarchoan, R., Thomas, R., Jenkins, J. F., Broder, S. and Myers, C. E., 1987. Plasma and cerebrospinal fluid pharmacokinetics of 3'-azido-3'-deoxythymidine: a novel pyrimidine analog with potential application for the treatment of patients with AIDS and related diseases. *Clin Pharmacol Ther* **41,** 407-412.

Knupp, C. A., Shyu, W. C., Dolin, R., Valentine, F. T., McLaren, C., Martin, R. R., Pittman, K. A. and Barbhaiya, R. H., 1991. Pharmacokinetics of didanosine in patients with acquired immunodeficiency syndrome or acquired immunodeficiency syndrome-related complex. *Clin Pharmacol Ther* **49,** 523-535.

Kool, M., de Haas, M., Scheffer, G. L., Scheper, R. J., van Eijk, M. J., Juijn, J. A., Baas, F. and Borst, P., 1997. Analysis of expression of cMOAT (MRP2), MRP3, MRP4, and MRP5, homologues of the multidrug resistance-associated protein gene (MRP1), in human cancer cell lines. *Cancer Res* **57,** 3537-3547.

Kornhauser, D. M., Petty, B. G., Hendrix, C. W., Woods, A. S., Nerhood, L. J., Bartlett, J. G. and Lietman, P. S., 1989. Probenecid and zidovudine metabolism. *Lancet* **2,** 473-475.

Le Hir, M. and Dubach, U. C., 1985. Concentrative transport of purine nucleosides in brush border vesicles of the rat kidney. *Eur J Clin Invest* **15,** 121-127.

Lee, K., Klein-Szanto, A. J. and Kruh, G. D., 2000. Analysis of the MRP4 drug resistance profile in transfected NIH3T3 cells. *J Natl Cancer Inst* **92,** 1934-1940.

Leung, S. and Bendayan, R., 1999. Role of P-glycoprotein in the renal transport of dideoxynucleoside analog drugs. *Can J Physiol Pharmacol* **77,** 625-630.

Lewis, D. L., Hagstrom, J. E., Loomis, A. G., Wolff, J. A. and Herweijer, H., 2002. Efficient delivery of siRNA for inhibition of gene expression in postnatal mice. *Nat Genet* **32,** 107-108.

Lewis, D. L. and Wolff, J. A., 2005. Delivery of siRNA and siRNA expression constructs to adult mammals by hydrodynamic intravascular injection. *Methods Enzymol* **392,** 336-350.

Li, W. T., Zhou, G. Y., Song, X. R., Chi, W. L., Ren, R. M. and Wang, X. W., 2005. Modulation of BCRP mediated atypical multidrug resistance phenotype by RNA interference. *Neoplasma* **52,** 219-224.

Liu, Y. and Hu, M., 2000. P-glycoprotein and bioavailability-implication of polymorphism. *Clin Chem Lab Med* **38,** 877-881.

Maher, J. M., Slitt, A. L., Cherrington, N. J., Cheng, X. and Klaassen, C. D., 2005. Tissue distribution and hepatic and renal ontogeny of the multidrug resistance-associated protein (Mrp) family in mice. *Drug Metab Dispos* **33,** 947-955.

Maliepaard, M., Scheffer, G. L., Faneyte, I. F., van Gastelen, M. A., Pijnenborg, A. C., Schinkel, A. H., van De Vijver, M. J., Scheper, R. J. and Schellens, J. H., 2001. Subcellular localization and distribution of the breast cancer resistance protein transporter in normal human tissues. *Cancer Res* **61,** 3458-3464.

Matheny, C. J., Lamb, M. W., Brouwer, K. R. and Pollack, G. M., 2001. Pharmacokinetic and pharmacodynamic implications of P-glycoprotein modulation. *Pharmacotherapy* **21,** 778-796.

Matsui, Y., Kobayashi, N., Nishikawa, M. and Takakura, Y., 2005. Sequence-Specific Suppression of mdr1a/1b Expression in Mice via RNA Interference. *Pharm Res*

McCaffrey, A. P., Meuse, L., Pham, T. T., Conklin, D. S., Hannon, G. J. and Kay, M. A., 2002. RNA interference in adult mice. *Nature* **418,** 38-39.

Meyers, J. A., Sanchez, D., Elwell, L. P. and Falkow, S., 1976. Simple agarose gel electrophoretic method for the identification and characterization of plasmid deoxyribonucleic acid. *J Bacteriol* **127,** 1529-1537.

Morisaki, K., Robey, R. W., Ozvegy-Laczka, C., Honjo, Y., Polgar, O., Steadman, K., Sarkadi, B. and Bates, S. E., 2005. Single nucleotide polymorphisms modify the transporter activity of ABCG2. *Cancer Chemother Pharmacol* **56,** 161-172.

Morse, G. D., Shelton, M. J. and O'Donnell, A. M., 1993. Comparative pharmacokinetics of antiviral nucleoside analogues. *Clin Pharmacokinet* **24,** 101-123.

Pan-Zhou, X. R., Cretton-Scott, E., Zhou, X. J., Xie, M. Y., Rahmani, R., Schinazi, R. F., Duchin, K. and Sommadossi, J. P., 1997. Comparative metabolism of the antiviral dimer 3'-azido-3'-deoxythymidine-P-2',3'-dideoxyinosine and the monomers zidovudine and didanosine by rat, monkey, and human hepatocytes. *Antimicrob Agents Chemother* **41,** 2502-2510.

Perry, C. M. and Balfour, J. A., 1996. Didanosine. An update on its antiviral activity, pharmacokinetic properties and therapeutic efficacy in the management of HIV disease. *Drugs* **52,** 928-962.

Pichler, A., Zelcer, N., Prior, J. L., Kuil, A. J. and Piwnica-Worms, D., 2005. In vivo RNA interference-mediated ablation of MDR1 P-glycoprotein. *Clin Cancer Res* **11,** 4487-4494.

Plotkin, S. A., Drew, W. L., Felsenstein, D. and Hirsch, M. S., 1985. Sensitivity of clinical isolates of human cytomegalovirus to 9-(1,3-dihydroxy-2-propoxymethyl)guanine. *J Infect Dis* **152,** 833-834.

Ray, A. S., Olson, L. and Fridland, A., 2004. Role of purine nucleoside phosphorylase in interactions between 2',3'-dideoxyinosine and allopurinol, ganciclovir, or tenofovir. *Antimicrob Agents Chemother* **48,** 1089-1095.

Resetar, A. and Spector, T., 1989. Glucuronidation of 3'-azido-3'-deoxythymidine: human and rat enzyme specificity. *Biochem Pharmacol* **38,** 1389-1393.

Rolinski, B., Bogner, J. R., Sadri, I., Wintergerst, U. and Goebel, F. D., 1997. Absorption and elimination kinetics of zidovudine in the cerebrospinal fluid in HIV-1-infected patients. *J Acquir Immune Defic Syndr Hum Retrovirol* **15,** 192-197.

Ross, D. D., 2000. Novel mechanisms of drug resistance in leukemia. *Leukemia* **14,** 467-473.

Sahai, J., Gallicano, K., Garber, G., Pakuts, A. and Cameron, W., 1995. Pharmacokinetics of simultaneously administered zidovudine and didanosine in HIV-seropositive male patients. *J Acquir Immune Defic Syndr Hum Retrovirol* **10,** 54-60.

Sampath, J., Adachi, M., Hatse, S., Naesens, L., Balzarini, J., Flatley, R. M., Matherly, L. H. and Schuetz, J. D., 2002. Role of MRP4 and MRP5 in biology and chemotherapy. *AAPS PharmSci* **4,** E14.

Schaub, T. P., Kartenbeck, J., Konig, J., Spring, H., Dorsam, J., Staehler, G., Storkel, S., Thon, W. F. and Keppler, D., 1999. Expression of the MRP2 gene-encoded conjugate export pump in human kidney proximal tubules and in renal cell carcinoma. *J Am Soc Nephrol* **10,** 1159-1169.

Schaub, T. P., Kartenbeck, J., Konig, J., Vogel, O., Witzgall, R., Kriz, W. and Keppler, D., 1997. Expression of the conjugate export pump encoded by the mrp2 gene in the apical membrane of kidney proximal tubules. *J Am Soc Nephrol* **8,** 1213-1221.

Schinkel, A. H., 1999. P-Glycoprotein, a gatekeeper in the blood-brain barrier. *Adv Drug Deliv Rev* **36,** 179-194.

Schinkel, A. H. and Jonker, J. W., 2003. Mammalian drug efflux transporters of the ATP binding cassette (ABC) family: an overview. *Adv Drug Deliv Rev* **55,** 3-29.

Schuetz, J. D., Connelly, M. C., Sun, D., Paibir, S. G., Flynn, P. M., Srinivas, R. V., Kumar, A. and Fridland, A., 1999. MRP4: A previously unidentified factor in resistance to nucleoside-based antiviral drugs. *Nat Med* **5,** 1048-1051.

Sidtis, J. J., Gatsonis, C., Price, R. W., Singer, E. J., Collier, A. C., Richman, D. D., Hirsch, M. S., Schaerf, F. W., Fischl, M. A., Kieburtz, K. and et al., 1993. Zidovudine treatment of the AIDS dementia complex: results of a placebo-controlled trial. AIDS Clinical Trials Group. *Ann Neurol* **33,** 343-349.

Siegmund, W., Ludwig, K., Giessmann, T., Dazert, P., Schroeder, E., Sperker, B., Warzok, R., Kroemer, H. K. and Cascorbi, I., 2002. The effects of the human MDR1 genotype on the expression of duodenal P-glycoprotein and disposition of the probe drug talinolol. *Clin Pharmacol Ther* **72,** 572-583.

Sim, S. M., Back, D. J. and Breckenridge, A. M., 1991. The effect of various drugs on the glucuronidation of zidovudine (azidothymidine; AZT) by human liver microsomes. *Br J Clin Pharmacol* **32,** 17-21.

Singlas, E., Pioger, J. C., Taburet, A. M., Colaneri, S. and Fillastre, J. P., 1989. Comparative pharmacokinetics of zidovudine (AZT) and its metabolite (G.AZT) in healthy subjects and HIV seropositive patients. *Eur J Clin Pharmacol* **36,** 639-640.

Somogyi, A., 1996. Renal transport of drugs: specificity and molecular mechanisms. *Clin Exp Pharmacol Physiol* **23,** 986-989.

Stagg, M. P., Cretton, E. M., Kidd, L., Diasio, R. B. and Sommadossi, J. P., 1992. Clinical pharmacokinetics of 3'-azido-3'-deoxythymidine (zidovudine) and catabolites with formation of a toxic catabolite, 3'-amino-3'-deoxythymidine. *Clin Pharmacol Ther* **51,** 668-676.

Stoeckler, J. D., Cambor, C. and Parks, R. E., Jr., 1980. Human erythrocytic purine nucleoside phosphorylase: reaction with sugar-modified nucleoside substrates. *Biochemistry* **19,** 102-107.

Su, F., Ouyang, N., Zhu, P., Ouyang, N., Jia, W., Gong, C., Ma, X., Xu, H. and Song, E., 2005. Psychological stress induces chemoresistance in breast cancer by upregulating mdr1. *Biochem Biophys Res Commun* **329,** 888-897.

Szebeni, J., Patel, S. S., Hung, K., Wahl, L. M. and Weinstein, J. N., 1991. Effects of thymidine and uridine on the phosphorylation of 3'-azido-3'-deoxythymidine

(zidovudine) in human mononuclear cells. *Antimicrob Agents Chemother* **35,** 198-200.

Takeda, M., Khamdang, S., Narikawa, S., Kimura, H., Kobayashi, Y., Yamamoto, T., Cha, S. H., Sekine, T. and Endou, H., 2002. Human organic anion transporters and human organic cation transporters mediate renal antiviral transport. *J Pharmacol Exp Ther* **300,** 918-924.

Thiebaut, F., Tsuruo, T., Hamada, H., Gottesman, M. M., Pastan, I. and Willingham, M. C., 1987. Cellular localization of the multidrug-resistance gene product P-glycoprotein in normal human tissues. *Proc Natl Acad Sci U S A* **84,** 7735-7738.

Tornevik, Y., Ullman, B., Balzarini, J., Wahren, B. and Eriksson, S., 1995. Cytotoxicity of 3'-azido-3'-deoxythymidine correlates with 3'-azidothymidine-5'-monophosphate (AZT-MP) levels, whereas anti-human immunodeficiency virus (HIV) activity correlates with 3'-azidothymidine-5'-triphosphate (AZT-TP) levels in cultured CEM T-lymphoblastoid cells. *Biochem Pharmacol* **49,** 829-837.

Unadkat, J. D., Collier, A. C., Crosby, S. S., Cummings, D., Opheim, K. E. and Corey, L., 1990. Pharmacokinetics of oral zidovudine (azidothymidine) in patients with AIDS when administered with and without a high-fat meal. *Aids* **4,** 229-232.

van Aubel, R. A., Smeets, P. H., Peters, J. G., Bindels, R. J. and Russel, F. G., 2002. The MRP4/ABCC4 gene encodes a novel apical organic anion transporter in human kidney proximal tubules: putative efflux pump for urinary cAMP and cGMP. *J Am Soc Nephrol* **13,** 595-603.

Veal, G. J. and Back, D. J., 1995. Metabolism of Zidovudine. *Gen Pharmacol* **26,** 1469-1475.

Wang, X., Furukawa, T., Nitanda, T., Okamoto, M., Sugimoto, Y., Akiyama, S. and Baba, M., 2003. Breast cancer resistance protein (BCRP/ABCG2) induces cellular resistance to HIV-1 nucleoside reverse transcriptase inhibitors. *Mol Pharmacol* **63,** 65-72.

Wang, X., Nitanda, T., Shi, M., Okamoto, M., Furukawa, T., Sugimoto, Y., Akiyama, S. and Baba, M., 2004. Induction of cellular resistance to nucleoside reverse transcriptase inhibitors by the wild-type breast cancer resistance protein. *Biochem Pharmacol* **68,** 1363-1370.

Watanabe, T., Onuki, R., Yamashita, S., Taira, K. and Sugiyama, Y., 2005. Construction of a functional transporter analysis system using MDR1 knockdown Caco-2 cells. *Pharm Res* **22,** 1287-1293.

Weibel, M., Balzarini, J., Bernhardt, A. and Mamont, P., 1994. Potentiating effect of (2-[2-[(2-amino-1,6-dihydro-6-oxo-9H-purin-9-yl)methyl]-phenyl]ethenyl) -phosphonic acid (MDL 74,428), a potent inhibitor of purine nucleoside phosphorylase, on the antiretroviral activities of 2',3'-dideoxyinosine combined with ribavirin in mice. *Biochem Pharmacol* **48,** 245-252.

White, D. A., Heffron, F., Miciak, A., Middleton, B., Knights, S. and Knight, D., 1990. Chemical synthesis of dual-radiolabelled cyclandelate and its metabolism in rat hepatocytes and mouse J774 cells. *Xenobiotica* **20,** 71-79.

Wijnholds, J., Mol, C. A., van Deemter, L., de Haas, M., Scheffer, G. L., Baas, F., Beijnen, J. H., Scheper, R. J., Hatse, S., De Clercq, E., Balzarini, J. and Borst, P., 2000. Multidrug-resistance protein 5 is a multispecific organic anion transporter able to transport nucleotide analogs. *Proc Natl Acad Sci U S A* **97,** 7476-7481.

Xu, J., Liu, Y., Yang, Y., Bates, S. and Zhang, J. T., 2004. Characterization of oligomeric human half-ABC transporter ATP-binding cassette G2. *J Biol Chem* **279,** 19781-19789.

Yao, S. Y., Ng, A. M., Sundaram, M., Cass, C. E., Baldwin, S. A. and Young, J. D., 2001. Transport of antiviral 3'-deoxy-nucleoside drugs by recombinant human and rat equilibrative, nitrobenzylthioinosine (NBMPR)-insensitive (ENT2) nucleoside transporter proteins produced in Xenopus oocytes. *Mol Membr Biol* **18,** 161-167.

Yarchoan, R., Klecker, R. W., Weinhold, K. J., Markham, P. D., Lyerly, H. K., Durack, D. T., Gelmann, E., Lehrman, S. N., Blum, R. M., Barry, D. W. and et al., 1986. Administration of 3'-azido-3'-deoxythymidine, an inhibitor of HTLV-III/LAV replication, to patients with AIDS or AIDS-related complex. *Lancet* **1,** 575-580.

Yarchoan, R., Pluda, J. M., Thomas, R. V., Mitsuya, H., Brouwers, P., Wyvill, K. M., Hartman, N., Johns, D. G. and Broder, S., 1990. Long-term toxicity/activity profile of 2',3'-dideoxyinosine in AIDS or AIDS-related complex. *Lancet* **336,** 526-529.

Zakharova, O. D., Tarrago-Litvak, L., Maksakova, G., Andreola, M. L., Dufour, E., Litvak, S. and Nevinsky, G. A., 1995. High-affinity interaction of human immunodeficiency virus type-1 reverse transcriptase with partially complementary primers. *Eur J Biochem* **233,** 856-863.

IX. CURRICULUM VITAE

Name: Sung-Hack Lee

Position: Head of Drug Metabolism and Pharmacokinetics
LG Life Sciences, Ltd. / R&D
104-1 Munji-dong, Yuseong-gu, Daejeon
305-380, Korea
Phone: 82-42-866-2287
E-mail: shleeap@lgls.com

Professional Activity and License:
Manager, 2006-Present, DMPK Team, LG Life Sciences, Korea

Teaching Assistant, 2003-2006, Ernest Mario School of Pharmacy, Rutgers, The State University of New Jersey

Graduate Assistant, 2001-2003, Ernest Mario School of Pharmacy, Rutgers, The State University of New Jersey

Research Scientist, 1996-2001, Department of DMPK, LG Life Sciences, Korea

Pharmacist License, 1994, Ministry of Health and Welfare, Korea

Educations:
Ph.D., 2008, Pharmaceutics, Rutgers, The State University of New Jersey (Major Adviser: Patrick J. Sinko, Ph.D.)

M.S., 1996, Pharmaceutics, Seoul National University, Korea (Major Adviser: Chang-Koo Shim, Ph.D.)

B.S., 1994, Manufacturing Pharmacy, Seoul National University, Korea

Scholarships:
 - Nam-Chuck Scholarship (3/91-2/94), Full tuition

Research Interests and Techniques:
 - Transporter mediated pharmacokinetic boosting of HIV protease inhibitors
 - Transporter mediated BBB efflux of anti-cancer and/or anti-HIV drugs
 - Differentiation of intestinal and hepatic first pass effect of drugs in rabbit model
 - General drug metabolism using hepatic S9 and/or microsomal fraction
 - In vivo preclinical pharmacokinetics in the rats, dogs, and monkeys
 - Development and validation of bioanalytical method using HPLC and LC/MS-MS

Publications:

1. Su Y, Hu P, Lee SH, Sinko PJ. Using novobiocin as a specific inhibitor of breast cancer resistant protein to assess the role of transporter in the absorption and disposition of topotecan. *J Pharm Pharm Sci.* 2007;10(4):519-36.

2. Su Y, Lee SH, Sinko PJ. Inhibition of efflux transporter ABCG2/BCRP does not restore mitoxantrone sensitivity in irinotecan-selected human leukemia CPT-K5 cells: evidence for multifactorial multidrug resistance. *Eur J Pharm Sci.* 2006:29:102-110.

3. Lee SH, Sinko PJ. siRNA--getting the message out. *Eur J Pharm Sci.* 2006:27:401-410.

4. Kunta JR, Lee SH, Perry BA, Lee YH, Sinko PJ. Differentiation of gut and hepatic first-pass loss of verapamil in intestinal and vascular access-ported (ivap) rabbits. *Drug Metab Dispos* 2004;32:1293-1298.

5. Su Y, Lee SH, Sinko PJ. Practical aspects of transporter model systems: a case study involving SQV. *Drug Metab Rev* 2004;36:377-389.

6. Lalloo AK, Luo FR, Guo A, Paranjpe PV, Lee SH, Vyas V, Rubin E, Sinko PJ. Membrane transport of camptothecin: facilitation by human P-glycoprotein (ABCB1) and multidrug resistance protein 2 (ABCC2). *BMC Med* 2004;2:16.

7. Hong J, Lambert JD, Lee SH, Sinko PJ, Yang CS. Involvement of multidrug resistance-associated proteins in regulating cellular levels of (-)-epigallocatechin-3-gallate and its methyl metabolites. *Biochem Biophys Res Commun* 2003;310:222-227.

8. Park J, Lee SH, Kim A. Microparticle and liquid formulation of a novel HIV protease inhibitor. *Pharm Dev Technol* 2002;7:297-303.

9. Lee K, Jung WH, Kang M, Lee SH. Noncovalent thrombin inhibitors incorporating an imidazolylethynyl P1. *Bioorg Med Chem Lett* 2000;10:2775-2778.

10. Lee K, Jung WH, Hwang SY, Lee SH. Fluorobenzamidrazone thrombin inhibitors: influence of fluorine on enhancing oral absorption. *Bioorg Med Chem Lett* 1999;9:2483-2486.

11. Lee K, Jung WH, Park CW, Hong CY, Kim IC, Kim S, Oh YS, Kwon OH, Lee SH, Park HD, Kim SW, Lee YH, Yoo YJ. Benzylamine-based selective and orally bioavailable inhibitors of thrombin. *Bioorg Med Chem Lett* 1998;8:2563-2568.

12. Lee SH, Choi YJ, Jeong YN, Kim HS, Lee SH, Kim IC, Oh YS, Lee YH. High-performance liquid chromatographic determination of a new oral thrombin inhibitor in the blood of rats and dogs. *J Chromatogr B Biomed Sci Appl* 1998;714:379-383.

13. Hong SS, Lee SH, Lee YJ, Chung SJ, Lee MH, Shim CK. Accelerated oral absorption of gliclazide in human subjects from a soft gelatin capsule containing a PEG 400 suspension of gliclazide. *J Control Release* 1998;51:185-192.

Patent:

Kyo-Han Ahn, Suk-Jong Lee, Sung-Hack Lee, Jae-Sun Kim, Chang Yong Hong, Tae-Kyo Park, Jung-In Oh, Hee-Dong Park, Hee-Jin Kim, and Chang-Ho Lee N-(4-amino) butyl-3-phenylpyrrolidine derivative, it's synthesis and formulation as an anxiolytic and antidepressant agent, KR0237542 (1999)